Phytoestrogen coumestrol as an anti-cancer therapy against triple-negative inflammatory breast cancer

By

Keishla M. Rodríguez-Mártir

Submitted to the Faculty of Natural Sciences
Department of Biology

In fulfillement of the requirements for the degree of
Doctor of Philosophy
at the University of Puerto Rico, Rio Piedras Campus
May 12, 2022

List of contents

List of figures

List of tables

List of abbreviations

Cou: coumestrol

E2: estrogen

IC_{50}: half-maximal inhibitory concentration

TN-IBC: triple-negative inflammatory breast cancer

IBC: inflammatory breast cancer

TNBC: triple-negative breast cancer

SERM: selective estrogen receptor modulator

SERD: selective estrogen receptor degrader

DMSO: dimethyl sulphoxide

NF-kB: nuclear factor kappa

ER-α66: estrogen receptor alpha 66

ER-α36: estrogen receptor alpha 36

ER-β: estrogen receptor beta

ER: estrogen receptor

PR: progesterone receptor

GPR30: G protein-coupled receptor 30

HER2: human epidermal growth factor receptor 2

EGFR: epidermal growth factor receptor

DMEM: Dulbecco's Modified Eagle Medium

RPMI: Roswell Park Memorial Institute Medium

FBS: fetal bovine serum

PBS: phosphate buffered saline

HBSS: Hanks Balanced Salt Solution

TBST: tris-buffered saline and Tween 20

PVDF: poly (vinylidene fluoride)

BSA: bovine serum albumin

RCV: relative cell viability

CO2: carbon dioxide

SDS-PAGE: sodium dodecyl-sulfate polyacrylamide gel electrophoresis

ECL: enhanced chemiluminescence

ANOVA: analysis of variance

ECM: extracellular matrix

TIPARP: TCDD Inducible Poly (ADP-Ribose) Polymerase

PCR: polymerase chain reaction

qRT-PCR: quantitative reverse transcription polymerase chain reaction

DEGs: differentially expressed genes

ACCEPTED BY THE FACULTY OF NATURAL SCIENCES
DEPARTMENT OF BIOLOGY
UNIVERSITY OF PUERTO RICO RIO PIEDRAS CAMPUS
IN PARTIAL FULFILLMENT OF THE REQUIREMENTS FOR THE DEGREE OF
DOCTOR OF PHILOSOPHY
IN THE SUBJECT OF BIOLOGY

_____
Esther A. Peterson-Peguero
THESIS DIRECTOR

_____
Beatriz Zayas, Ph.D.
DISSERTATION COMMITTEE MEMBER

_____
Pablo Vivas, Ph.D.
DISSERTATION COMMITTEE MEMBER

_____
José Agosto, Ph.D.
DISSERTATION COMMITTEE MEMBER

_____
José A. Rodríguez-Martínez, Ph.D.
DISSERTATION COMMITTEE MEMBER

Abstract

Coumestrol (Cou) is a phytoestrogen present in soy and clover sprouts which is structurally similar to estrogen (E2) and has a cytotoxic effect in breast cancer cell lines. Nevertheless, the molecular mechanism by which Cou can exert its effect in the most aggressive breast cancer subtype, triple-negative inflammatory breast cancer (TN-IBC), is still unknown. Studies show that TN-IBC cell lines are unresponsive to hormonal therapies, but E2 can activate signaling pathways involved in pro-oncogenic phenotypes such as motility and invasion by activating a rapid estrogen-dependent non-genomic signaling. Therefore, the objective of this study was to determine the anti-cancer effect of Cou in TN-IBC cell lines (using 2D and 3D culture models) and the molecular mechanism Cou exerts for its anti-cancer activity. Dose-response curves of Cou in 2D and 3D culture models of TN-IBC cell lines were generated to determine the half-maximal inhibitory concentration (IC_{50}). Relative cell viability was measured in ER-positive, triple-negative, TN-IBC, and HER2-amplified IBC cell lines. Functional assays were performed in TN-IBC cell lines to determine the effect of E2, Cou, and E2/Cou combination treatments on cell viability, migration, invasion, proliferation, and tumor emboli growth. Additionally, the effect of Cou and E2 treatments on phosphorylation of downstream kinases was analyzed by a proteome profile human phospho-kinase array. RNA-seq was performed in TN-IBC cell lines to identify transcriptome changes after Cou treatment. Our data demonstrated that Cou treatment using the IC_{50} (13µM in 2D models and 50µM in 3D models) decreased cell viability in TN-IBC cell lines. Similarly, Cou treatment reduces triple-

negative non-IBC cell viability. In comparison with E2, Cou decreases migration, invasion, proliferation, and tumor emboli growth in TN-IBC cell lines. Finally, Cou treatment reduces the phosphorylation of kinases MAPK/ERK and PI3K/AKT that promote pro-oncogenic phenotypes and upregulate genes such as TIPARP, recently involved in breast cancer phenotype suppression. In summary, this study guide us in elucidating a signaling pathway affected by Cou's anti-cancer activity. More importantly, it opens the opportunities to design more effective targeted therapeutic strategies to improve the prognosis and survival rates of IBC patients.

Dedication

I dedicate my dissertation work to my family, specifically my mother, Betzaida Martir-Arce. You taught me to fight for my dreams and never give up, even in difficult situations. You are my greatest example to follow. You are the woman I love the most in this world. I would have never made it without your support, nursing, and love.

Also, I want to dedicate my dissertation to the memory of my grandmother, Dominica Arce. You always instilled in me the importance of studying and believed in my abilities. I know that from heaven, you are celebrating my achievements.

Acknowledgements

This project is supported by UPR Fondos Institucionales para la Investigación (FIPI to E. Peterson), NIH 1R21CA253609-01 and RISE program (5R25GM061151-20).

I would like to express my most profound appreciation to my principal investigator (PI), Dr. Esther Peterson-Peguero. Thanks for believing in my project idea and conveying a spirit of adventure regarding research. Without her guidance and persistent help, this dissertation would not have been possible.

I want to thank my committee members, Dr. Jose Rodriguez-Martinez, Dr. Pablo Vivas, Dr. Beatriz Zayas, and Dr. Jose Agosto, whose work demonstrated your engagement with your profession and scientific community. Thanks for all your support, advice and for accepting the challenge of being part of this project.

In addition, a special thanks to Carlos S. Morales-Rivera, Emanuel A. Carrasquillo-Dones, Ayeisha N. Colon-Ortiz, Dalissa Negron-Figueroa, and Jesús M. Rosario-Rivera. First, I would like to thank Carlos for performing the RNA-sequencing analysis. Thanks to Emanuel for being my cheerleader, lab partner and give me support in all my graduate studies. Also, thanks to my three undergraduates Ayeisha, Dalissa and Jesús for helping me perform the experiments of this dissertation and giving me the opportunity to provide mentoring in their studies. All of you are extremely special to me. My grad school would never be the same if I had never met them.

Biography

Keishla began her university studies in August 2012 at the University of Puerto Rico at Aguadilla Campus (UPRAg) in the biology program with a concentration in Biomedical Sciences. After completing her first year in college, she performed research with Dr. Adrianne Tossas called “Inventory of birds in coastal habitat restoration”. Then, she works for two years under the research lead of Dr. Yadira Malavez, “*Tamarindus indica* from Puerto Rico as an antimicrobial agent against Gram-negative and Gram-positive bacteria.”

Keishla firmly believes that every biologist must integrate into the society in which they live to identify the current needs in their community and make contributions. For this reason, she organizes fundraising for cancer patients. These awoke in Keishla a desire to learn more about this disease and contribute to research in that area. For this reason, since it was her last year as an undergraduate student in UPRAg and she was taking two courses, Keishla drove for two hours to visit Dr. Peterson’s lab (breast cancer research lab) once a week to work as a volunteer in her lab. Then, she formally started her graduate studies creating a thesis based on the analysis of a natural compound as a treatment for triple-negative inflammatory breast cancer under the mentoring of Dr. Esther A. Peterson-Peguero at the University of Puerto Rico at Rio Piedras Campus. She submitted the first article of her thesis called “Phytoestrogen coumestrol induces anti-proliferative and anti-migration effects on triple-negative inflammatory breast cancer”. Also, after starting graduate school, Keishla had the opportunity to teach General Biology and Microbiology Laboratory courses to undergraduate students.

Chapter I: Introduction

1.1 Breast Cancer

Breast cancer is the most common cancer in females worldwide (Britt, 2021; Goldman, 2020; Lukong, 2017). However, in the United States, breast cancer is the second most common disease in women (Division of Cancer Prevention and Control, 2021; Feng et al., 2018). Also, both genders (female and male) can develop breast cancer, but it is rare in men (Clinic, 2020; Lukong, 2017). Among 1 in 8 women and 1 in 833 men in the United States will develop breast cancer in their lives (Breastcancer.org, 2021; Feng et al., 2018). Additionally, it's estimated that about 30% of newly diagnosed cancers in women will be breast cancers (AmericanCancerSociety, 2022).

Even though women are at higher risk of developing breast cancer, other factors can also increase the odds of being diagnosed with breast cancer (Sun et al., 2017). One factor is age because all cancers risk increases as you age (Sun et al., 2017). Also, beginning your period at a younger age (<12 years), beginning menopause at an older age, having your first child at an older age (>30 years), and never being pregnant increases the probability of developing breast cancer (Sun et al., 2017). Being obese, drinking alcohol, and having a personal and family history of breast cancer increases the risk of developing breast cancer (Sun et al., 2017). Interestingly, BRCA genes, under normal conditions, are tumor suppressor genes involved in regulating the growth of breast and other types of cells. Mutations in BRCA1 and BRCA2 genes increase your risk of developing breast cancer by up to 72% (Sun et al., 2017). Despite this, having one or even several

breast cancer risk factors doesn't necessarily mean you'll develop breast cancer (Sun et al., 2017).

There are many changes that any woman and man can make in their life to reduce the risk of developing breast cancer. After 20 years old, breast self-exams should be done monthly (Kolak et al., 2017). Other ways to reduce the risk of breast cancer are to perform exercise most days of the week and control everything we consume (Kolak et al., 2017). Examples are reducing alcohol intake and maintaining a healthy diet based on fruits, vegetables and legumes (Kolak et al., 2017). Also, the best-known way to save lives is early detection. Mammography is one of the most common early detection methods. Despise this, mammography do not prevent the development of breast cancer.

The earliest descriptions of breast cancer dates back to 3,000 B.C. (Britt, 2021; Goldman, 2020; Lukong, 2017). Since that time, theories have developed to try to explain the causes of breast cancer (Britt, 2021; Lukong, 2017). The first theory was the humoral theory developed by Hippocrates (460 B.C.) (Britt, 2021; Lukong, 2017).This theory establishes that the body consists of four humors, and an imbalance of these humors induces diseases or even death (Britt, 2021; Lukong, 2017). Also, an excess of black biles (one of the humors) could cause breast tumors (Britt, 2021; Lukong, 2017). Then, in 168 B.C., the Galenic humoral theory (generated by Galen) was developed, which is the same Hippocrates humoral theory but suggests a treatment like a form of lumpectomy in which an incision was made around the tumor and the entire mass was removed (Lukong, 2017). Also, Galen suggests using opium, castor oil, licorice, and sulfur as

medication (Lukong, 2017). These new recommended treatments arose since the Roman physicians in the first century crudely excised affected breasts with a hot cautery in a procedure that sometimes removed the pectoralis muscles (Lukong, 2017). In the 1500s, two doctors created the infectious disease theory, which proposed that cancer was contagious (Britt, 2021). Then, in the ~1600s, a new theory called the lymphatic theory was proposed, the lymphatic theory replaced the humoral theory and suggested that the lymphs formed cancer (Britt, 2021; Lukong, 2017). Finally, in 1838, the blastema theory replaced lymphatic theory, proposing that cancer consists of cells and cancerous cells derived from other cells (Britt, 2021; Lukong, 2017).

Since the ~1880s, various methods or treatments have been developed to detect breast cancer and treat breast cancer patients. The first method developed to treat breast cancer was the radical mastectomy performed by William Halstead in 1882 (Britt, 2021; Goldman, 2020).Thirteen years later, the first x-ray was taken, which facilitated the development of mammograms to detect this disease (Britt, 2021; Goldman, 2020). In 1937, radiation therapy was used in addition to surgery by the recommendation of Sir Geoffrey Keynes (Britt, 2021; Goldman, 2020).

After determining the role of estrogen and HER2 receptors in breast cancer progression, scientists developed various drugs which modulated or regulated the receptor or its ligand (targeted therapies). The first antiestrogen drug approved by the Food and Drug Administration (FDA) as a breast cancer treatment was Tamoxifen (Nolvadex) in 1978 (Britt, 2021; Goldman, 2020). Then, in 1998, the National Surgical Adjuvant Breast and Bowel Project Breast Cancer Prevention

Trial showed that Tamoxifen decreases the risk of developing breast cancer in at-risk women by 50 percent (Britt, 2021; Goldman, 2020). Also, the second treatment approved by the FDA was anastrozole (Arimidex) which blocks the production of estrogen (Britt, 2021; Goldman, 2020). Since 1984 researchers discovered that overexpression of HER2 is related to breast cancer aggressiveness. In 1998 the FDA approved the third drug Trastuzumab (Herceptin) (Britt, 2021; Goldman, 2020). Herceptin is a drug that targets cancer cells that overexpress HER2 (HER2-positive) (Britt, 2021; Goldman, 2020). Also, the FDA approved ado-trastuzumab emtansine (T-DM1) in 2013 and Enhertu in 2019 (Britt, 2021; Goldman, 2020). Both approved drugs proved to be an effective treatment for HER2-positive breast cancer patients (Britt, 2021; Goldman, 2020). In 2020, the FDA approved Trodelvy, a drug for treating metastatic triple-negative breast cancer (Britt, 2021; Goldman, 2020).

Once scientists developed some of the targeted therapies, experts established molecular or intrinsic subtypes of breast cancer: Luminal A, Luminal B, Normal-like, HER2-enriched, and Triple-Negative/Basal-like (Figure 1) (Britt, 2021; Eliyatkın et al., 2015; Feng et al., 2018; Goldman, 2020; Nascimento & Otoni, 2020; Yersal & Barutca, 2014). The breast cancer classifications allowed targeted therapies to be a specific treatments depending on the molecular subtype (Table 1). In other words, targeted therapies are therapies against particular receptors used to develop the molecular subtype classification. Around 75% of breast cancers are positive or express both the estrogen-receptor (ER) and the progesterone-receptor (PR) (Yersal & Barutca, 2014), and express genes that

encode proteins of luminal epithelial cells (Yersal & Barutca, 2014). Thus, tumors that express these receptors and molecular markers are called luminal groups consisting of two subclasses, Luminal-A and Luminal-B (Yersal & Barutca, 2014). Luminal-A is the most common subtype and is defined by an absence in the overexpression of HER2, low Ki67 (proliferation cell nuclear antigen), and has a good prognosis (Figure 1 and Table 1) (Eliyatkın et al., 2015; Nascimento & Otoni, 2020; Yersal & Barutca, 2014). In contrast, Luminal-B affects around ~20% of breast cancers and has a higher expression of Ki67 (Figure 1 and Table 1) (Feng et al., 2018; Nascimento & Otoni, 2020; Yersal & Barutca, 2014). Also, this molecular subtype could be HER2 positive or negative and has an overall worse prognosis (Eliyatkın et al., 2015; Feng et al., 2018; Nascimento & Otoni, 2020; Yersal & Barutca, 2014). Similar to Luminal-A, the Normal-like subtype can express ER and PR, low levels of Ki67, and is HER2 negative (Figure 1 and Table 1) (Feng et al., 2018). Even though the normal-like subtype has a good prognosis, it is worse compared to Luminal-A (Feng et al., 2018). HER2-enriched is another molecular subtype characterized by an overexpression of HER2 and the absence of ER and PR (Figure 1 and Table 1) (Eliyatkın et al., 2015; Feng et al., 2018; Nascimento & Otoni, 2020; Yersal & Barutca, 2014). In addition, it has a worse prognosis, and the cancer cells have a higher proliferation compared to the luminal group (Feng et al., 2018; Yersal & Barutca, 2014). Breast cancer patients with Luminal-A, Luminal-B, and Normal-like have two treatment options: hormonal and targeted therapies (Feng et al., 2018). Tamoxifen is one targeted therapy administered to Luminal-A, Luminal-B, and Normal-like breast cancer patients

(Table 1). HER-2 enriched breast cancer patients can receive targeted therapies such as Trastuzumab (Herceptin) (Table 1) (Feng et al., 2018). The molecular subtype, Triple-negative/Basal-like, is diagnosed at a younger age and women with BRCA1 gene mutation have a higher risk of developing this subtype (Eliyatkın et al., 2015; Feng et al., 2018). It's the most aggressive molecular subtype and is characterized by a lack of ER, PR, and HER2 protein expression (Table 1 and Figure 1) (Eliyatkın et al., 2015; Feng et al., 2018; Nascimento & Otoni, 2020; Yersal & Barutca, 2014). Also, triple-negative/Basal-like overexpress the epidermal growth factor receptor (EGFR) and has frequent mutations in p53 tumor protein (Eliyatkın et al., 2015; Yersal & Barutca, 2014). The study presented here focuses mainly in triple-negative breast cancer (TNBC) which has fewer effective treatments than the other subtypes due to the lack of estrogen (ER), progesterone (PR) and HER2 receptors to make hormone therapy or targeted HER2 drugs work. The treatment options are limited and include standard chemotherapy, surgery and/or radiation when it has not metastasize. If TNBC has spread to other parts of the body, therapies such as platinum drugs, PARP inhibitors or immunotherapy might be considered. This gap in effective therapies for TNBC stress out the importance of identifying druggable targets and characterize novel targeted therapies.

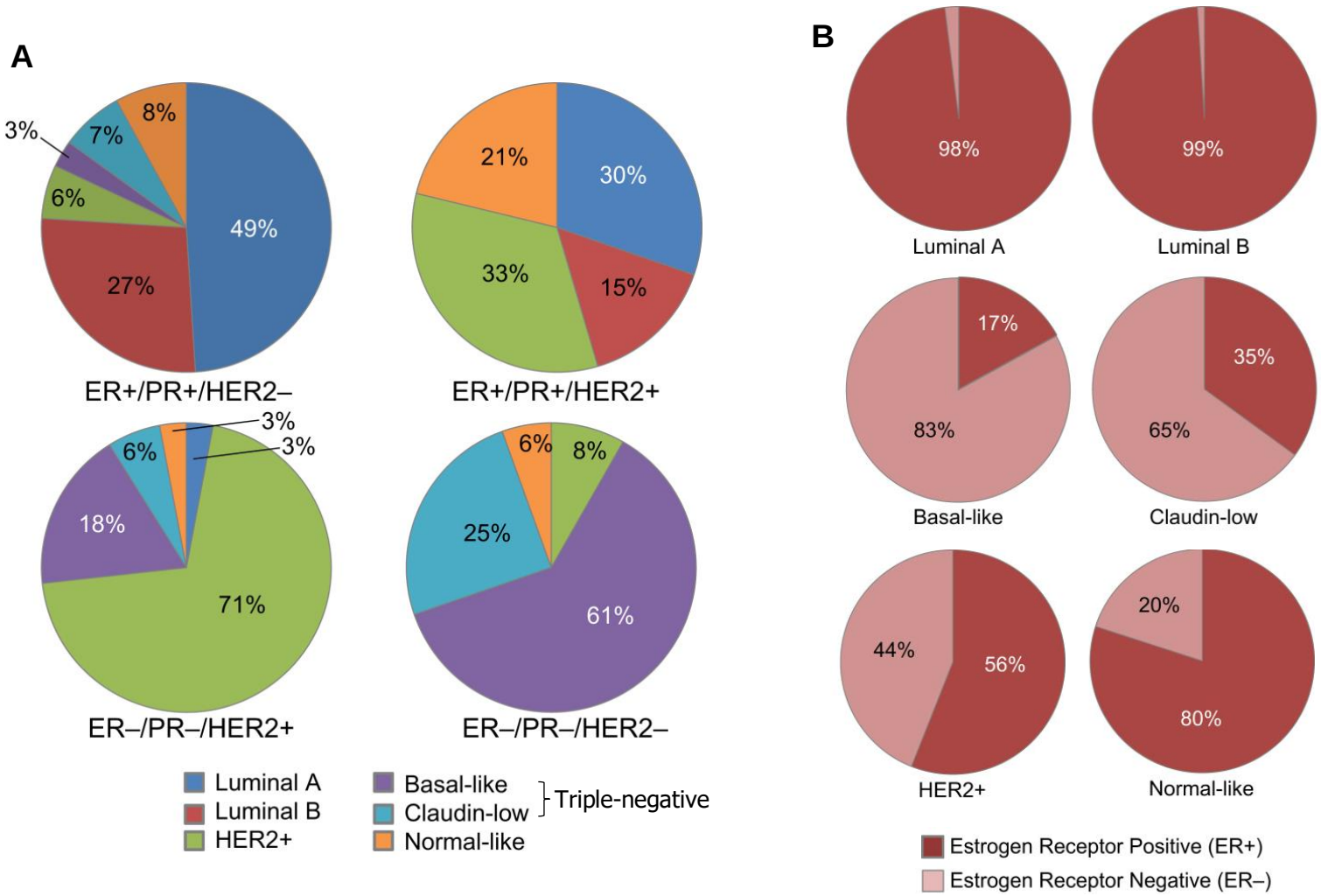

Figure 1. Breast cancer molecular subtypes. Expression of estrogen (**A and B**), progesterone (**A**) and HER2 (**A**) receptors in the breast cancer molecular subtypes. Modified from (Rivenbark et al., 2013).

Table 1: Molecular or intrinsic breast cancer subtypes

	Molecular signatures	Incidence in all the breast cancer	Other characteristics	Examples of targeted therapies	References
Luminal-A	ER + PR + HER2 -	~40%	• Low Ki67 • Good prognosis	• SERM (Tamoxifen) • SERD (Fulvestrant) • Aromatase inhibitor (Anastrozole)	(Yersal & Barutca, 2014) (Feng et al., 2018) (Eliyatkın et al., 2015) (Nascimento & Otoni, 2020)
Luminal-B	ER + PR + HER2 +/-	~20%	• High Ki67 • Intermediate prognosis • Most aggressive form of ER+	• SERM (Tamoxifen) • SERD (Fulvestrant)	(Yersal & Barutca, 2014) (Feng et al., 2018) (Eliyatkın et al., 2015) (Nascimento & Otoni, 2020)
Normal-like	ER + PR + HER2 -	Rare	• Low Ki67 • Good prognosis	• SERM (Tamoxifen)	(Yersal & Barutca, 2014) (Feng et al., 2018) (Eliyatkın et al., 2015) (Nascimento & Otoni, 2020)
HER2-enriched	ER - PR - HER2 +	~15%	• High Ki67 • Poor prognosis • Propensities to metastasis • 40% have p53 mutations	• Herceptin • Kinase inhibitor (Lapatinib)	(Yersal & Barutca, 2014) (Feng et al., 2018) (Eliyatkın et al., 2015) (Nascimento & Otoni, 2020)
Triple-negative/Basal-like	ER + PR + HER2 -	~20%	• High Ki67 • Poor prognosis • Frequent p53 mutations • Associated with BRCA1 mutations • Prevalent in young women • Low expression of cellular junction proteins	-	(Yersal & Barutca, 2014) (Feng et al., 2018) (Eliyatkın et al., 2015) (Nascimento & Otoni, 2020)

1.2 Inflammatory Breast Cancer

Inflammatory Breast Cancer (IBC) is the most aggressive and lethal breast cancer subtype. It affects approximately 2 to 4% of all breast cancer patients and accounts for 7% of all breast cancer–related deaths in the United States (George Somlo, 2018; Menta et al., 2018). Interestingly, based on the molecular breast cancer subtypes, 40% and 30% of IBC are classified as HER-2 positive and TNBC, respectively (Menta et al., 2018). The incidence of IBC cases that express hormone receptors is relatively lower than the other molecular subtypes (Menta et al., 2018). African American, Hispanic American/Latina, and American Indian/Alaskan women are more likely to develop this type of breast cancer (Dushkin & Cristofanilli, 2011; George Somlo, 2018; van Uden et al., 2015). It is also more prevalent in young women and is associated with a high body mass index (Dushkin & Cristofanilli, 2011; van Uden et al., 2015). Based on race, Hispanic women had the youngest mean age of onset of 50.5 years as compared to a mean of age of onset of 55.2 years for African American women and 58.1 years for Caucasian women (van Uden et al., 2015). Generally, IBC patients have a significantly shorter median survival time (2.9 years or 33 months) (George Somlo, 2018; Rosenbluth & Overmoyer, 2019). Nevertheless, the median survival for African American women is 33.2 months, and 43.1 months in Hispanic American women (George Somlo, 2018). Interestingly, American Indian/Alaskan women and Asian American women have the lowest (24.8 months) and highest (49.7 months) median survival, respectively (George Somlo, 2018). Unfortunately, African American and Hispanic/Latin ethnicity correlate with socioeconomic status,

which implies they are less likely to get an adequate screening of diverse diseases such as breast cancer and have limited access to care and treatment.

IBC has a distinct clinical presentation that makes it hard to get a correct diagnosis, such as enlargement or inflammation of the breast (sometimes increasing in size 2-3 fold within a few weeks) and itchiness (Dushkin & Cristofanilli, 2011). Other symptoms are "peau-d'orange" erythema, and edema caused by the blockage of lymph vessels by diffusion of tumor cell clusters called tumor emboli, one of the hallmarks of IBC (Dushkin & Cristofanilli, 2011; Menta et al., 2018; van Uden et al., 2015; Yamauchi et al., 2012). Also, it is thought that tumor emboli are responsible for its aggressive and rapid metastasis phenotype (Vermeulen et al., 2010). Based on the absence of a palpable tumor mass, unfortunately, these symptoms can be easily confused with a breast infection, dermatitis or mastitis, producing a delay in proper diagnosis (Dushkin & Cristofanilli, 2011; Menta et al., 2018; van Uden et al., 2015; Yamauchi et al., 2012). Also, IBC tumor emboli are difficult to detect in a mammogram, detecting only 43% of primary lesions (Dushkin & Cristofanilli, 2011; Menta et al., 2018). Better detection alternatives include breast MRI and molecular breast imaging (MBI) that show higher sensitivity in the detection of IBC (Dushkin & Cristofanilli, 2011; Menta et al., 2018).

There is a myth that breast cancer only affects women. It is even socially inconceivable to think that a man needs a mammography if he has a high risk of developing breast cancer. Although rare, breast cancer can occur in men especially in those individuals with a family history of breast cancer or hereditary

breast cancer syndrome (Tanhueco & Youssef, 2021). Moreover, IBC can also occur in men, but diagnosis may be missed and often delayed (Tanhueco & Youssef, 2021). Interestingly, there is a poor prognosis for male patients with IBC (Hyakudomi et al., 2013). Scientists thought this occurred because IBC in males tends to be triple-negative (Hyakudomi et al., 2013). For these reasons stated above and in addition to the lack of knowledge/understanding of IBC in males, there is an urgent need to identify and characterize pathways that are deregulated in IBC that will help us develop novel effective treatments for this disease (Tanhueco & Youssef, 2021).

1.2.1 Inflammatory Breast Cancer Therapies

IBC patient's treatment is a trimodality therapy, which includes upfront systemic therapy, chemotherapy, total mastectomy, axillary lymph node dissection, radiation to the chest wall, and regional draining of lymph nodes (Figure 4) (Hester et al., 2021; Rosenbluth & Overmoyer, 2019). Regardless of the molecular subtype, IBC patients are first treated with chemotherapy such as anthracycline or taxane as a neoadjuvant treatment (chemotherapy before surgery) (AmericanCancerSociety, 2021; Menta et al., 2018). This neoadjuvant treatment can be combined with hormone, targeted, or immunotherapy depending on the molecular subtype (AmericanCancerSociety, 2021). The purpose of this treatment (pre-operative treatment) is to convert the IBC into a disease that can be removed by surgery, help reduce the size of a tumor and control the microscopic metastasis (AmericanCancerSociety, 2021; Rosenbluth & Overmoyer, 2019; Selli & Sims, 2019). The combination of treatments given varies depending on the

molecular subtype of breast cancer. Patients with IBC that express the hormone receptors can be treated with a combination of standard chemotherapy with hormone and targeted therapy as a neoadjuvant treatment (AmericanCancerSociety, 2021). HER2-positive IBC patients can combine chemotherapy with targeted therapy drugs such as trastuzumab (Herceptin) and pertuzumab (Perjeta) (AmericanCancerSociety, 2021; Rosenbluth & Overmoyer, 2019). Interestingly, there are no effective targeted therapeutics for triple-negative IBC (TN-IBC) patients (Table 1) (Dawood et al., 2011; Li et al., 2011; Masuda et al., 2013). Despite this, an immunotherapy drug (pembrolizumab) combined with chemotherapy can be administrated to TN-IBC patients (AmericanCancerSociety, 2021). Furthermore, if cancer advances after chemotherapy or neoadjuvant treatment, IBC patients could receive breast radiation (AmericanCancerSociety, 2021) as a source of therapy.

Surgery is the next step for IBC patients' treatment (AmericanCancerSociety, 2021). Breast-conserving surgery cannot be performed for these patients since this cancer has substantial lymph node involvement and clusters of cells without a demarcated tumor (AmericanCancerSociety, 2021). Unfortunately, regardless of the molecular subtype, surgeons must perform a complete mastectomy to remove the entire breast and lymph nodes under the arm (Figure 2) (AmericanCancerSociety, 2021; Rosenbluth & Overmoyer, 2019). After surgery and depending on the amount of cancer tissue found in the breast, IBC patients with cancer cells that express hormone receptors could receive chemo, targeted, and hormone therapy as adjuvant treatment (treatment given after the

primary treatment) (Figure 4) (AmericanCancerSociety, 2021). Also, the oral chemotherapy capecitabine (inhibitor of DNA synthesis and reduced tumor growth) could be prescripted for triple-negative IBC patients (AmericanCancerSociety, 2021; Arora et al., 2017). For HER2-positive patients, trastuzumab, pertuzumab, and ado-trastuzumab emtansine could be prescribed (AmericanCancerSociety, 2021). Finally, if breast radiation is not given before surgery, the radiation is given as adjuvant therapy to lower the chance of the cancer coming back (AmericanCancerSociety, 2021). Despite all the treatments administrated or performed to improve the prognosis of IBC patients, nearly 50% of patients die of metastatic disease (Arora et al., 2017).

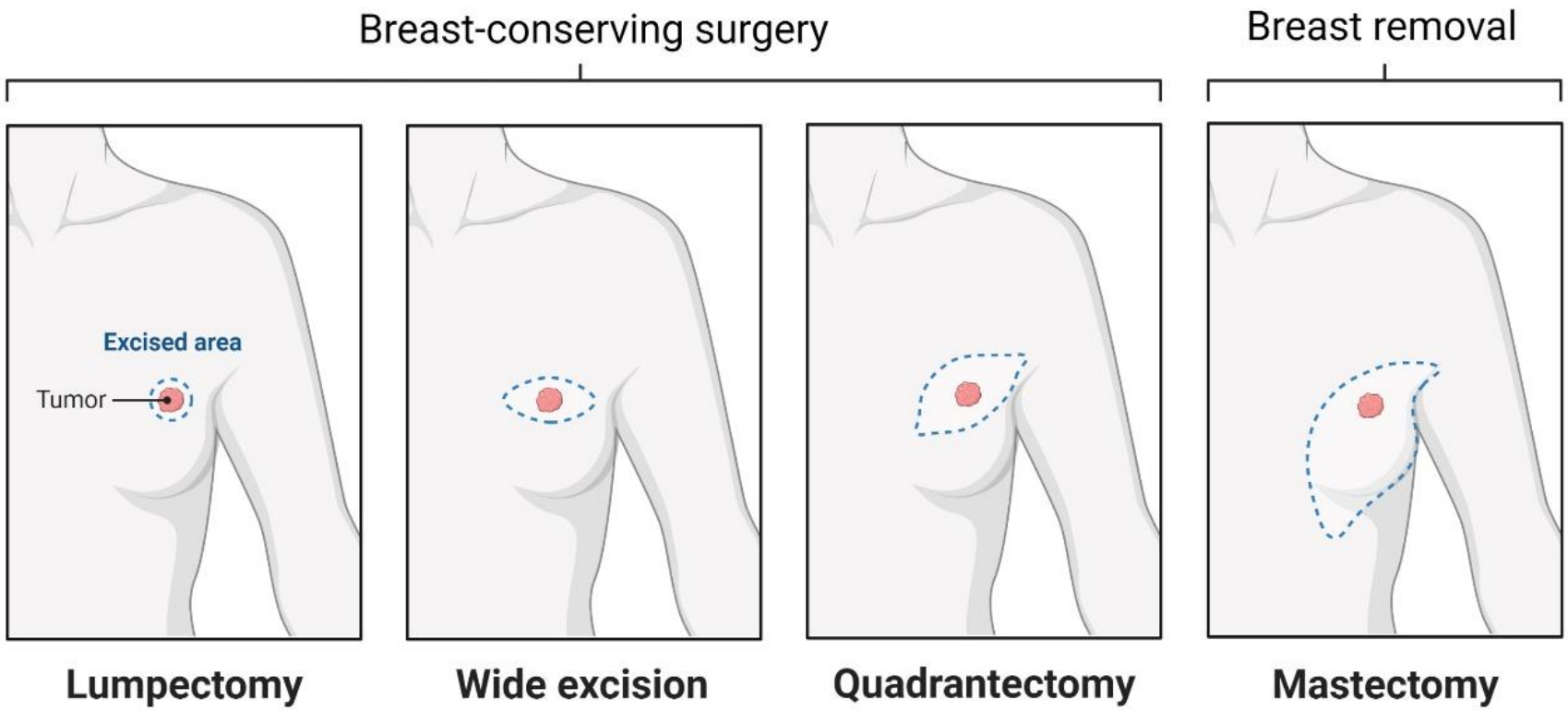

Figure 2. Type of breast cancer surgeries. (Adapted from “Breast Cancer Surgery Types”, by BioRender.com)

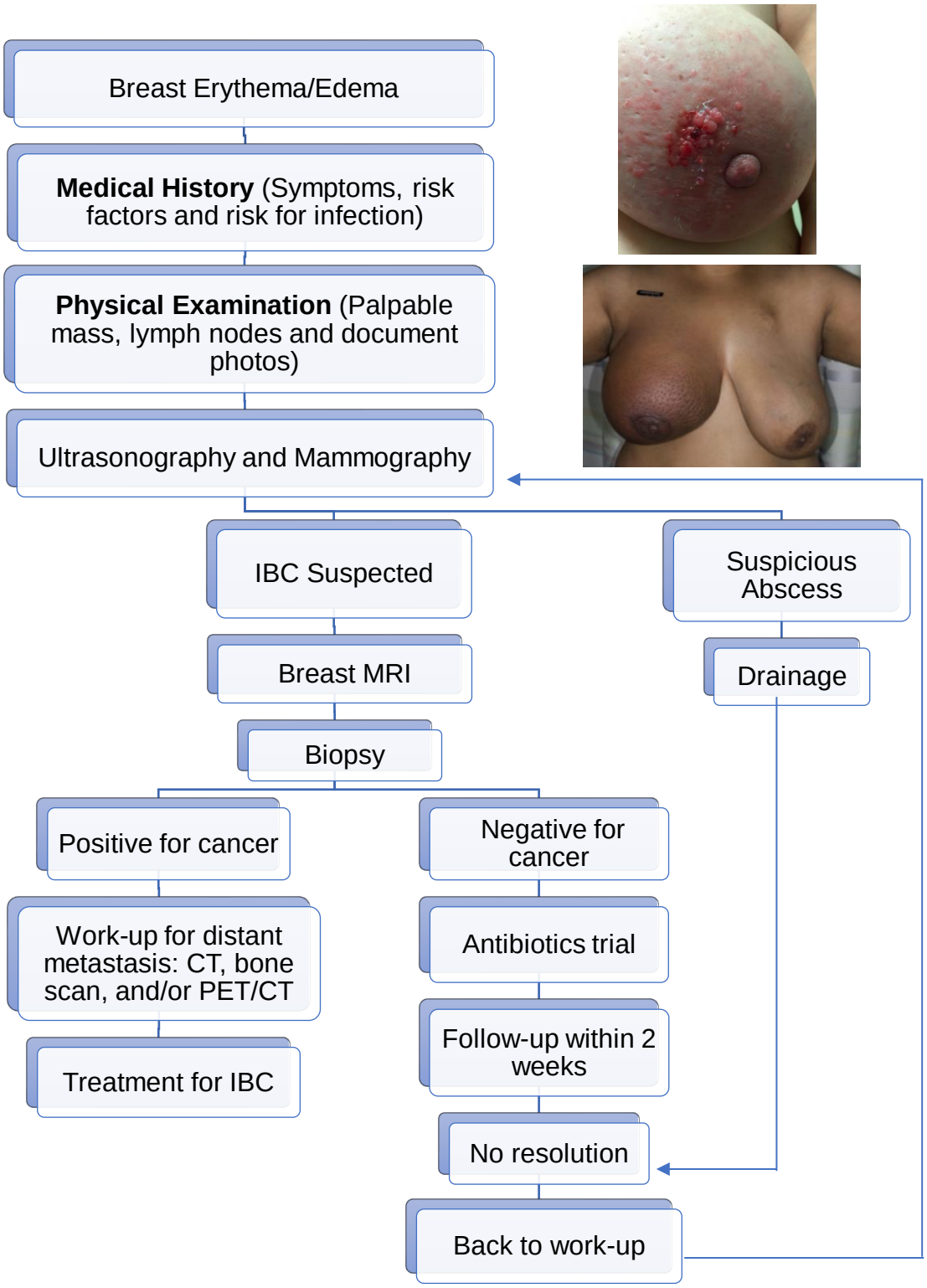

Figure 3. Examination for IBC patients. (George Somlo, 2018; Menta et al., 2018; Yamauchi et al., 2012)

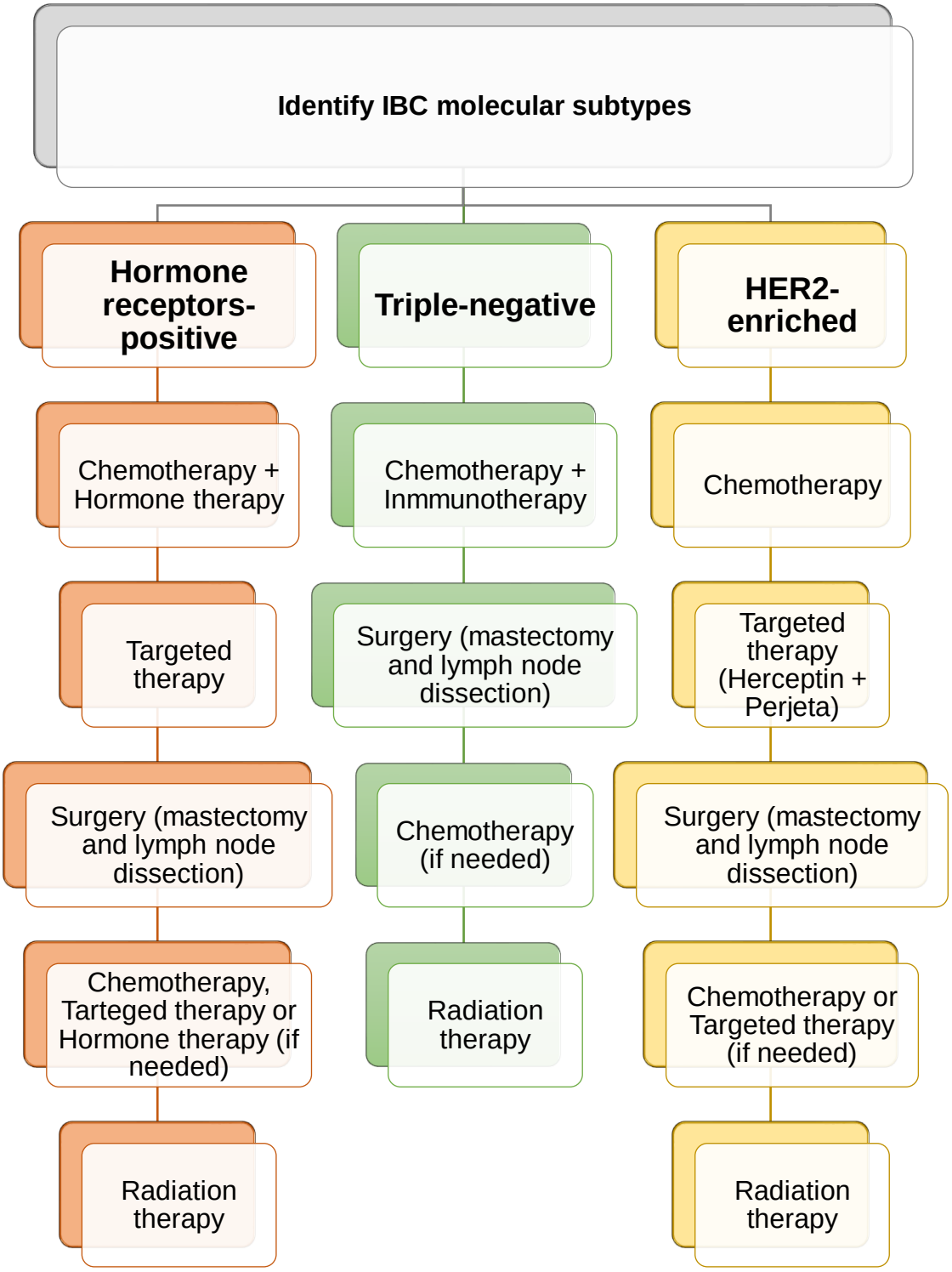

Figure 4. Treatments for IBC patients. (AmericanCancerSociety, 2021)

1.2.2 Estrogen Non-genomic Signaling in Triple-Negative Breast Cancer

Around half of diagnosed IBC cases are classified as triple-negative (TN-IBC), meaning they lack expression of hormonal receptors: canonical estrogen receptor alpha 66 (ER-α66), progesterone receptor (PR), and amplification of the human epidermal growth factor receptor 2 (HER2). Interestingly, a recent study demonstrated that TN-IBC cell lines express alternate estrogen receptors such as estrogen receptor alpha 36 (ER-α36) and GPR30 (Ohshiro et al., 2012).

ER-α36 is a 36kDa novel variant of ER-α66 (Figure 5). It's highly expressed in the majority of ER-α66 negative breast cancer cell lines but is also expressed in ER-α66 positive breast cancer cell lines (Gu et al., 2014; Rao et al., 2011; Su et al., 2014; Wang & Yin, 2015). ER-α66 mRNA encodes for 595 amino acids, resulting in a protein with a molecular weight of 66kDa. ER-α36 transcript is directly spliced into exon 2–6 of the ER-α66 gene regulated by an unidentified promoter located in the first intron of the ER-α66 gene (Figure 5) (Su et al., 2014). The last 138 amino acids encoded by the final exon seven and exon eight are replaced by an unique 27-amino-acid sequence at C-terminus (Figure 5) (Gu et al., 2014). Compared to ER-α66, ER-α36 lacks both transactivation domains, AF-1 and AF-2, but retains the DNA-binding domains (Figure 5) (Gu et al., 2014; Rao et al., 2011; Su et al., 2014; Wang & Yin, 2015). Also, it retains protein dimerization domains and can form heterodimers with ER-α66 or ER-β (Wang & Yin, 2015). Interestingly, ER-α36 responds to E2α, E2β, E3, E4, and even tamoxifen, an estrogen antagonist (Su et al., 2014).

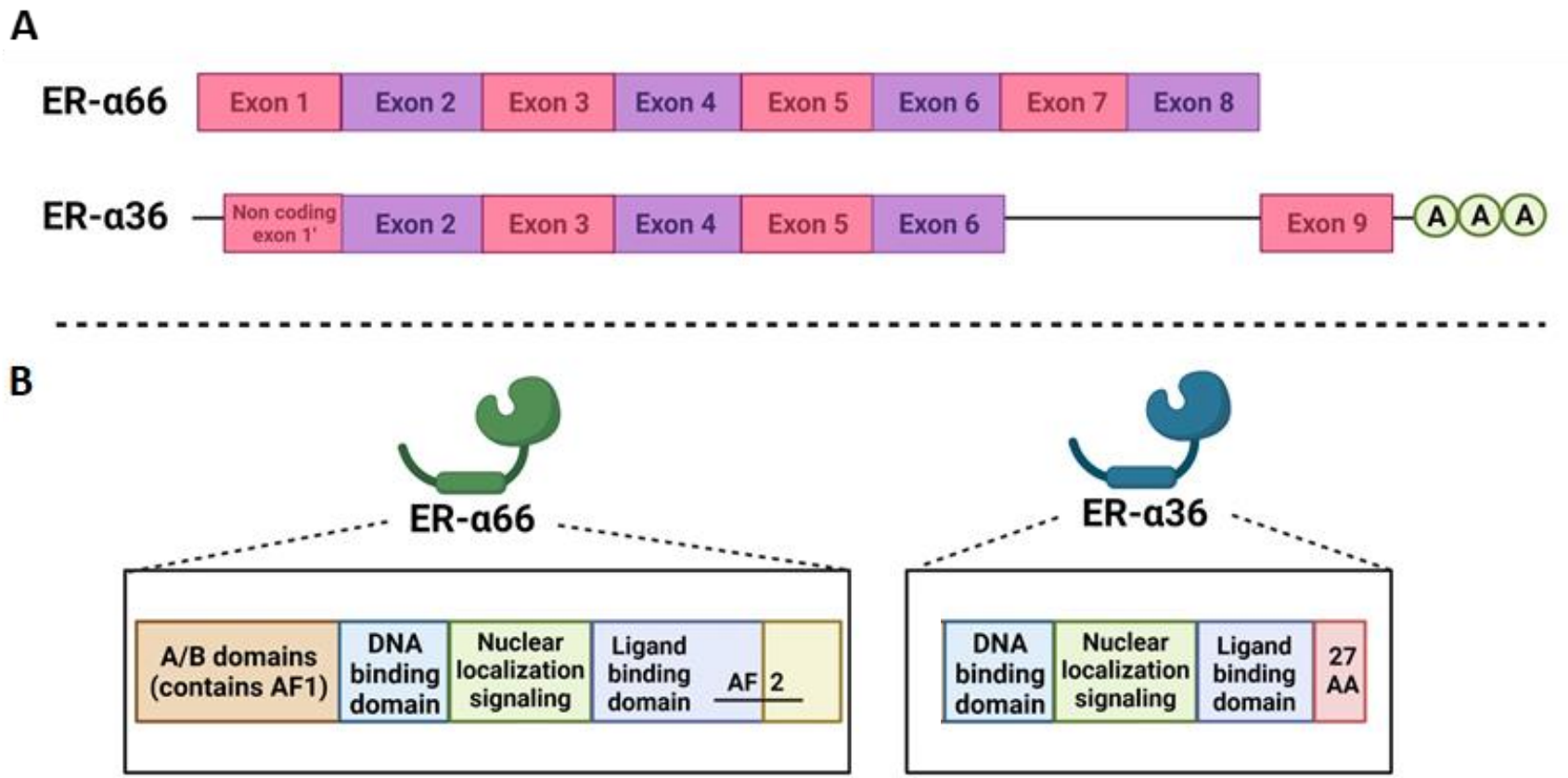

Figure 5. Similatiries and differences between estrogen alpha 66 (ER-α66) and estrogen alpha 36 (ER-α36) receptors. ER-α36 is an splice variant of ER-α66. **(A)** ER-α36 transcript is directly spliced into exon 2–6 of the ER-α66 gene because it has a non-coding exon (exon 1'). Also, it has a unique C-terminal 27 amino acid domain. **(B)** Compared to ER-α66, ER-α36 lacks both transactivation domains, AF-1 and AF-2, but retains the DNA-binding domain, nuclear localization signaling and ligand-binding domain. (Gu et al., 2014) (Created with BioRender.com)

Tamoxifen is an adjuvant targeted therapy for ER-positive breast cancer cell lines because it blocks the ligand-binding site of ER-α66 and its genomic signaling pathway (Gu et al., 2014; Su et al., 2014). Despite the similarities between ER-α66 and ER-α36, studies showed that ER-α36 has resistance to the targeted therapies designed against ER-α66 (Figure 6). A study in cells lacking ER-α66 expression showed that tamoxifen binds to ER-α36 to enhance nuclear translocation and induces stem cell-like properties by increasing the expression of the stem-cell marker ALDH1 (Wang et al., 2018). ALDH1 is involved in the proliferation and metastasis of breast cancer stem cells (Wang et al., 2018). Thus, tamoxifen therapy promotes breast cancer metastasis and proliferation via activation of ER-α36 and its non-genomic mechanisms, which implies that tamoxifen functions as an agonist of ER-α36 to promote the stemness of breast cancer stem cells (Wang et al., 2018). Also, the literature suggests ER-α36 is not only involved in de novo non-genomic activities providing resistance to targeted therapies like tamoxifen but promotes their agonist activity (Gu et al., 2014; Kang et al., 2010).

Another targeted therapy available for ER-positive breast cancer patients is fulvestrant (ICI182,780). Fulvestrant binds to ER-α66 to impair its dimerization and nuclear localization (Gu et al., 2014; Su et al., 2014). Interestingly, fulvestrant accelerates the degradation of ER-α66 without any reduction of ER-α66 mRNA, but it fails to induce degradation of ER-α36 (Figure 6) (Gu et al., 2014; Su et al., 2014). A possible explanation is that ER-α36 has a truncated ligand-binding domain lacking the helix 9–12 of ER-α66 (Gu et al., 2014; Su et al., 2014). The helix 12 is essential for protein degradation induced by fulvestrant (Gu et al., 2014).

Aromatase inhibitors (anastrazole and letrozole) are endocrine treatments that block the aromatase enzyme to repress the levels of estrogen (E2) (Gu et al., 2014; Kang et al., 2010). Interestingly, cells with a high expression of ER-α36 can respond to a very low concentration of E2, which means that they induce estrogen hypersensitivity (Figure 6) (Gu et al., 2014; Kang et al., 2010). Therefore, this estrogen hypersensitivity in ER-negative breast cancer cells is a possible reason for its resistance to aromatase inhibitors treatments such as anastrazole and letrozole (Gu et al., 2014).

In summary, ER-α36 is a variant of ER-α66, but it has different characteristics and functions. In addition, even though both estrogen receptors have similar ligand-binding domains, no targeted therapies have an antagonistic effect against ER-α36. In other words, the expression of ER-α36 induces an agonist instead of antagonist effect upon tamoxifen and fulvestrant treatment (targeted therapies). This implies an urgent need to explore new targeted approaches for ER-negative breast cancer cells treatment.

It is essential to develop research that describes the possible mechanisms by which ER-α36 exerts its carcinogenic activity. These discoveries would help the scientific community to develop ER-α36 inhibitors or therapies against ER-negative and HER2 breast cancer cell lines that express this variant of the estrogen receptors.

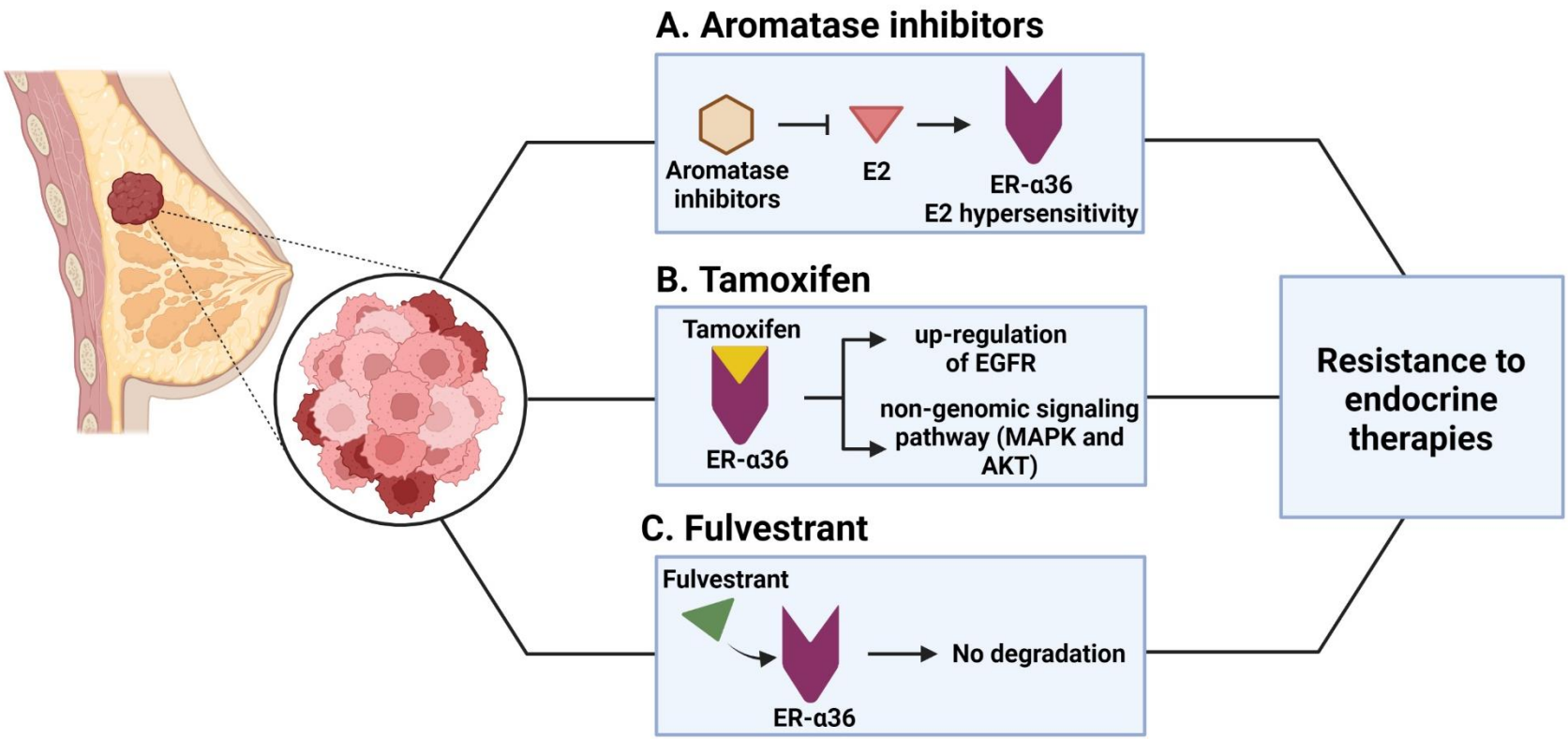

Figure 6. ER-α36 shows resistance to endocrine therapies. **(A)** High expression of ER-α36 induces estrogen hypersensitivity of the receptor. This hypersensitivity could explain the failure of aromatase inhibitors (AIs). **(B)** Tamoxifen (TAM) has an agonist effect in ER-α36 by upregulating EGFR and promoting the non-genomic signaling pathway (MAPK and AKT kinases). **(C)** Fulvestrant's (ICI 182,780) mechanism of action (degradation of estrogen receptor) fails in ER-α36. (Gu et al., 2014) (Created with BioRender.com)

1.3 Estrogen Non-Genomic Signaling Pathway

The estrogen non-genomic signaling pathway refers to the estrogen binding to estrogen receptors to induce rapid (occurs in seconds to minutes) activation of kinases involved in promoting pro-oncogenic phenotypes (Figure 7). On the contrary, the genomic signaling pathway (occurs in hours to days) is when estrogen binds to ER-α66, then the receptor dimerize and translocate to the nucleus to bind to an estrogen response element (ERE) sequence and act or bind to a transcription factor to regulate the expression of specific target genes (Figure 7) (Wang & Yin, 2015). Therefore, there is a distinct difference between the non-genomic and genomic signaling pathways. The main difference is that the non-genomic pathway could activate more transcription factors because the genomic pathway refers to when the estrogen receptor acts as a transcription factor. Thus, the non-genomic signaling pathway can control more genes that regulate cellular growth, survival, motility, and invasion (Su et al., 2014).

Triple-negative inflammatory breast cancer expresses alternate estrogen receptors (ER-α36 and GPR30) that promote proliferation, migration, and invasion via a non-genomic signaling pathway (MAPK/ERK and PI3K/AKT kinases) upon estrogen treatment (Figure 9) (Ohshiro et al., 2012). The activation of these kinases can induce the expression of the proto-oncogene c-Myc (Su et al., 2014). c-Myc plays a role in cell cycle regulation, metabolism, apoptosis, differentiation, cell adhesion, and tumorigenesis (Su et al., 2014). Also, ER-α36 induces the activation of JNK, which is another member of the MAPK family that regulates differentiation, cell proliferation, and migration (Figure 9) (Gu et al., 2014).

ER-α36 is involved in the cross-activation or phosphorylation of membrane tyrosine kinase receptors, EGFR (Figure 8 and 9) (Gu et al., 2014; Vrtačnik et al., 2014). Interestingly, half of the cases of TN-IBC overexpress EGFR (Table 2) (Masuda et al., 2012). A possible explanation is a positive feedback loop between EGFR and ER-α36 which means that EGFR signaling activates transcription of ER-α36 through an activator-protein-1-binding site (Figure 8) (Su et al., 2014). Also, ER-α36 interacts with the EGFR/Src/Shc complex to stabilize EGFR protein (Figure 8) (Su et al., 2014). Phosphorylation of EGFR promotes the activation of MAPK/ERK and STAT5 (Su et al., 2014). Also, Src/EGFR/STAT5 pathway activates cyclin D1, which is a regulator of cell cycle progression (Gu et al., 2014; Su et al., 2014). These previous findings demonstrated that ER-α36/EGFR complex might be critical in the estrogen non-genomic signaling (Gu et al., 2014).

GPR30 mediates cell proliferation, viability, and motility in TNBCs cell lines, via activation of MAPK/ERK signaling upon treatment with estradiol and GPR30 agonist, G1 (Yu et al., 2014). Also, the high expression of GPR30 has been associated with metastases and poor survival in breast cancer patients (Arias-Pulido et al., 2010). Contradictory, other studies revealed that GPR30 functions as a tumor suppressor for TNBC (Wei et al., 2014). Therefore, those findings demonstrated that the role of GPR30 in TNBCs cell lines through estrogen non-genomic signaling is still not clear (Kang et al., 2010). For example, a study showed that the estrogen non-genomic effects seen after treatment with G1 (GPR30 agonist ligand) were mediated only in the presence of ER-α36, and those effects were abolished when ER-α36 was inhibited (Kang et al., 2010). Also, this study

showed that ER-α36 mediates the estrogen non-genomic signaling independently of GPR30, but GPR30 induces ER-α36 expression (Kang et al., 2010). These findings suggest that the activities of GPR30 in response to estrogen occur through its ability to induce expression of ER-α36 (Kang et al., 2010). Developing antagonist therapies against the oncogenic effects of ER-α36 and GPR30 could be an effective alternative to improve the survival rate of triple-negative breast cancer patients.

Table 2: Molecular signature (several proteins) of inflammatory breast cancer

GENE/PROTEIN	ALTERATION	ROLE OR FUNCTION	REFERENCES
E-CADHERIN	Over-expression	• Tumor emboli • Metastasis • Resistance to chemotherapy	(Ye et al., 2010) (Wang et al., 2017) (Di Bonito et al., 2019)
RHO C GTPASE	Over-expression	• Cytoskeletal reorganization • Regulation of angiogenic growth factors • Production of inflammatory cytokines • Up-regulation of VEGF	(Van der Auwera et al., 2007) (van Golen et al., 1999) (Van Laere et al., 2005) (Di Bonito et al., 2019)
NF-κB	Over-expression	• Hyperactivation of MAPK • Tumor emboli • Pro-inflammatory cytokines	(Van der Auwera et al., 2007) (Arora et al., 2017) (Van Laere et al., 2005) (Di Bonito et al., 2019)
ERBB TYROSINE KINASES (EGFR)	Over-expression	• Activation of NF-kB • Angiogenesis • Uncontrolled growth	(Masuda et al., 2012) (Wang et al., 2017)
WISP3	Loss of expression	• Inhibits angiogenesis and invasion	(Van der Auwera et al., 2007) (Kleer et al., 2002) (Di Bonito et al., 2019)
IGF-1	Alterations	• Pro-inflammatory microenvironment	(Di Bonito et al., 2019)
COX-2	Over-expression	• Tumor extravasation • Mediator of inflammation • Metastasis	(Wang et al., 2017) (Di Bonito et al., 2019)

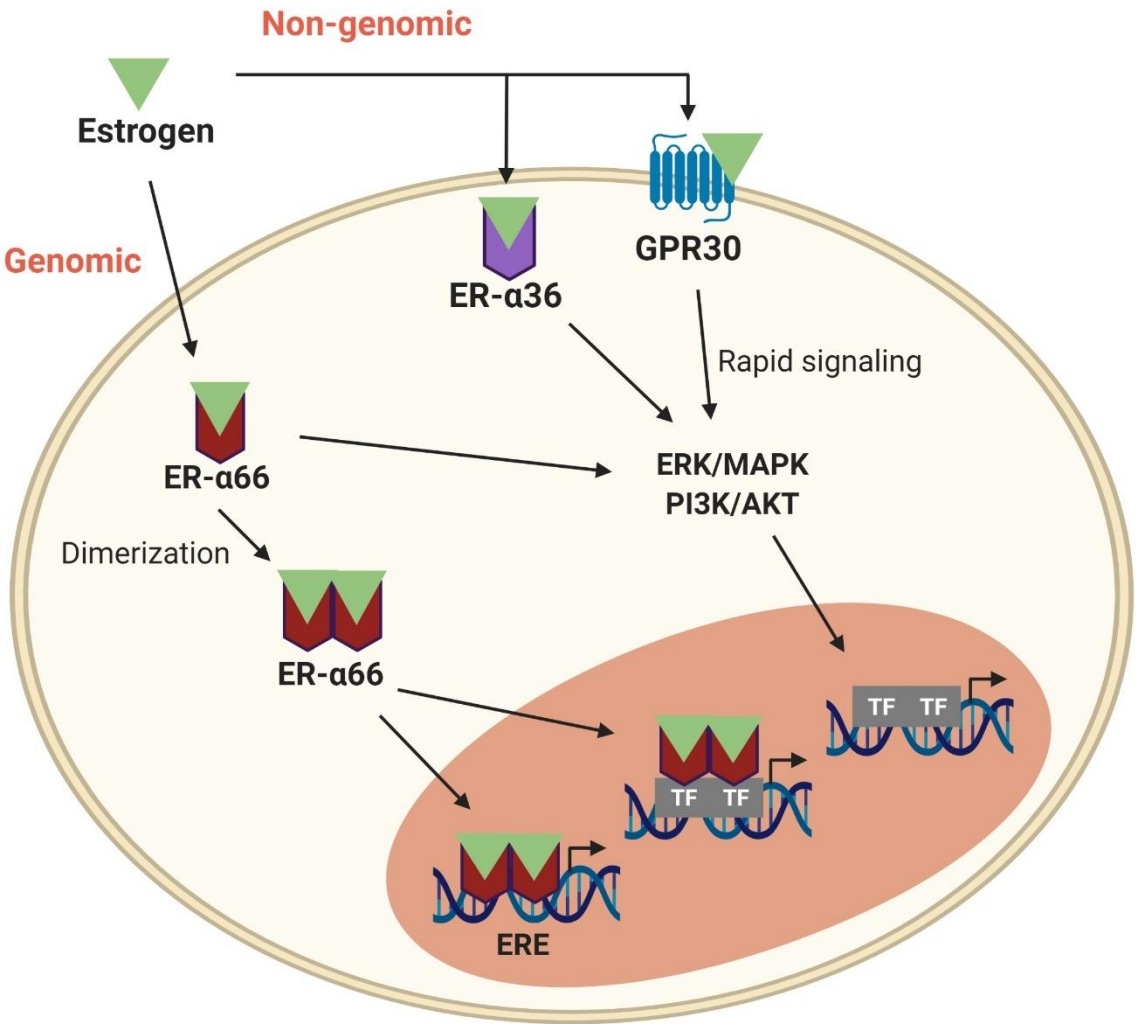

Figure 7. Differences between the estrogen genomic and non-genomic signaling pathways. The genomic signaling pathway shows a dimerization of the estrogen receptors (ER) after estrogen binding and their ability to induce gene expression. The non-genomic signaling pathway shows the rapid signaling that the receptors send to the cytoplasm after estrogen binding. The non-genomic signaling concludes by inducing gene expression. Abbreviations in the figure: (ERE) estrogen responsive elements, and (TF) transcription factor (Słowikowski et al., 2017). (Created with Biorender.com)

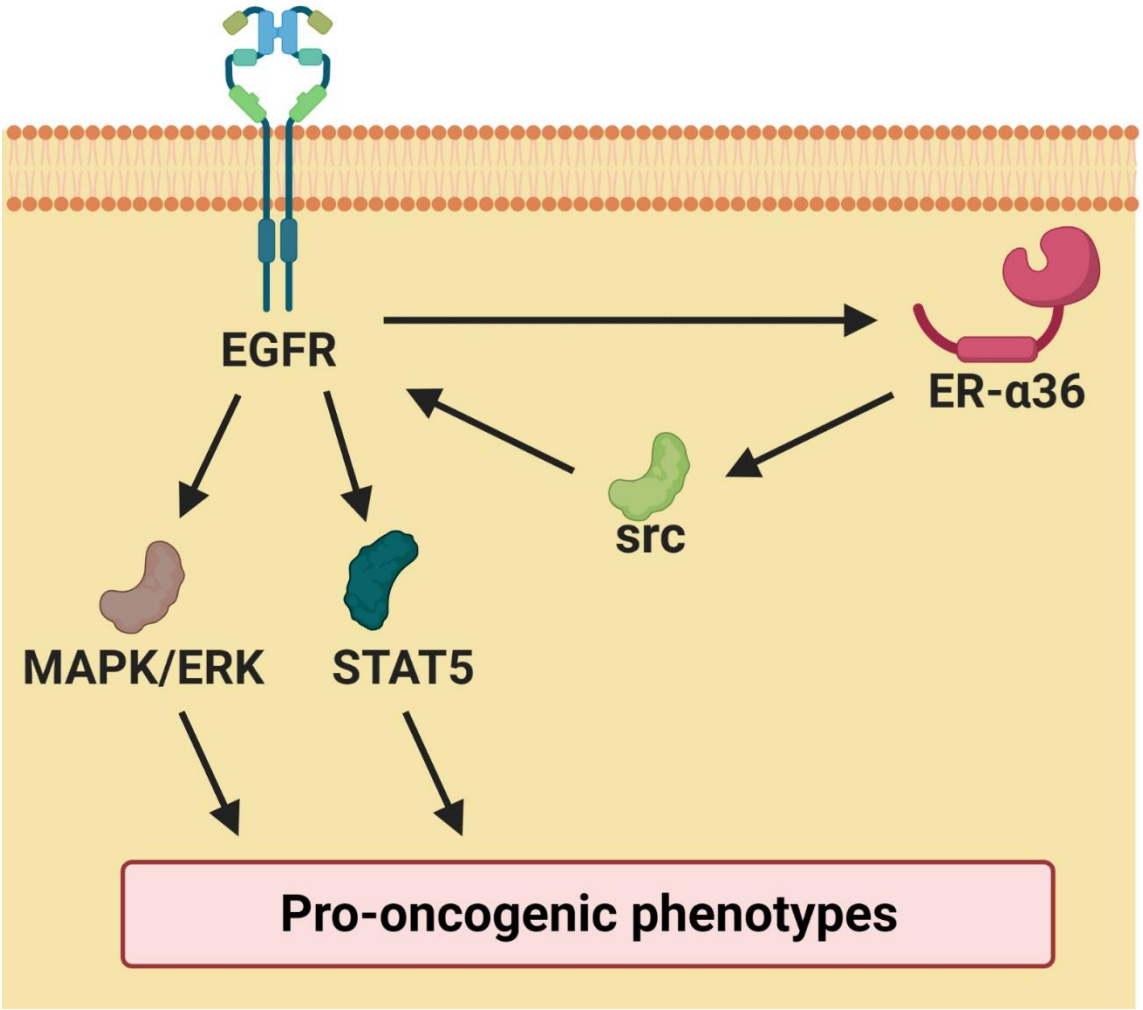

Figure 8. Correlation between EGFR and ER-α36. EGFR induces the activation of ER-α36, which in turn stabilizes the EGFR protein and induces the activation of kinases that promote pro-oncogenic phenotypes (Su et al., 2014). (Created with BioRender.com)

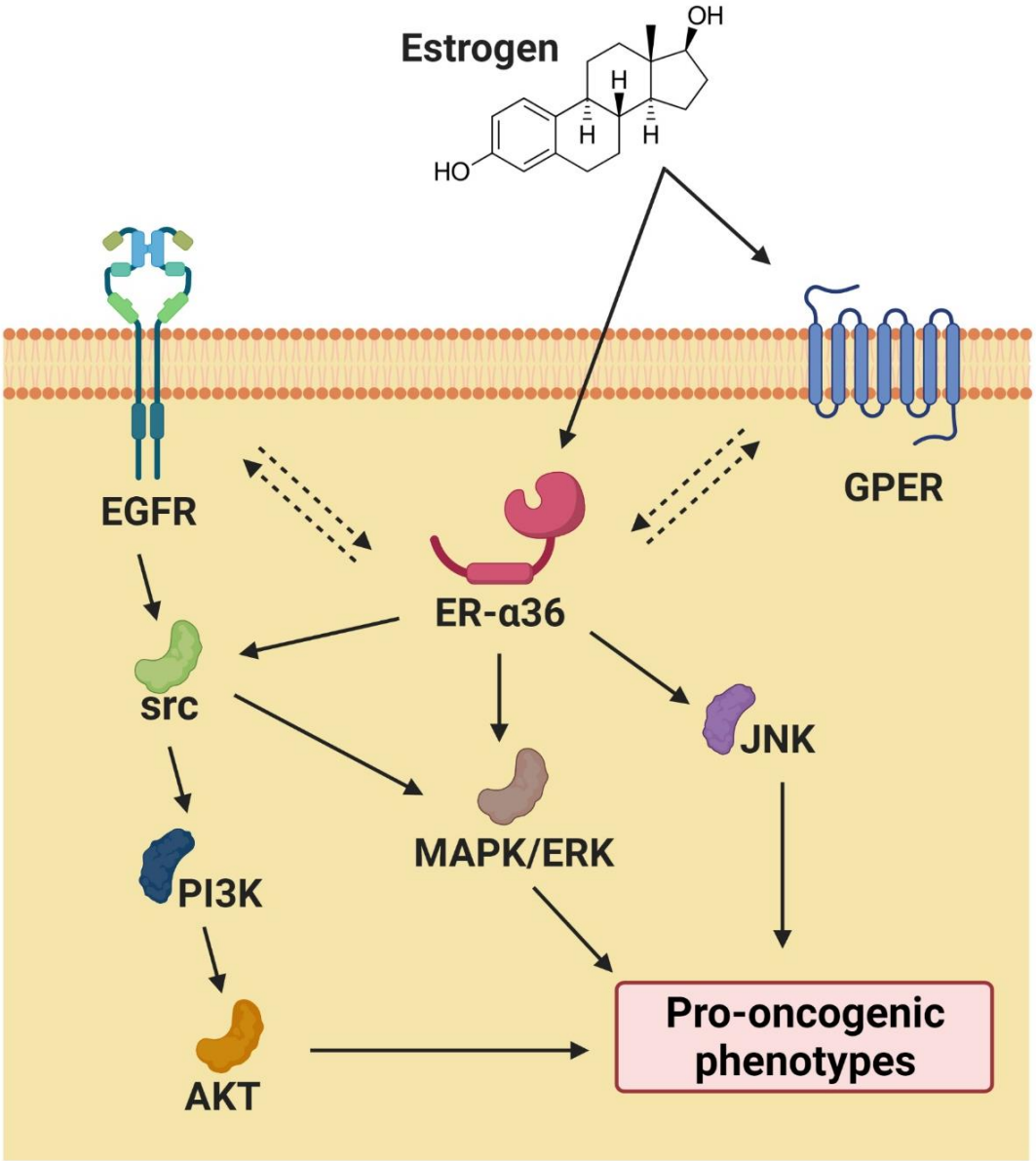

Figure 9. ER-α36 effects in the non-genomic signaling pathway. ER-α36 interacts with the EGFR and GPER receptors and activates diverse kinases that promote pro-oncogenic phenotypes by the non-genomic signaling pathway. (Gu et al., 2014) (Created with BioRender.com)

1.4 Phytoestrogen as a potential therapy

Phytoestrogens are natural substances that exhibit a chemical structure similar to estradiol (E2) (Figure 10) (Basu & Maier, 2018). The phytoestrogen's phenolic rings have a hydroxyl group that corresponds to the hydroxyl groups on the aromatic rings of E2 (Basu & Maier, 2018). Because of this, phytoestrogens can weakly bind to estrogen receptors and compete with estradiol for the ligand-binding domain of said receptors (Basu & Maier, 2018). Also, phytoestrogens induce agonist or antagonist effects depending on their concentration (Basu & Maier, 2018).

The major groups of phytoestrogens are isoflavones, coumestans, stilbenes, and lignans (Figure 10) (Basu & Maier, 2018). The most studied group is the isoflavones particularly, daidzein and genistein (Basu & Maier, 2018; Cos et al., 2003). Isoflavones are founded in soybeans, and their concentration varies depending on the varieties and processing of the soybeans (Table 3) (Cos et al., 2003). Other isoflavones are biochanin A and formononetin, methylated precursors of genistein and daidzein, respectively (Basu & Maier, 2018). Calycosin and glycitein are O-methylated isoflavones (Basu & Maier, 2018). Two members of the stilbenes group are resveratrol and pterostilbene, which are founded in grapes skin, peanuts, and red wine (Table 3) (Basu & Maier, 2018; Cos et al., 2003). Resveratrol is found in red wine since it has been manufactured with prolonged exposure to grape skin (Cos et al., 2003). Also, several scientists believe that resveratrol is the wine component responsible for the French paradox (Cos et al., 2003). The French paradox is the observation of low coronary heart

disease (CHD) death rates despite the high intake of dietary cholesterol and saturated fats (Ferrières, 2004). The lignans phytoestrogens are arctigenin, manassantin A, matairesinol, pharbilignan C, secoisolariciresinol, taiwanin A, and many others (Basu & Maier, 2018). This phytoestrogen type is mainly found in oilseeds, cereals, grains, vegetables, and (Table 3) (Cos et al., 2003). The smallest phytoestrogen group, which this study is focused on, is coumestans which only has coumestrol as a member, and it has been found in alfalfa, soybeans, and clover sprouts (Table 3) (Basu & Maier, 2018; Cos et al., 2003). Interestingly, coumestans exhibit a structure similar to isoflavones (Cos et al., 2003).

Table 3: Dietary sources of phytoestrogens (Basu & Maier, 2018; Cos et al., 2003)

Phytoestrogen	Dietary sources
Isoflavones	• Soybeans and soy products: bean paste, cheese, flakes, flour, milk, sauce, tempeh, tofu, and okara • Other beans: kidney beans, navy beans, and lentils • Sprouts: mung bean sprouts • Legume: red clover
Stilbenes	• Fruits: grapes • Beverage: Red wine • Peanuts
Lignans	• Grains: buckwheat, millet, oat, wheat, brown rice • Nuts: cashew, hazelnut • Seeds: sesame, oilseeds, sunflower, chickpea, pea, soybean • Fruits: apple, banana, cantaloupe, grape, kiwi, lemon, orange, pineapple, red raspberry, strawberry • Vegetables: asparagus, avocado, carrot, cauliflower, cucumber, garlic, onion, potato, and tomato • Beverage: coffee, wine, and tea
Coumestans	• Sprouts: alfalfa, and clover sprouts • Legume: red clover • Vegetables: spinach, Brussel sprouts and broccoli • Beans: mung beans

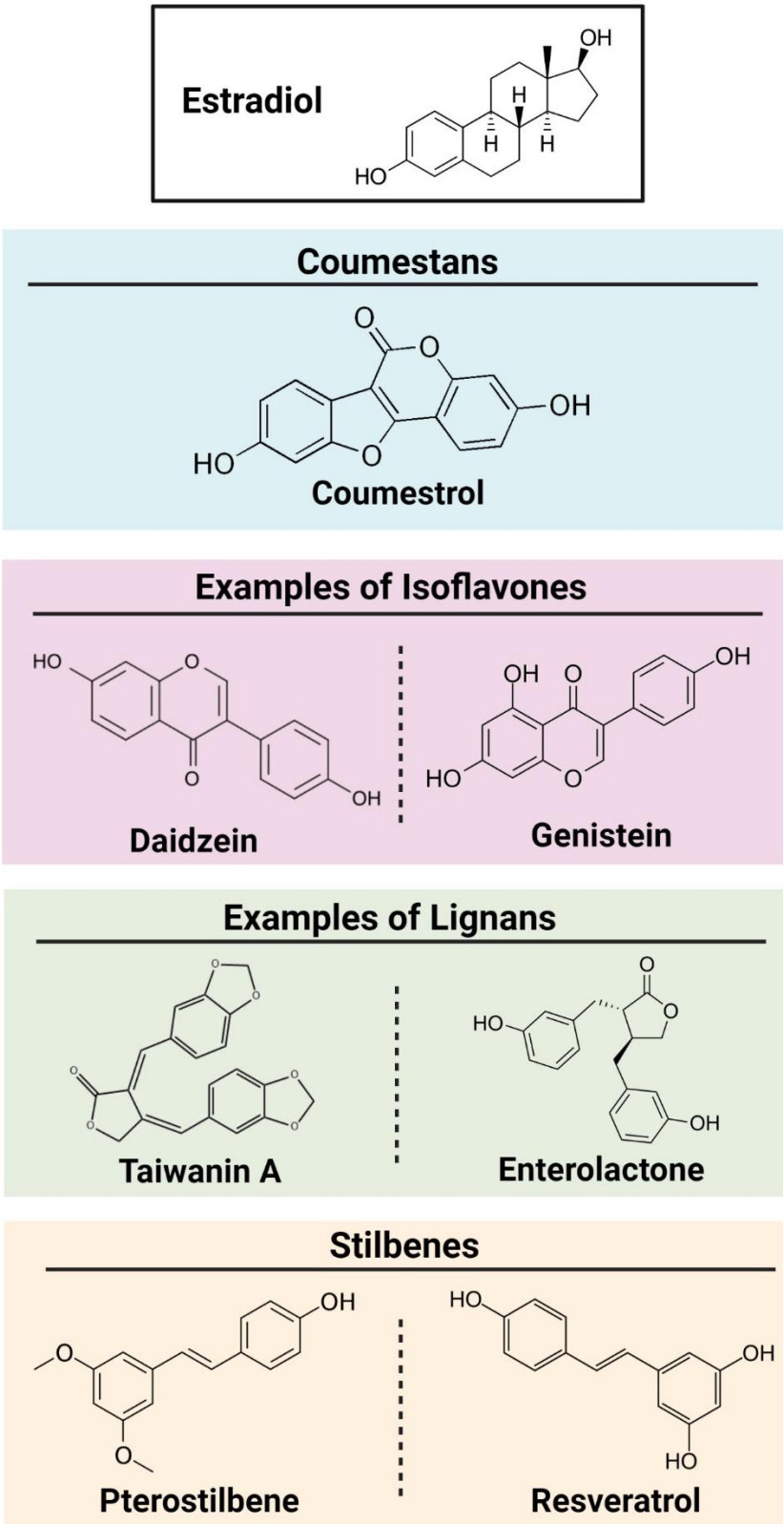

Figure 10. Estradiol and phytoestrogens chemical structures. (Basu & Maier, 2018) (Created with BioRender.com)

1.4.1 Mechanisms of action of phytoestrogens

Phytoestrogens can bind to estrogen receptors (ER) by a weak affinity (1000-10000 times less than that of estradiol) (Bilal et al., 2014). Despite this, some phytoestrogens such as genistein, coumestrol and apigenin have a higher affinity (10-100 times that of estradiol) to ERs (Bilal et al., 2014). Also, phytoestrogens can interact with growth factors and cytokine signaling pathways (Figure 11) (Bilal et al., 2014). Thus, all these bindings or interactions can modulate the responses to growth factors or activate/inhibit kinases (Figure 11) (Bilal et al., 2014). Additionally, phytoestrogens may alter the ligand-independent transcriptional activity of ERs or other transcription factors such as AP-1 and NF-κB (Bilal et al., 2014). One example is that genistein is a tyrosine kinase inhibitor and affects the activation of ERK and AKT kinases (Bilal et al., 2014). Down-regulation of AKT has been observed after long-term treatment of breast cancer cells with genistein (Bilal et al., 2014). Interestingly, in addition to phytoestrogens affecting kinases and receptors involved in pro-oncogenic phenotypes, they also affect the cell cycle (Figure 11).

Cell cycle consists of a series of events in which cells increase in size, duplicate their DNA and and divide their cytoplasm and organelles to produce two daughter cells. Transition in the cell cycle is regulated by cyclins and the activation of cyclin-dependent kinases (CDKs). However, the effects of phytoestrogens in the cell cycle are controversial. Studies reported that high concentrations of phytoestrogen (>10μM) inhibit the expression of cyclin D1 (regulates the G1 to S phase of the cell cycle) (Bilal et al., 2014). High doses of phytoestrogens increase

the expression of p21, p27, and p53 (CDK inhibitors), promoting apoptosis and decreasing proliferation (Bilal et al., 2014).

Interestingly, phytoestrogens, specifically isoflavones, weakly inhibit aromatase (Figure 11) (Bilal et al., 2014). Aromatase is an enzyme responsible for converting androgens into estrogen. Also, phytoestrogens inhibit 17β-hydroxysteroid dehydrogenase (HSD) type 1, which reduces oestrone (E1) to E2 and 17β-HSD type 5 that converts androstenedione to testosterone, which can subsequently be converted to E2 by aromatase (Bilal et al., 2014). Therefore, this data demonstrated that phytoestrogens could inhibit steroid synthesis (Bilal et al., 2014).

Another phytoestrogen mechanism of action is epigenetic changes (Figure 11 and 12). Epigenetic changes are heritable changes that do not change the DNA sequence. Scientists suggest that epigenetic events could be involved in childhood protection since early exposure to phytoestrogens could protect against breast cancer in later life (Bilal et al., 2014). Phytoestrogens promote the expression of tumor suppressor genes ($p21^{WAF1}$ and $p16^{INK4a}$) (Bilal et al., 2014). The induction of these genes was associated with a small reduction in the activity of histone deacetylases (HDACs) but a large increase in the activity of histone methyltransferases (HMTs) (Bilal et al., 2014). Also, phytoestrogens decreased the activity of DNA methyltransferases (DNMT) (Bilal et al., 2014). Long-term treatment with high doses of phytoestrogens downregulated the expression of acetylated histone 3, cyclin D1, and pro-caspase 9 (Bilal et al., 2014). Understanding all these epigenetic modifications and their contributions to

breast tumorigenesis opens the opportunity to further understand the potential role of pythoestrogen in breast cancer patients' diagnosis, prognosis, and therapy (Dagdemir et al., 2013).

In summary, phytoestrogens have antagonist effects in estrogen receptors (ERs), modulate cell signaling pathways, and regulate the cell cycle (Figure 11) (Bilal et al., 2014). Also, phytoestrogens have anti-oxidant properties, regulate angiogenesis, and are involved in epigenetic alterations (Figure 11 and 12) (Bilal et al., 2014).

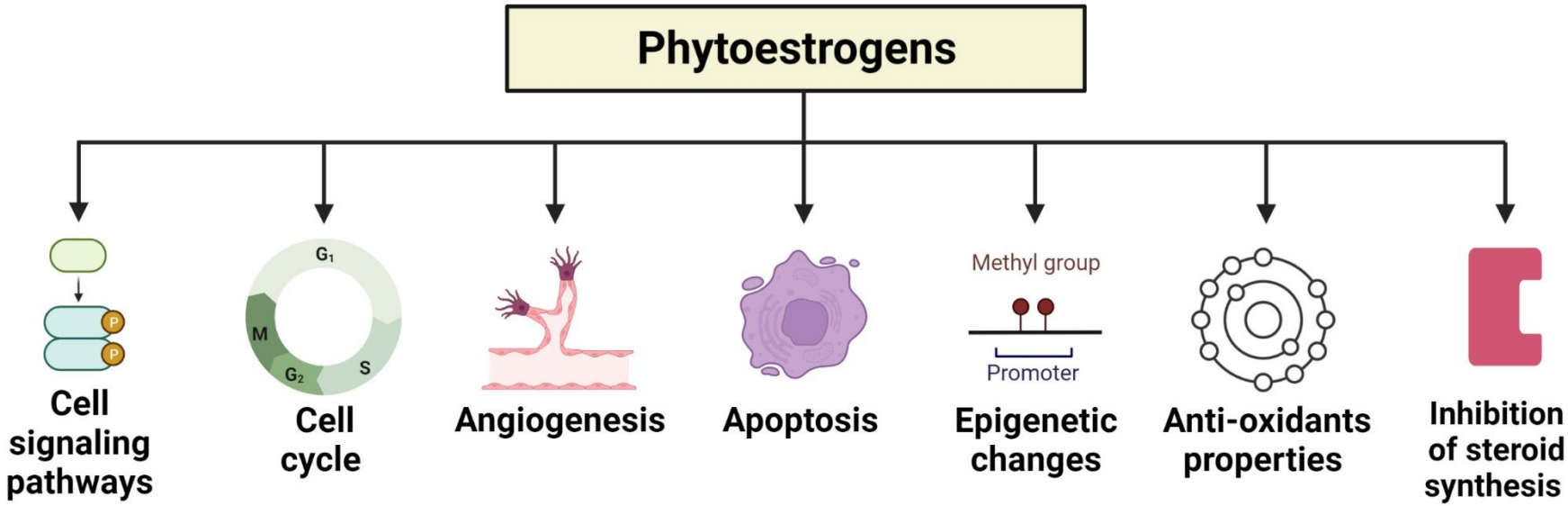

Figure 11. Summary of the phytoestrogens mechanism of action. (Bilal et al., 2014) (Created with BioRender.com)

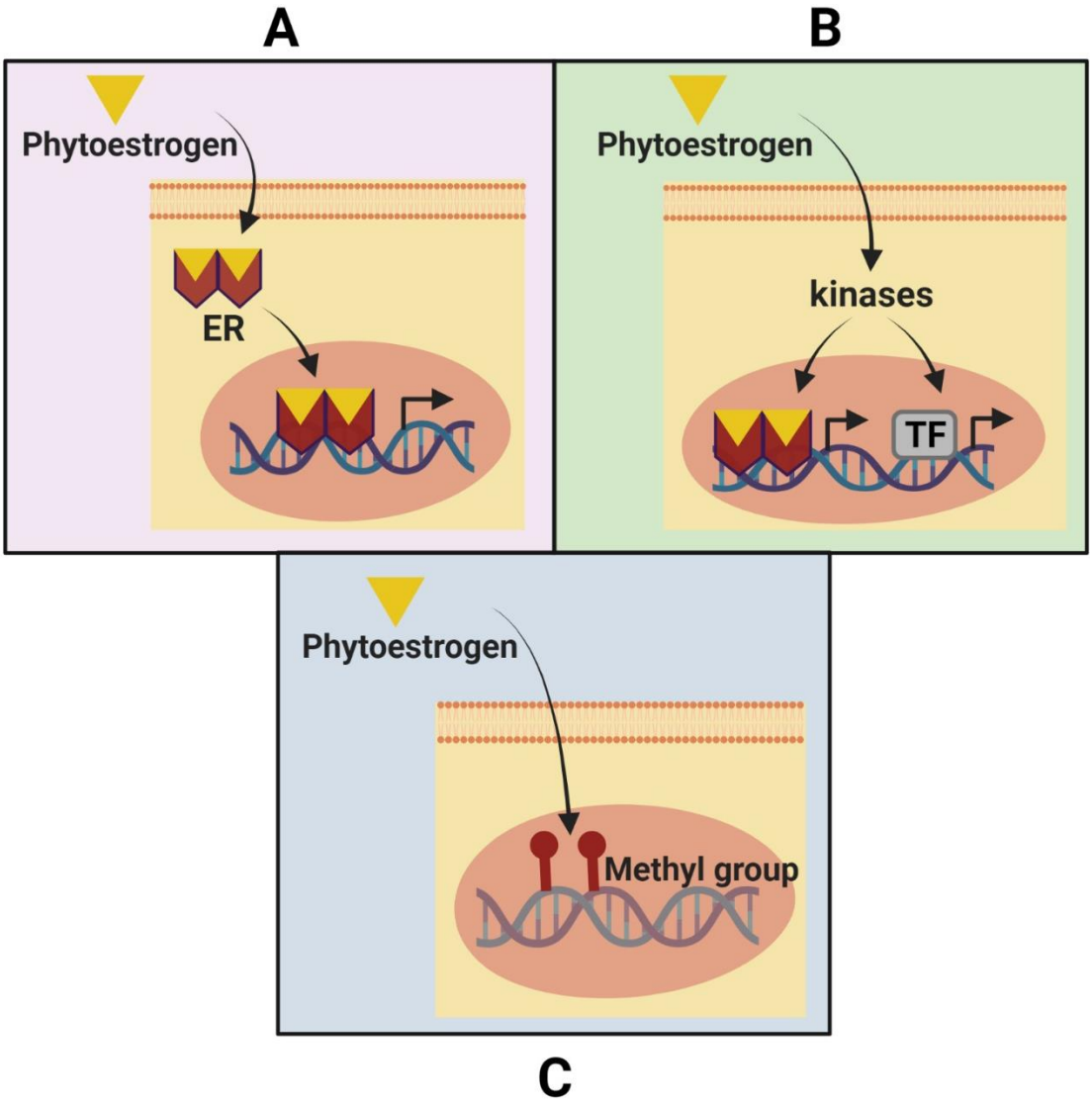

Figure 12. Mechanism by which phytoestrogens alter the transcription of genes. (A) Phytoestrogen binds to the estrogen receptors (ER) and induces transcriptional activity as an agonist or antagonist ligand. **(B)** Phytoestrogens can activate kinases involved in promoting gene transcription. **(C)** Phytoestrogen induces epigenetic changes (Bilal et al., 2014).

1.4.2 Phytoestrogens and breast cancer

Asian women and vegetarians have a diet rich in high phytoestrogen foods (Figure 13). The average intake of soy and isoflavones in Asian populations is 50g/day and 30mg/day, respectively (Bilal et al., 2014; Cos et al., 2003). On the contrary, the Western populations intake 1 g/day of soy and 1mg/day of isoflavones (Bilal et al., 2014; Cos et al., 2003). Coincidentally, Asian and vegetarian women have the lowest breast cancer risk and the highest excretion of urinary phytoestrogens (Wang & Kurzer, 1998). Also, there is a trend of reduced risk in breast cancer with increased soy intake in both pre- and postmenopausal Asian women (Obiorah et al., 2014).

For Chinese women previously diagnosed with ER-positive breast cancer, higher consumption of soy (>15.31 gram/day) was associated with the lowest mortality and recurrence rate in comparison to women that had the lowest consumption of soy (=<5.31 gram/day) (Shu et al., 2009). In fact, Chinese women that use tamoxifen and have low to moderate levels (5.32-9.45 gram/day) of soy food intake have the lowest mortality (Shu et al., 2009). Similarly, high soy consumption during childhood and adolescence is associated with a reduced risk of breast cancer in adults (Cos et al., 2003; Obiorah et al., 2014). In an *in vitro* study, phytoestrogens stimulated ER-positive breast cancer cell growth at low pharmacologic concentrations. In contrast, at high concentrations (>5 μmol/L), phytoestrogen inhibits the proliferation of cancer cells (Obiorah et al., 2014). Nevertheless, phytoestrogens' prolonged exposure could decrease ER-α66 mRNA expression (Obiorah et al., 2014). Based on the inverse relationship

between soy consumption and breast cancer risk in Asian countries, an interest in using phytoestrogens in breast cancer prevention has been triggered (Obiorah et al., 2014).

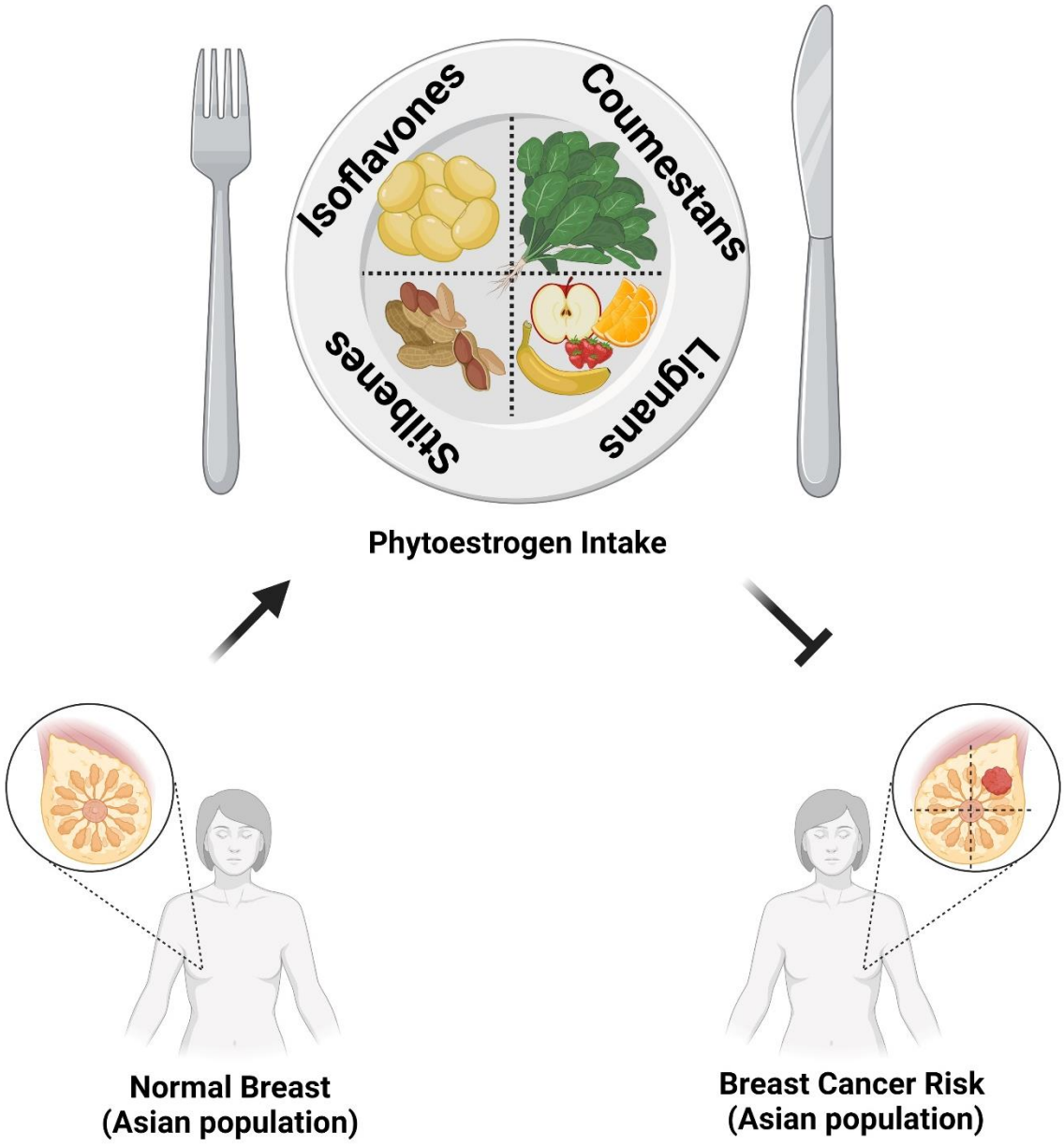

Figure 13. Phytoestrogen intake reduces breast cancer risk in Asian population. (Created with Biorender.com)

1.4.3 Phytoestrogens and inflammatory breast cancer

Genistein is the most studied phytoestrogen and is the only one that has been studied in triple-negative inflammatory breast cancer (TN-IBC) cell lines. A study demonstrated that Genistein (50µM) induces apoptosis in BRCA1-mutant cells (SUM149PT) (Privat et al., 2010). Furthermore, Genistein induced a cytotoxic effect against TN-IBC cell lines; suggesting that other phytoestrogens could cause a similar cytotoxic effect. Thus, there is an urgent need to evaluate the anti-carcinogenic effect of other phytoestrogens as a possible targeted therapies alone or in combination with other therapeutic options.

1.4.4 Coumestrol

Coumestrol (Cou) is a polyphenolic compound structurally similar to estradiol (E2) and can compete for binding to an unfilled cytoplasmic estrogen receptor or unfilled nuclear estrogen receptor sites (Martin et al., 1978). Also, it is derived from Daidzein, an isoflavone like Genistein (Basu & Maier, 2018). It was described as an antagonist of ER-α66 and ER-β receptors with an IC_{50} of 11nM and 2nM, respectively (Chen et al., 2004; Hopert et al., 1998). An increased interest in studying the effects of Cou against breast, prostate, and ovarian cancer have emerged recently (Lim et al., 2017; Lim et al., 2016; Zafar et al., 2017; Zafar et al., 2018). Recent studies performed in ER-positive (MCF-7) and ER-negative or TNBC (MDA-MB-231) breast cancer cell lines treated with Cou showed a G1/S cell cycle arrest and promotion of mitochondrial-mediated apoptosis (Zafar et al., 2017; Zafar et al., 2018). Also, Cou cytotoxicity was found to be mediated by increasing DNA damage and activating an apoptotic response (Wang & Kurzer,

1998; Zafar et al., 2017; Zafar et al., 2018). Similar effects were seen in prostate and ovarian cancers as Cou decreased proliferation and migration and induced apoptosis by regulating the activity of PI3K/AKT, ERK1/2, and JNK/MAPK signaling pathways (Lim et al., 2017; Lim et al., 2016).

Decades ago, Cou was found to bind competitively to the estrogen receptor proteins in rat uterine cytosol, a rat model of 7,12-Dimethylbenz[a]anthracene (DMBA)-induced mammary tumors, and in human mammary tumor tissue (Verdeal et al., 1980). Using this model, Cou was not antiestrogenic, but did not support growth of mammary tumors when given orally to the animals (Verdeal et al., 1980). Despite this, earlier studies involving Cou are conflictive. Diverse studies demonstrated that Cou (10 µM) inhibits ER-positive cancer cells growth, but other studies only showed that the inhibitory effects of Cou (1 µM) were restricted to an estrogen-depleted state (Dixon-Shanies & Shaikh, 1999; Hess-Wilson et al., 2006; Obiorah et al., 2014). Also, studies performed in ER-positive breast cancer cells showed that Cou (1 µM) and other phytoestrogens are inhibitors of apoptosis and have robust transactivation of ER-α66 and ER-β receptors (Harris et al., 2005; Schmidt et al., 2005). Interestingly, scientists demonstrated that low doses of phytoestrogens are generally found to stimulate the growth of breast cancer cells and only concentrations >10 µM are considered as high dose (Bilal et al., 2014).

Since there are no previous studies that have demonstrated the effect of Cou in IBC models, our research focuses in the study of Cou as a potential anticancer agent against TN-IBC. Our study will take into consideration the effects of Cou in the presence and absence of 17β-estradiol (E2). Both conditions will help

us determine if the anticancer activity of Cou is affected by E2 levels, which in the long-term will help us determine if the potential treatment will benefit pre and/or postmenopausal women. Our research opens an opportunity for scientists in the field to explore natural compounds like phytoestrogens with the potential of antagonizing the estrogen non-genomic signaling pathway. The data gathered from this thesis is pivotal to achieve the long-term goal of developing effective targeted therapies for IBC to improve patients' prognosis, survival rates and quality of life.

Specific aims

Aim 1: Determine if coumestrol inhibits pro-oncogenic phenotypes in IBC cell lines. Studies showed that Cou has a cytotoxic effect in ER-positive and TNBC cell lines. Due to the similar expression of estrogen receptors between TNBC (MDA-MB-231) and TN-IBC (SUM149PT), the working hypothesis for this aim is that treatment with coumestrol can inhibit oncogenic phenotypes in IBC cell lines. In order to answer our hypothesis, we will analyze the effects on cellular responses, including migration using two-dimensional (2D culture model) and cell proliferation, migration, invasion, and tumor emboli formation using three-dimensional (3D culture model) cell cultures.

Aim 2. Characterize the molecular mechanism by which coumestrol inhibits cell proliferation and migration in IBC cell lines. Based on the affinity of Cou to the estrogen receptors, *we proposed that Cou exerts its anti-cancer activity by modulating the estrogen non-genomic signaling pathway of TN-IBC.* However, coumestrol anti-cancer activity may also be independent of modulating the estrogen non-genomic signaling. Characterization of the molecular mechanism of Cou anti-cancer activity will be done by analyzing the levels of phosphorylation of kinases involved in the estrogen non-genomic signaling pathway and the transcriptome chages elicit by coumestrol treatment.

Chapter II. Coumestrol as an inhibitor of pro-oncogenic phenotypes

2.1 Introduction

Triple-Negative Inflammatory Breast Cancer expresses alternate estrogen receptors that promote proliferation, migration, and invasion via a non-genomic signaling pathway (Ohshiro et al., 2012). In other words, estrogen is a hormone responsible for inducing pro-oncogenic phenotypes in TN-IBC. Also, Inflammatory Breast Cancer is a type of breast cancer that does not produce a palpable mass but induces breast inflammation (Dushkin & Cristofanilli, 2011; Vermeulen et al., 2010). Inflammation of the breast is caused by the continuous growth of tumor cells within the lymphatic vessels that eventually block drainage from the tissue resulting in the edema (Vermeulen et al., 2010). Experts in IBC pathogenesis think that IBC's rapid metastasis is induced by tumor emboli formation, a hallmark of IBC (Vermeulen et al., 2010).

Studying molecules that target metastasis and other pro-oncogenic phenotypes in IBC is crucial for improving the survival of patients with TN-IBC. This study expands our current knowledge of possible anti-cancer effects of compounds that are considered antagonists of estrogen signaling, such as Cou (Chen et al., 2004; Hopert et al., 1998). The rationale for performing functional assays is that Cou has a structure similar to estradiol (E2) that facilitates its function as a ligand for estrogen receptors and its antagonist effect. Based on this, *we propose that Cou exerts an anti-cancer activity on TN-IBC.* Therefore, Cou will inhibit pro-oncogenic phenotypes such as proliferation, migration, invasion, and tumor emboli formation. **Our hypothesis was that Cou exerts its anti-cancer effect by**

inhibiting kinases involved in proliferation, migration, and invasion and impairing IBC tumor emboli formation.

2.2 Materials and methods

Cell lines and cell culture

ER-positive (MCF-7) and triple-negative non-IBC (MDA-MB-231) cell lines were purchased from ATCC and cultured in DMEM (Sigma Aldrich) or RPMI (Sigma Aldrich), respectively. Also, each medium was supplemented with 10% heat-inactivated fetal bovine serum (FBS) and 1% penicillin and streptomycin (P/S) (Fisher Scientific) (Table 4). Triple-negative inflammatory breast cancer cell lines (TN-IBC), SUM149PT, were purchased from BioIVT. The Medical University of South Carolina (Dr. Stephen P. Ethier) provided HER-2 amplified inflammatory breast cancer cell line (SUM190PT). SUM149PT and SUM190PT cells were cultured in F12 (Fisher Scientific) supplemented with 10% heat-inactivated fetal bovine serum (FBS, Sigma Aldrich), 1% penicillin and streptomycin (Fisher Scientific), 0.5 mg/ml insulin (Sigma Aldrich), and 1 mg/ml hydrocortisone (hydro) (Sigma Aldrich) (Table 4). All the cell lines were seeded in tissue culture-treated dishes (100 mm plates) or T25 flasks and maintained at 37ºC in a 5% CO2 incubator. The medium was changed every 2 or 3 days (Table 5).

Once MCF-7, MDA-MB-231, and SUM149PT cells reached 90-100% confluency, they were split into different flasks (Table 4). SUM190PT cells were split at 80% of confluency (Table 4). We removed the medium and washed the plate with 2mL of 1X HBSS. Then, 1mL of TrypLE™Express (trypsin) (Gibco) was added to detach each cell line from the tissue culture plate and gently rocked to

cover the cells. After 5-12 minutes of incubation, we collected the trypsin with the detached cells and centrifuged them in a 15 mL tube for 10 minutes at 1.2 rpm at room temperature. The supernatant was removed and the desired volume to perform the desired split/passage was added. Each resuspended cell volume was transferred in a tissue culture plate or flask and fresh media was added in accordance to the plate or flask used (Table 5).

Table 4: Culture media for maintenance of breast cancer cell lines

	MCF-7	MDA-MB-231	SUM149PT	SUM190PT
Growth Medium Recipe	• 45mL DMEM • 5mL 10% FBS • 500µl 1% P/S	• 45mL RPMI • 5mL 10% FBS • 500µl 1% P/S	• 44mL F12 • 5mL 10% FBS • 25µl 0.5mg/ml insulin • 50µl 1mg/ml hydro • 500µl 1% P/S	• 44mL F12 • 5mL 10% FBS • 25µl 0.5 mg/ml insulin • 50µl 1mg/ml hydro • 500µl 1% P/S
Split	1:3 or 1:4	1:3 or 1:4	1:3 or 1:4	1:2
Detached time	5-8 minutes	5-8 minutes	8-12 minutes	5-8 minutes

Table 5: Volume of medium required per tissue culture dishes or flasks

T25 flasks	100mm plates
• 5mL of medium	• 8-10mL of medium

Compounds

Coumestrol (27885) and β-estradiol (E8875) were purchased from Sigma Aldrich. Both drugs were dissolved in dimethyl sulphoxide (DMSO) and stored at -20ºC. Coumestrol and estradiol have been prepared in a stock concentration of 93mM and 100mM, respectively (Table 6). The amount of DMSO added to prepare the stock concentration was calculated using GraphPad Molarity Prism. For each experiment performed, the drugs were diluted with a starving medium (DMEM/F12

without phenol red and 1% Charcoal Stripped Fetal Bovine Serum) to obtain the working concentration for each experiment before adding it to the cells.

Table 6: Dilution of drugs

	Coumestrol [93.2mM]	β-estradiol (estrogen) [100mM]
Dilution	• 50mg coumestrol • 2ml of DMSO	• 1g estrogen • 36.71ml of DMSO
Solubility	25mg/ml in DMSO	DMSO to 100mM
Storage time	1 year	1 year

Dose-response curves and relative cell viability (RCV)

Cells seeded in a T25 flask, or 100mm tissue culture dish were grown under a starving medium (medium without hormones or growth factors) (DMEM/F12 without phenol red, and 1% Charcoal Stripped Fetal Bovine Serum) at 37ºC in a 5% CO2 incubator. After 48 hours, for 2D cultures dose-response curves, ten thousand cells per well were plated in a 96-well plate in 200µl of starving medium prepared in a 2-fold serial dilution (6.25µM, 12.5µM, 25µM, 50µM, 100µM, and 200µM) of Cou concentrations. After 24, 48, and 72 hours, the starving medium containing the treatment was removed, and 100µl of alamarBlue™ cell viability reagent (Thermo Fisher Scientific) was added. After 3 hours, fluorescence was measured using an Infinite2000 PRO Microplate Reader (Tecan). In the Tecan, we determine the fluorescence intensity with the plate without cover, emission in 585nm, excitation in 550nm, and optimal gain. The time points (24, 48, and 72 hours) were performed in individual 96-wells plates with three technical and biological replicates per treatment. For the experiments, we used two controls: 1. no treatment control was cells treated with vehicle (DMSO) alone, and 2. negative control was alamarBlue™ without cells.

For the 3D culture system, each well was coated with 30µl of Matrigel® (Corning) first and placed in the incubator for 30 minutes. Then, ten thousand cells were plated in the coating wells under 100µl of starving medium prepared with a 2-fold serial dilution of Cou and 5% of Matrigel®. After 24, 48, and 72 hours, the medium was removed and 100µl of alamarBlue™ Reagent was added. After 3 hours, the alamarBlue™ Reagent was removed from the coated wells and added to a new 96-well plate for fluorescence measurement using the Tecan microplate reader using the same parameters of the 2D dose-response curves. Using GraphPad Prism 9.0, we generated a dose-response curve to determine the half-maximal inhibitory concentration (IC_{50}) of Cou for 2D and 3D models. For this, an XY table was created with an average of the normalized cell viability and %CV. alamarBlue™ alone (negative control) was subtracted from all measurements. Then, the data was normalized to DMSO and transformed to logarithms. The nonlinear regression parameters and sigmoidal dose-response (variable slope) was selected to generate the dose-response curve. To determine the half-maximal inhibitory concentration (IC_{50}) of Cou, we use the formula, 10^{x}. The value of X was the Cou concentration when the cell viability was affected by 50%.

We used the same protocol for the relative cell viability (RCV), but the cells were treated only with the IC_{50} value determined by the 2D and 3D dose-response curves. A grouped table with an average of the normalized cell viability and the standard deviation (SD) was created using GraphPad Prism 9.0. alamarBlue™ alone (negative control) was subtracted from all measurements and the data was

normalized to DMSO. The time of treatments (measured in hours) were placed in the X-axis, while the mean and SD in the Y-axes for the grouped bar chart.

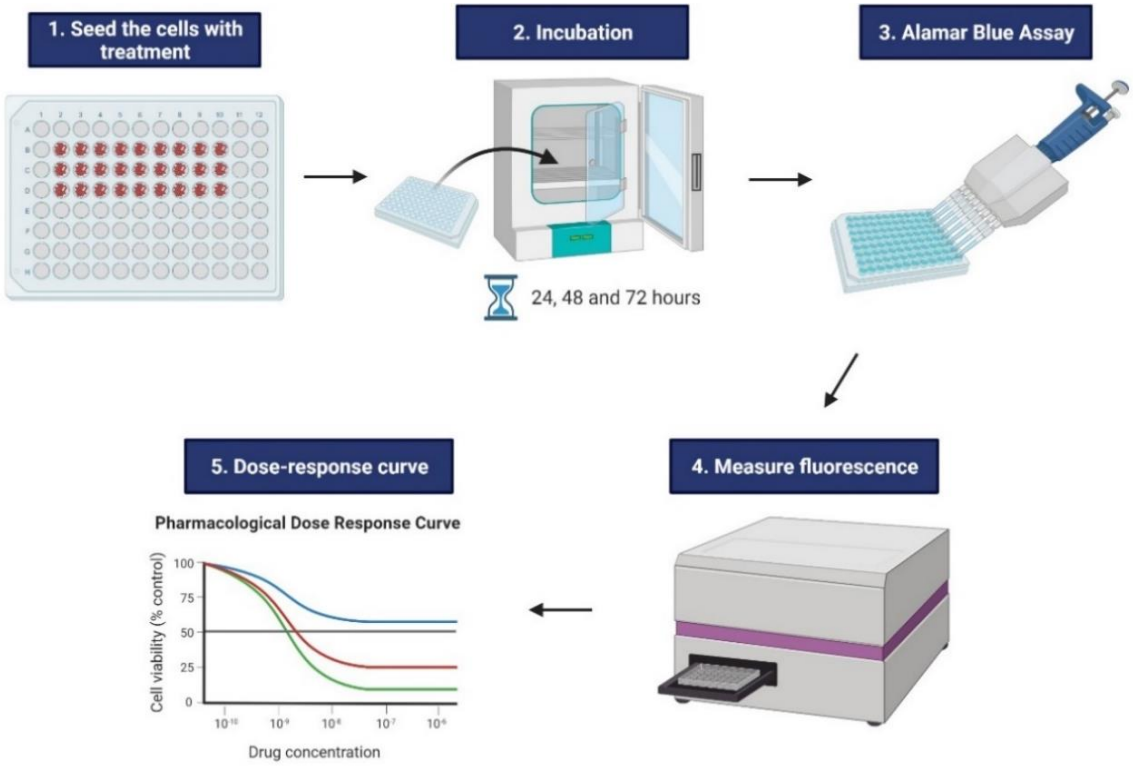

Figure 14. Summary of the dose-response curve and RCV protocol. (Created with Biorender.com)

3D Proliferation Assay

SUM149PT cells (100mm plate in a 50% confluency) were grown under starving medium (DMEM/F12 without phenol red, and 1% Charcoal Stripped Fetal Bovine Serum) at 37ºC in a 5% CO2 incubator for 48 hours. Then, a 12-well plate was coated with 150µl of Matrigel® Matrix (VWR) and placed for 30 minutes inside the 5% CO2 incubator at 37ºC. We added twenty thousand SUM149PT cells (250µl cells with medium) carefully to the 12-well Matrigel® Matrix covered plate. After 1 hour incubation, the cells were treated with 250µl of medium with E2 (10nM), Cou (50µM), or a combination of both treatments, and 5% of Matrigel®.

Every two days, the medium was changed and replace with fresh starving medium with the appropriate drug concentrations, and more Matrigel® Matrix (10%). After days 5 and 10, pictures of the colonies were taken using a Nikon Eclipse TS-2 microscope at 2,000X total magnification. Afterward, we used the Image J software to measure the colony area of fifty colonies per treatment. The area of each colony is a function of cell proliferation. Finally, a column chart with individual values per biological replicates was generated using GraphPad Prism 9.0. Then, Mann-Whitney correction was performed for the statistical analysis. Utilizing the Mann-Whitney median of the three biological replicates per treatment, a column chart was generated using GraphPad Prism 9.0. Then, another statistical analysis was perfomed using one-way Anova for determining the significance difference (p-value) between the treatments. * = $p<0.05$, ** = $p<0.01$, *** = $p<0.001$, **** = $p<0.0001$.

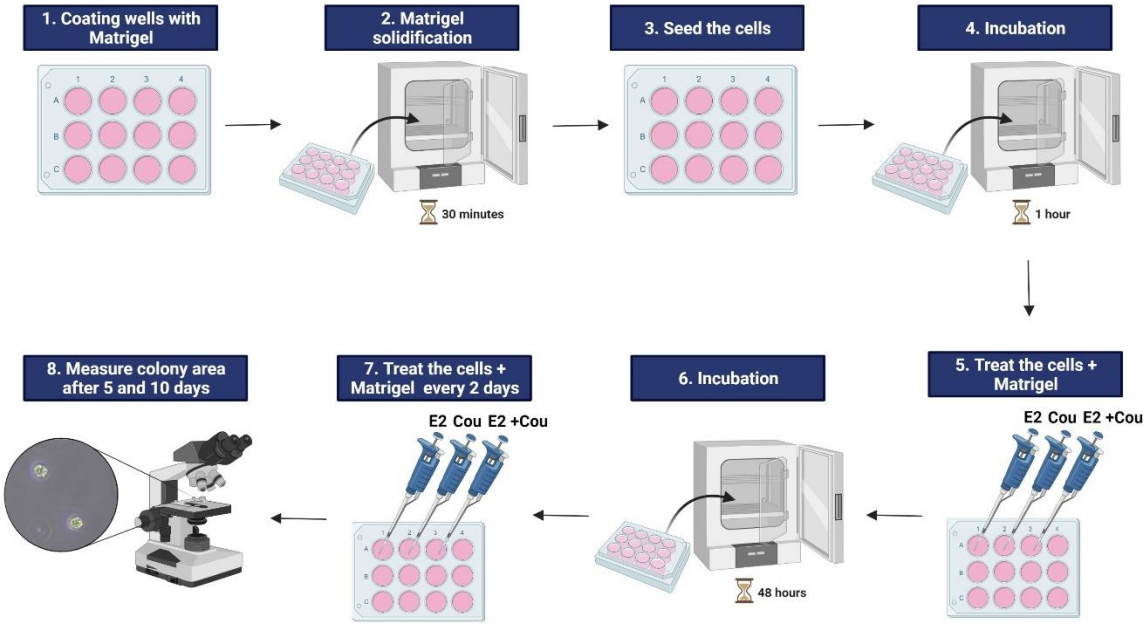

Figure 15. Summary of the 3D Proliferation Assay protocol. (Created with Biorender.com)

Wound Healing Assay

SUM149PT cells were plated in a 6-well plate under growth medium to obtain a confluent monolayer (100% confluency). After 24 hours, cells were placed under starving medium for 48 hours. Then, we removed the starving medium, and a wound was performed using a 10µL or P10 micropipette tip. We washed each well with 1X Hanks Balanced Salt Solution (HBSS) to remove any detached cells. Then, cells were treated with E2 (10nM), Cou (50µM), or a combination of both treatments under 2mL of starving medium for 19 hours. Two images were taken on each well, before (0h) and after (19h) treatment, at 1,000X total magnification. We drew two circles on the outside bottom of the plate to confirm that the taken images were in the same spot before and after the treatment. Then, we used image J software for quantifying the closed area of the wound. A column chart using GraphPad Prism 9.0 was generated for the three biological replicates per treatment and a t-test with non-parametric distribution was performed. * = $p<0.05$, ** = $p<0.01$, *** = $p<0.001$, **** = $p<0.0001$.

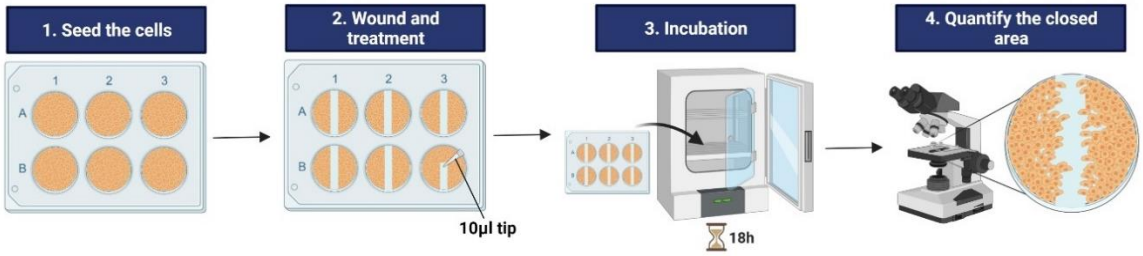

Figure 16. Summary of the Wound Healing Assay protocol. (Created with Biorender.com)

Boyden Chamber Assay

The Corning® FluoroBlok™ (insert) was placed in a well with 500µl of 1X PBS to rehydrate the membrane. Also, 100µl of 1X PBS was added inside the insert (Figure 17). After 5 minutes, 1X PBS inside the insert was removed and the insert was placed in an empty well. For the invasion assay, the insert was coated with 100µl of Matrigel® Matrix 200µg/ml and placed inside the 5% CO2 incubator at 37ºC for 30 minutes. Then, we detached the SUM149PT cells grown under a starving medium for 48 hours. After detaching, the cells were centrifuged at 1.2rpm for 10 minutes and add 1ml of non-chemo attract medium (0%DCC + 0.1%BSA + DMEM/F12 without phenol red). Count the cells and add 2 x 10^4 and 1 x 10^5 cells for migration and invasion assay, respectively. We added a total volume of 100µl inside with the counted cells, non-chemo attracts medium, and treatment. Also, we added 650µl of chemo attract medium (0.2%DCC + 0.1%BSA + DMEM/F12 without phenol red) in the wells that we placed the insert. The plate was incubated for 16 and 22 hours for migration and invasion assays, respectively. Following the incubation period, the media was removed from the insert and the insert was washed with 100µl of 1X HBSS. After, the insert was transferred to a well-containing 500µl of 1X HBSS and 12.44µl of calcein-AM 50µg (Abcam). After 1 hour in the 5%CO2 incubator, the insert was transferred to an empty well and dried using a wipe. To detect calcein-AM fluorescence, we used the Azure Sapphire™ Biomolecular Image in Cy2 dye, intensity number 8, and the pixels in 10µm. Finally, we used Image J software for measuring the fluorescence intensity.

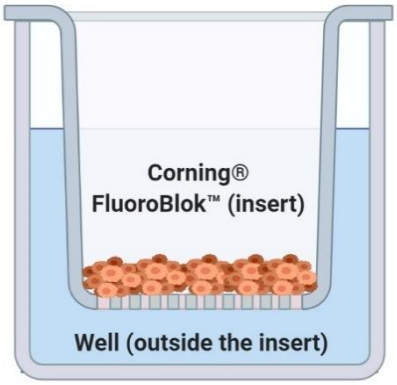

Figure 17. Parts of a Boyden Chamber Assay. (Created with Biorender.com)

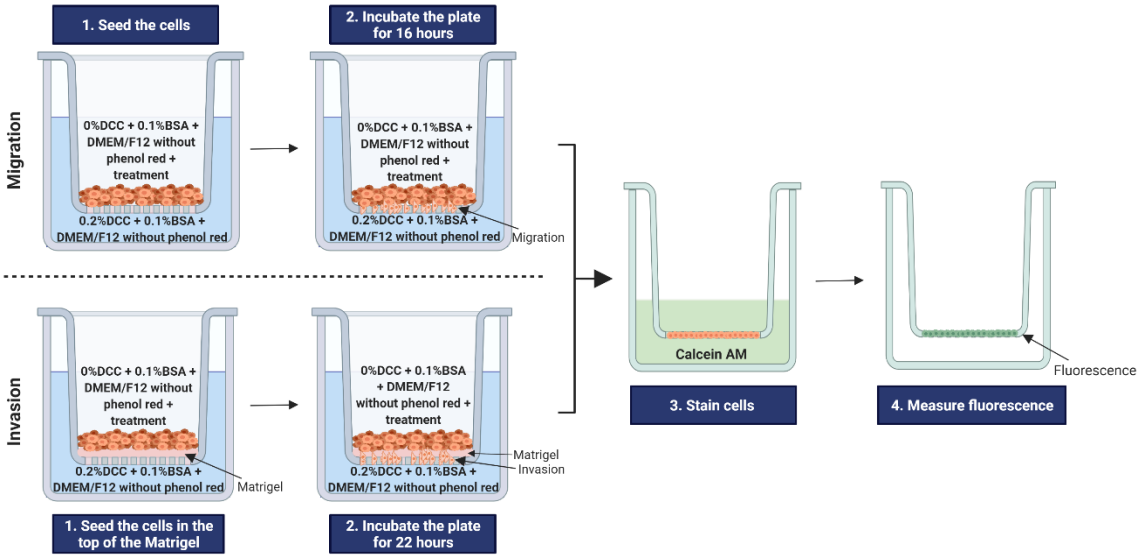

Figure 18. Summary of Boyden Chamber Assay protocol. (Created with Biorender.com)

In vitro 3D Tumor Emboli Assay

SUM149PT cells (250,000 cells) were plated in T75 low-attachment flasks with a growth medium supplemented with 2.25% PEG-8000 (Thermo Fisher Scientific). A total of 12mL of suspension (growth medium with 2.25% PEG-8000, cells, and treatment) was placed in each flask. Then, each flask was kept in an orbital shaking (40 rpm) at 37ºC in a 5% CO2 incubator. After 24, 48, 72, and 96

hours, we took images of all the formed tumor emboli at 400X total magnification. After each time point, we added a shot of the drug or treatment (DMSO or Cou 50µM) to each flask. Image J was used for quantifying the tumor emboli area. Using GraphPad Prism 9.0, a column chart with individual values per biological replicates was generated. A Mann Whitney test was performed for the statistical analysis. Also, a grouped chart was generated after determining the Mann-Whitney median of the three biological replicates per treatment. Finally, we analyzed the data using one-way ANOVA to determine the treatments' statistical significance difference (p-value). * = p<0.05, ** = p<0.01, *** = p<0.001, **** = p<0.0001.

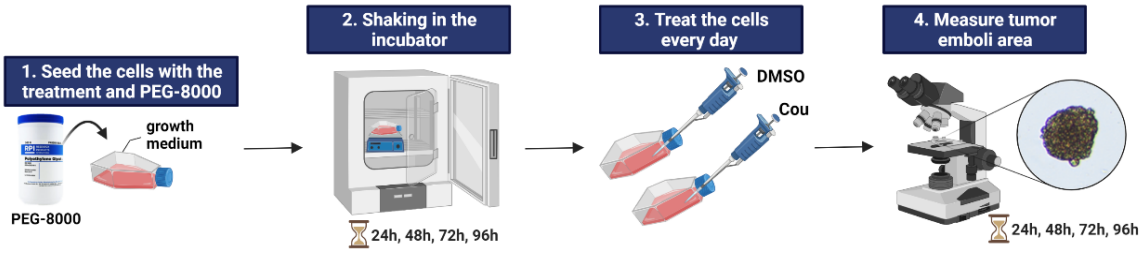

Figure 19. Summary of *in vitro* 3D Tumor Emboli Assay protocol. (Created with Biorender.com)

Trypan Blue Staining Assay

SUM149PT cells were seeded in a six wells plate in 25-30% confluency under a complete growth medium. After 24 hours, cells were placed under a free hormone or starving medium (DMEM/F12 without phenol red and 1% Charcoal Stripped Fetal Bovine Serum) for 48 hours. Then, the cells with 80-85% of confluency were treated with DMSO or Cou (50µM) and placed in a 5% CO2 incubator for 24 and 48 hours. After the incubation time, 250µl of TrypLE™Express (trypsin) (Gibco) was added to detach the cells from the tissue culture wells. The

detached cells were transferred into a microtube with 750µl of the starving medium. The suspension (cells + medium) was a total volume of 1mL. Then, a mixture of 10µl of the suspension and 10µl of trypan blue was performed in a new microtube. After resuspending the mixture, 10µl of the mixture was added to the Countess™ cell counter chamber slide. Finally, the slide was placed in the Countess™ Automated Cell Counter, and the percentage of live and dead cells was used to create a column chart with the three biological replicates per treatment. Finally, we analyzed the data using a t-test with non-parametric distribution to determine the treatments' statistical significance difference (p-value). * = $p<0.05$, ** = $p<0.01$, *** = $p<0.001$, **** = $p<0.0001$.

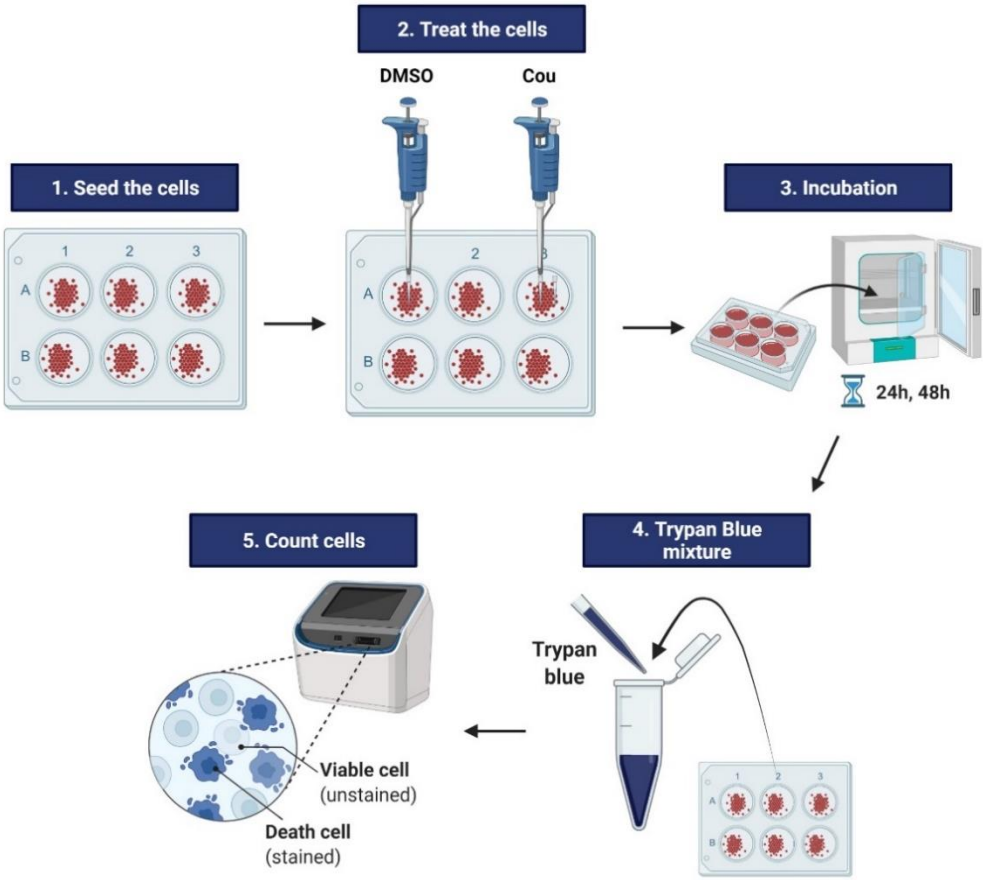

Figure 20. Summary of Trypan Blue Staining Assay Protocol. (Created with Biorender.com)

2.3 Results

Coumestrol decreases SUM149PT cell viability in 2D and 3D cell culture system

By performing a dose response (0 to 200 µM) experiment in 2D cell cultures, we identified that coumestrol decreased cell viability of a TN-IBC cell line, SUM149PT, as time progressed. The anti-proliferative effects of Cou against SUM149PT cells was in a time and dose dependent manner. After 24 hours of treatment, Cou decrease the cell viability of SUM149PT cells by 40%. A half of cell viability decrease after 48 and 72 hours with an IC_{50} value of 13.0 ± 0.4 µM and 8.0 ± 0.6 µM, respectively (Figure 21A).

In order to resemble *in vivo* cell environments, SUM149PT cells were seeded in a 3D (Matrigel) culture system and treated with Cou as described before. In comparison with the 2D culture system, Cou drastically decreased TN-IBC cell viability under a 3D culture system (Figure 21B). Under these culture conditions, after only 24 hours of Cou exposure, 50% inhibition of cell viability (IC_{50}) was achieved at a concentration of 50.0 ± 0.1 µM. Also, after 48 and 72 hours of treatment, SUM149PT cell viability decreased in a dose-dependent manner with an IC_{50} value of 17.0 ± 5.9 µM and 11.5 ± 1.7 µM, respectively.

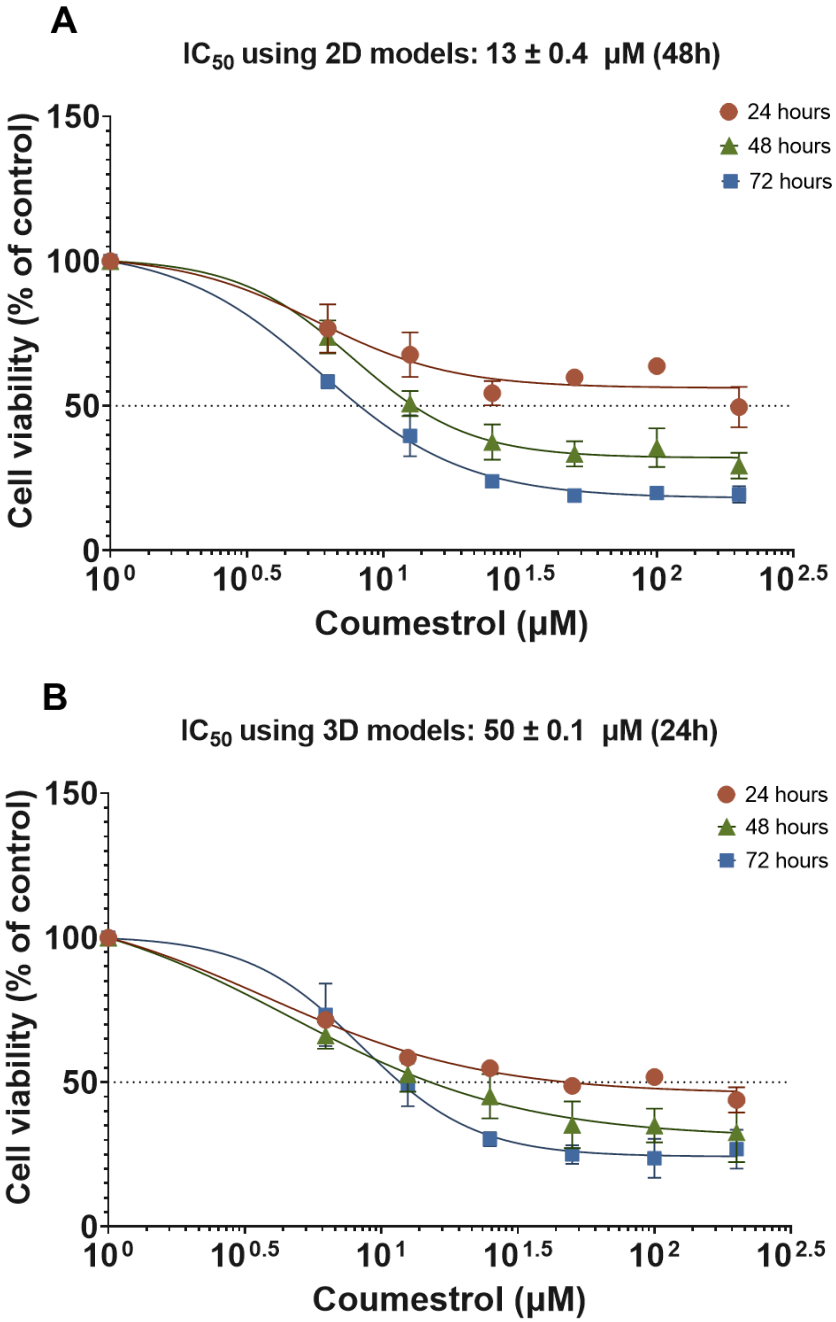

Figure 21. Cell viability decreased after coumestrol treatment in SUM149PT cells. The dose-response curve shows that increasing coumestrol concentrations (0 to 200µM) decreased SUM149PT cells viability. **(A)** Using 2D models, the IC50 of coumestrol was 13 and 8 µM after 48 and 72 hours of treatment, respectively. **(B)** After 24, 48, and 72 hours of treatment, the IC50 of coumestrol was 50, 17, and 11.5 µM using 3D models. Values expressed as mean ± SD of three independent biological replicates.

After determining the effects of Cou in SUM149PT cells, we wanted to analyze the effects of this phytoestrogen on another inflammatory breast cancer cell line, SUM190PT (HER2-amplified). The effect of Cou in SUM190PT cell viability is unknown. By performing a dose-response curve (0 to 200 µM) of Cou in 2D culture models, we observed that SUM190PT cells are resistant to the treatment. Cou did not significantly affect SUM190PT cell viability (Figure 22).

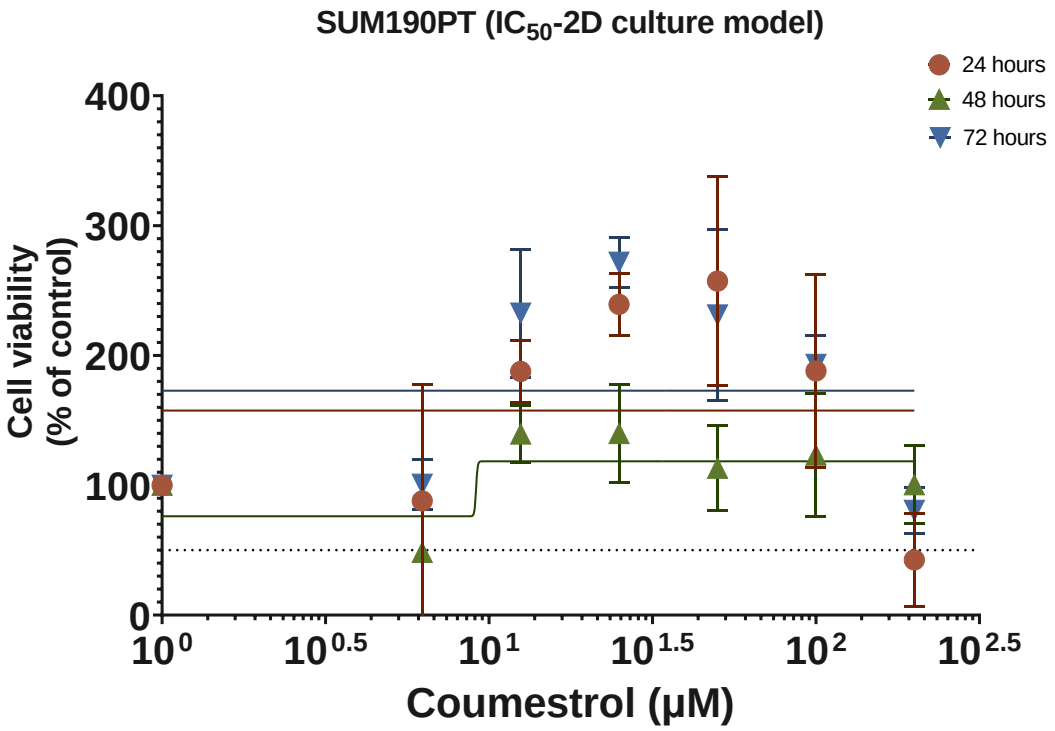

Figure 22. SUM190PT cell viability was not affected upon coumestrol treatment. The dose-response curve shows that the cell viability of SUM190PT does not decrease upon coumestrol treatments (0 to 200 µM). Also, an increase in cell viability was observed, suggesting that SUM190PT cells are resistant to coumestrol.

Based on the data obtained, relative cell viability (RCV) was measured to determine the effect on cell viability using the IC_{50}s calculated in 2D and 3D models on other subtypes of breast cancer. At all timepoints measured, 13 µM of Cou did

not significantly change the cell viability of MCF7 cells (ER-positive) (Figure 23A). However, Cou at this concentration reduces MDA-MB-231 (non-IBC triple-negative) viability by 21% after 24 hours, 50% after 48 hours, and 37% after 72 hours of treatment (Figure 23A). The viability of SUM149PT cells was not affected after 24 hours of Cou treatment at a concentration of 13µM which confirm the data obtained in the dose-response curve (Figure 23A). However, after 48 and 72 hours of Cou treatment, 50% inhibition of cell viability was achieved in SUM149PT cells (Figure 23A). In contrast, SUM190PT (HER2-amplified) cell viability slightly decreased after 48 and 72 hours of 13 µM Cou treatment (Figure 23A). Nevertheless, Cou slightly reduces SUM190PT cell viability by 14% after 48 hours and 19% after 72 hours of treatment, indicating a weak response of SUM190PT to Cou treatment (Figure 23A). These results confirm the data obtained in the dose-response curve, which suggests that SUM190PT cells are resistant to Cou treatment (Figure 22).

Increasing the concentration of Cou to 50 µM decreases MCF-7 cell viability by 38% after 24 hours, 40% after 48 hours, and 32% after 72 hours using 2D models (Figure 23B). Also, MDA-MB-231 and SUM149PT showed the highest reduction in cell viability after being treated with 50 µM of Cou (Figure 23). MDA-MB-231 cell viability decreases by 39% after 24 hours and 67% after 48 and 72 hours of treatment (Figure 23B). Cell viability of SUM149PT after 24 hours of Cou treatment (50 µM) was significantly decreased but did not reach 50% inhibition (Figure 23B). After 48 and 72 hours of treatment, SUM149PT cell viability was inhibited by 62% and 68%, respectively (Figure 23B). As expected from the dose

response curves, after 24 and 48 hours, SUM190PT showed resistance to 50 µM Cou treatment (Figure 23B).

An RCV assay using 3D cultures was performed to determine the effect of Cou in IBCs cell viability. SUM149PT cell viability was inhibited by 40% after 24 hours, 50% after 48 hours, and 66% after 72 hours of 50 µM Cou treatment using 3D models (Figure 24). In contrast, SUM190PT cells treated with Cou at 50 µM using 3D models showed a slightly decrease in cell viability after 24 hours and 72 hours, with an significant increase in cell viability at the 48 hours timepoint (Figure 24). Also, around half percentage of MDA-MB-231 viability decrease after Cou treatment (Figure 24). This data shows that both triple-negative breast cancer cell lines, MDA-MB-231 and SUM149PT, has the highest sensitivity upon Cou treatment. Overall, we can conclude that SUM190PT are resistant to Cou treatment, a phenomenon that might be partially explained by the presence of HER2 amplification. Also, triple-negative breast cancer cell lines, MDA-MB-231 and SUM149PT, have the highest sensitivity to Cou treatment suggesting that Cou anti-cancer effects are more significant against one of the molecular breast cancer subtypes, triple-negative.

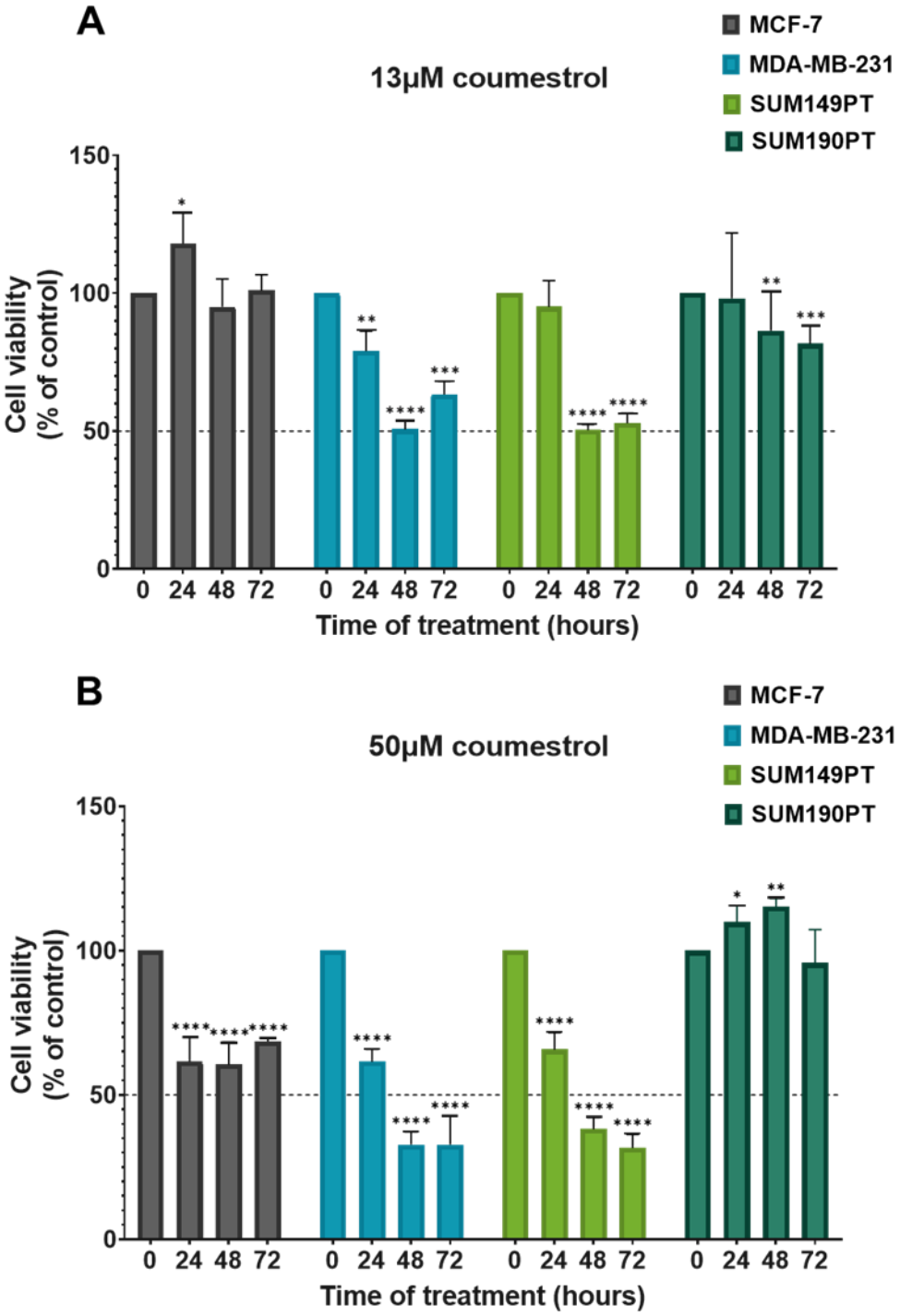

Figure 23. Relative cell viability of breast cancer cell lines treated with coumestrol IC50s in 2D models. MDA-MB-231 and SUM149PT cell lines treated with coumestrol 13 µM (**A**) and 50 µM (**B**) showed a decrease in cell viability in a dose-dependent manner. SUM190PT cell line showed resistance to coumestrol treatment. Values expressed as mean ± SD of three independent biological replicates. * = $p<0.05$, ** = $p<0.01$, *** = $p<0.001$, **** = $p<0.0001$.

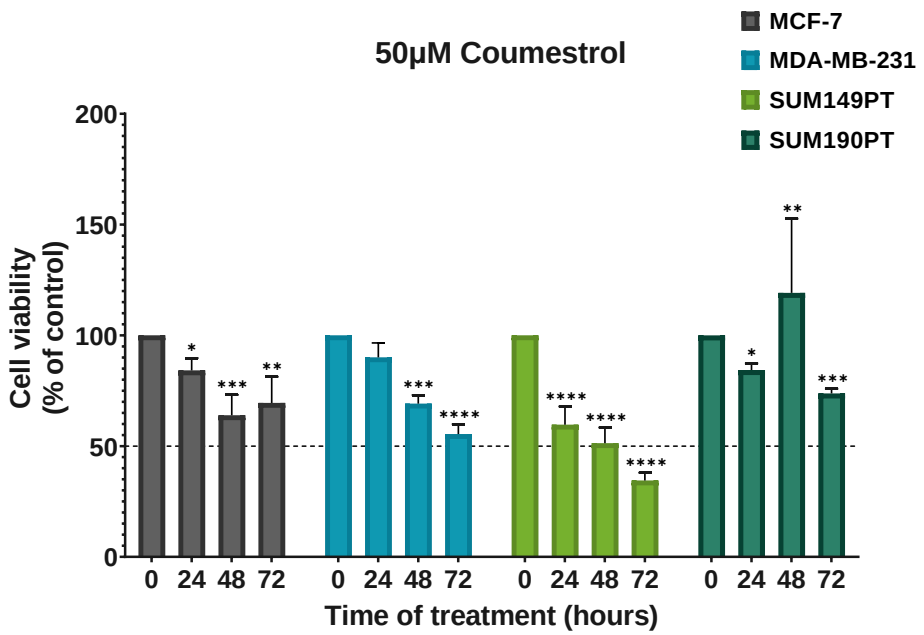

Figure 24. Relative cell viability of IBC cell lines treated with coumestrol IC_{50} in 3D models. Percent of MDA-MB-231 and SUM149PT cell viability decreased after 50 µM of coumestrol treatment. SUM190PT cell line showed resistance to coumestrol treatment after 48 hours of treatment. Values expressed as mean ± SD of three independent biological replicates. * = p<0.05, ** = p<0.01, *** = p<0.001, **** = p<0.0001.

Coumestrol inhibits SUM149PT cell proliferation in a 3D colony formation assay

A 3D culture system was used to study the inhibitory effect of Cou against SUM149PT cell proliferation. Cell proliferation was quantified as a function of colony area size. TN-IBC cells were treated for 10 days with E2 (10 nM), Cou (50 µM), and a combination of both treatments. After 5 and 10 days of treatment, the area of fifty colonies was measured. Estradiol treatment showed a significant increase in the area of colonies when compared to the vehicle (DMSO) control (Figure 25). After 5 days of treatment, E2 induces SUM149PT cell proliferation with an average of the medians of three independent biological replicates (mean value) of 11,542 square pixels in comparison to 6,789 square pixels in DMSO (Figure

25A). On the contrary, in comparison with E2, Cou (mean of 6,864 colony area) and the combination of treatments (mean of 8,341 colony area) affects cell proliferation by decreasing SUM149PT colony area after 5 days of treatment (Figure 25A). Finally, E2 promotes cell proliferation after 10 days of treatment with a mean value of 11,268 in comparison to 6,432 in DMSO (Figure 25B). Also, after 10 days of treatment, proliferation decreased more than a half after treating the cells with Cou (mean of 4,448 colony size) or a combination of both treatments (mean of 5,454 colony size) (Figure 25B). Notably, this data shows that the anti-cancer effects of Cou are not inhibited by the presence of E2.

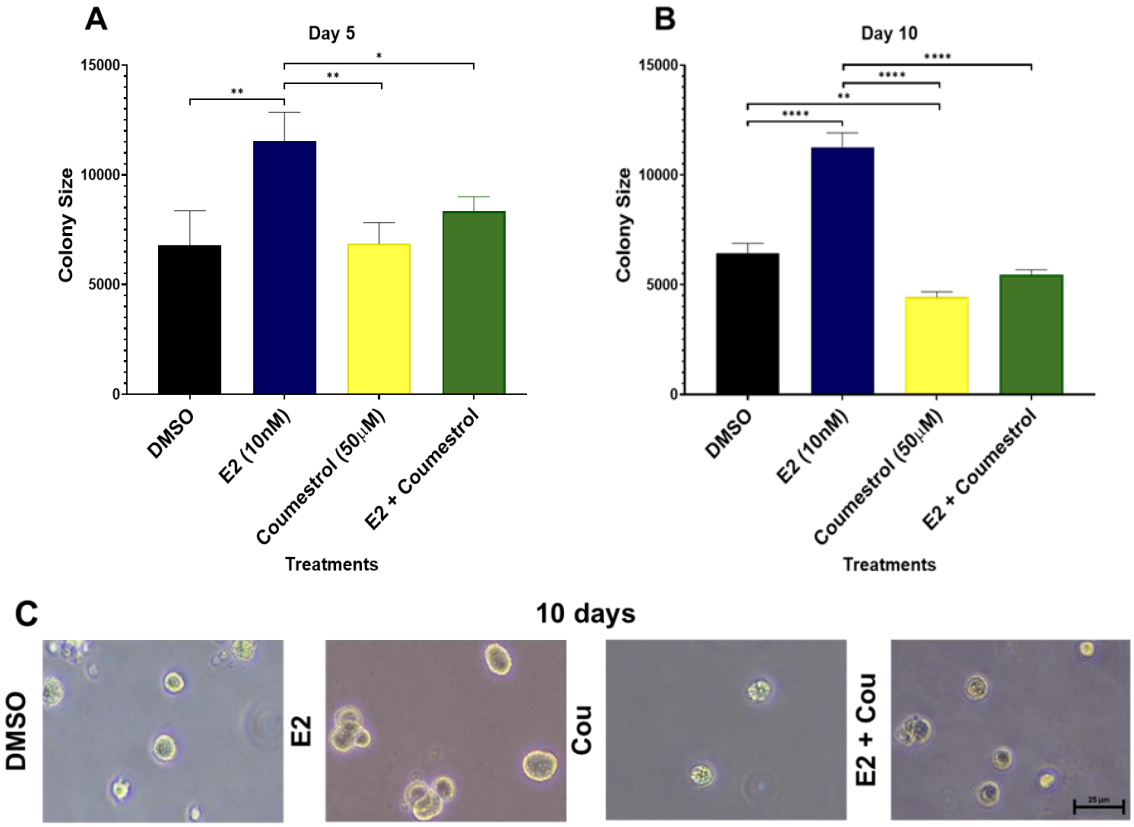

Figure 25. Coumestrol decreases IBC cell lines proliferation. (A) 3D Proliferation Assay in SUM149PT treated with estradiol (E2) (10nM) for five days showed increased in proliferation or colony size (square pixels) in comparison to coumestrol (n=50). **(B)** After ten days, coumestrol (50μM) induces a decrease in SUM149PT cells proliferation in comparison to E2 (10nM). Values expressed as mean of three independent experiments. * = $p<0.05$, ** = $p<0.01$, **** = $p<0.0001$.

Coumestrol inhibits migration and invasion induced by estradiol in SUM149PT cells

To further test the anticancer effect of Cou, we performed a wound healing assay to determine if Cou affects the migration of IBC cells. SUM149PT cells were treated with E2 (10 nM), Cou (15 µM or 50 µM), and combination. After 18 hours, the wound area for each treatment was measured, revealing migration patterns (Figure 26). SUM149PT cells under E2 alone had migrated significantly and had the most pronounced effect (Figure 26B).In comparison to E2, SUM149PT cell migration decreased 40% and 60% after Cou (15 µM or 50 µM) treatment, respectively (Figure 26A). Similarly, the combination of treatment showed a decrease in SUM149PT migration when compared to E2, indicating that the migratory effects of E2 were inhibited by Cou (Figure 26). Also, Boyden chamber assay performed for migration analysis confirmed the results obtained in the Wound Healing Assay (Figure 27A and 27B). The Boyden Chamber Assay showed that E2 alone increased and Cou alone decreased SUM149PT cell migration, despite not having a statistically significant difference (Figure 27A and 27B). Also, the Boyden Chamber Assay performed with the combination of treatments confirmed that Cou inhibited the migratory effects of E2 (Figure 27A). This data suggests that Cou has an active role in inhibiting invasion and metastasis processes.

Migration and invasion are pro-oncogenic phenotypes involved in the metastasis steps; specifically, invasion is the critical process in metastasis because it explains the capacity of a cancer cell to penetrate or invade neighboring

tissues. To study the effect of Cou in SUM149PT cell invasion, we performed a Boyden chamber assay coating with Matrigel® (Figure 27C and 27D). After 22 hours of treatment, an increase in invasion was observed upon E2 treatment in SUM149PT, despite not having a statistically significant difference (Figure 27C and 27D). SUM149PT cells invasion decreased upon Cou treatment (Figure 27C and 27D). Interestingly, the combination of treatments does not inhibit the invasion of SUM149PT but is slightly lower it in comparison with E2 alone (Figure 27C and 27D). This data suggests that the effect of E2 alone was slightly inhibited by the presence of Cou (Figure 27C and 27D).

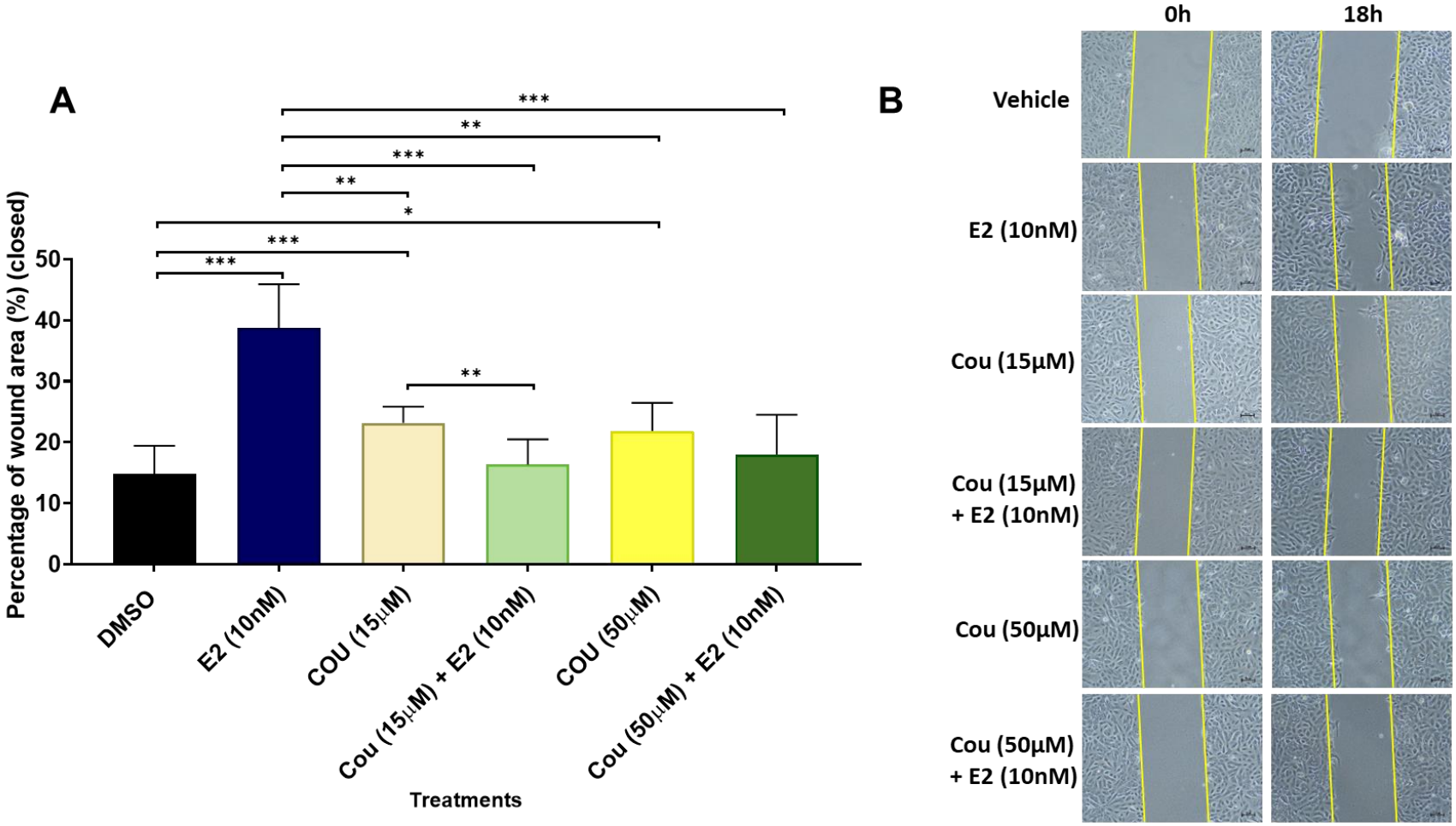

Figure 26. SUM149PT cells migration induced by estradiol is inhibited through coumestrol. (A) Wound Healing Assay after eighteen hours of estradiol (10nM) treatment showed an increase in SUM149PT migration (square pixels). **(B)** Illustration of the wound in the wells seeded with SUM149PT cells before and after the treatments. Values expressed as mean of three independent experiments. ** = $p<0.01$, *** = $p<0.001$, **** = $p<0.0001$.

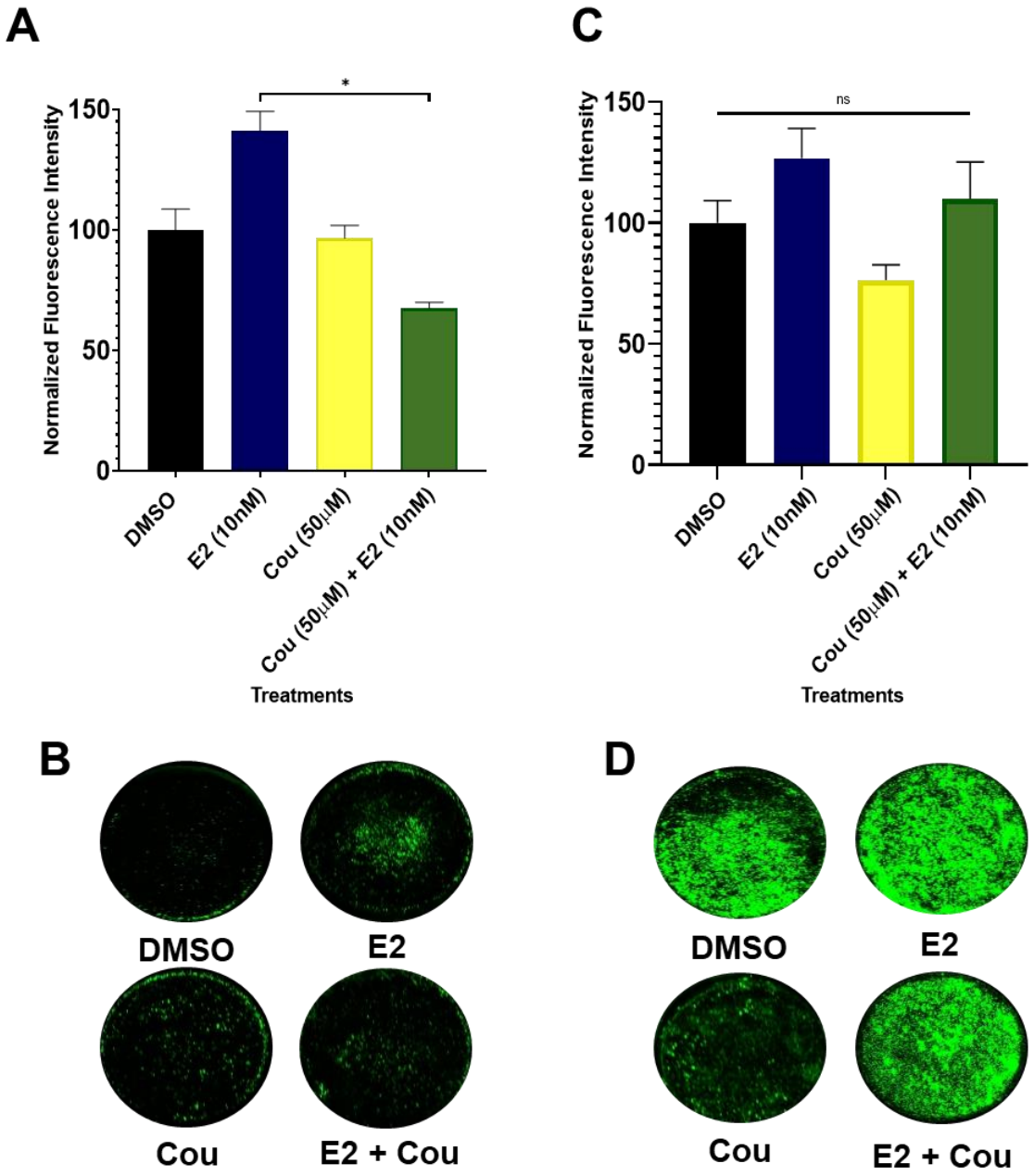

Figure 27. Boyden Chamber Assay in IBC cell lines treated with DMSO, coumestrol, estradiol or combination. Migration (A-B) and invasion (C-D) analysis was performed for sixteen and twenty-two hours of treatment, respectively. SUM149PT cell lines showed a decreased in migration (A) and invasion (C) after treated with coumestrol (50 µM). Also, a decreased in migration (A-B) had been observed after treated with coumestrol (50 µM) in combination with estradiol (10 nM). Illustration of SUM149PT cells migration (B) and invasion (D) treated with DMSO, estradiol, coumestrol, and the combination.

Coumestrol decreases tumor emboli growth but does not affect tumor emboli formation

Usually, IBC is diagnosed in an advanced stage with metastasis. Experts in IBC pathogenesis proposed that IBC rapid metastasis is induced by the tumor emboli formation, a hallmark of IBC (Dobiasova & Mego, 2020; Mohamed et al., 2014). Based on this unique characteristic of IBC cells, a 3D tumor emboli assay was performed to determine the effect of Cou on tumor emboli growth and formation. SUM149PT cell lines (TN-IBC) have been treated with DMSO or Cou 50 µM. After 24 hours, there was no difference in the area measured from the tumor emboli (Figure 28A and 28B). There is a slight but not statistically significant decrease in the sizes of tumor emboli after Cou treatment (31,718 mean of the tumor emboli area) when compared to DMSO (48,186 mean) (Figure 28A and 28B). However, after 72 hours of treatment, the data showed a decrease (55%) in tumor emboli area when the cells were treated with Cou (47,031 mean of the tumor emboli area) when compared to DMSO (86,463 mean of the tumor emboli area) (Figure 28A and 28B). Interestingly, after 96 hours of Cou treatment, the decrease in tumor emboli area was sustained with an average mean of 47,043 (Figure 28A and 28B). The data shows that Cou decreases tumor emboli growth as seen by a reduction in tumor emboli area (Figure 28A and 28B). Even though Cou does not affect tumor emboli formation, it significantly decrease in the growth rates of IBC tumor emboli (Figure 28C). The cells were not treated with a combination of both treatments because we used a complete growth medium for tumor emboli

formation which contain serum with growth factor and hormones including estrogen.

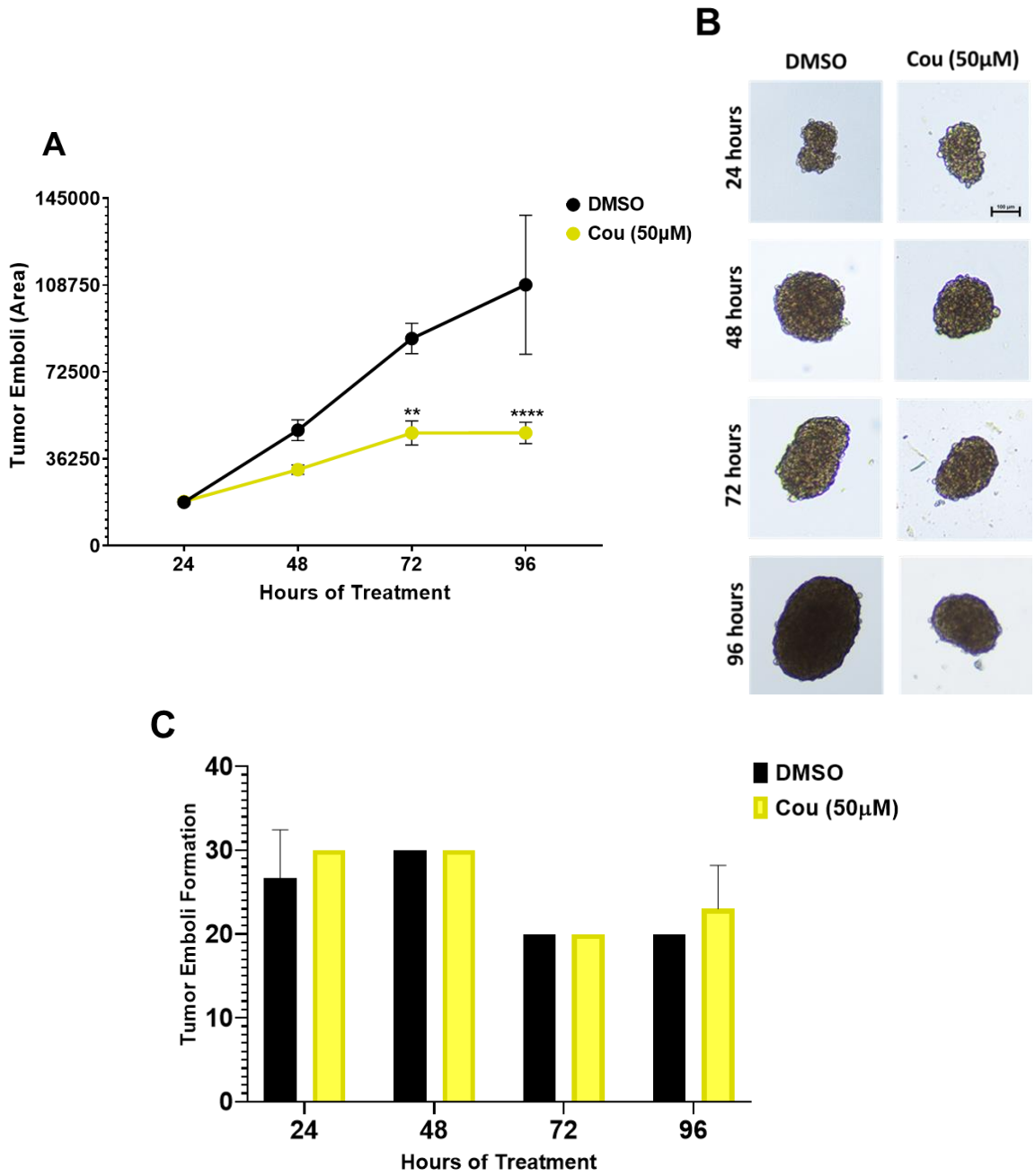

Figure 28. Inhibition of tumor emboli growth in IBC cell lines treated with coumestrol. **(A)** SUM149PT cell lines treated with coumestrol (50µM) showed decreased tumor emboli area (square pixels). **(B)** Illustration of SUM149PT tumor emboli after DMSO and coumestrol treatment. **(C)** Tumor emboli formation was not impaired by coumestrol treatment. Values expressed as mean of three independent experiments**.** ** = $p<0.01$, **** = $p<0.0001$.

Coumestrol induces cell death in SUM149PT cells

Recent studies demonstrated that Cou induces a cytotoxic effect in ER-positive (MCF-7) and TNBC (MDA-MB-231) cell lines (Zafar et al., 2017; Zafar et al., 2018). A Trypan Blue staining assay was performed to determine the effects of Cou in SUM149PT cell death. The cell viability was quantified by the trypan blue staining; stained cells indicated that the cell was dead, and the unstained cell showed live cells. TN-IBC cells were treated for 24 and 48 hours with DMSO or Cou(50 µM), and the percentage of live and dead cells was measured. After 24 hours of treatment, Cou showed an increase in the percentage of SUM149PT dead cells with an average of three independent biological replicates (mean value) of 67% in comparison to 25% in DMSO. Also, in comparison with DMSO (26%), Cou induced cell death of more than a half in SUM149PT cells after 48 hours. On the contrary, SUM149PT live cells decreased upon Cou treatment after 24 and 48 hours by 33% and 44%, respectively. These data show that Cou has a cytotoxic effect in SUM149PT cells, demonstrating that Cou can be considered as a novel treatment for patients with the most aggressive breast cancer subtype, inflammatory breast cancer.

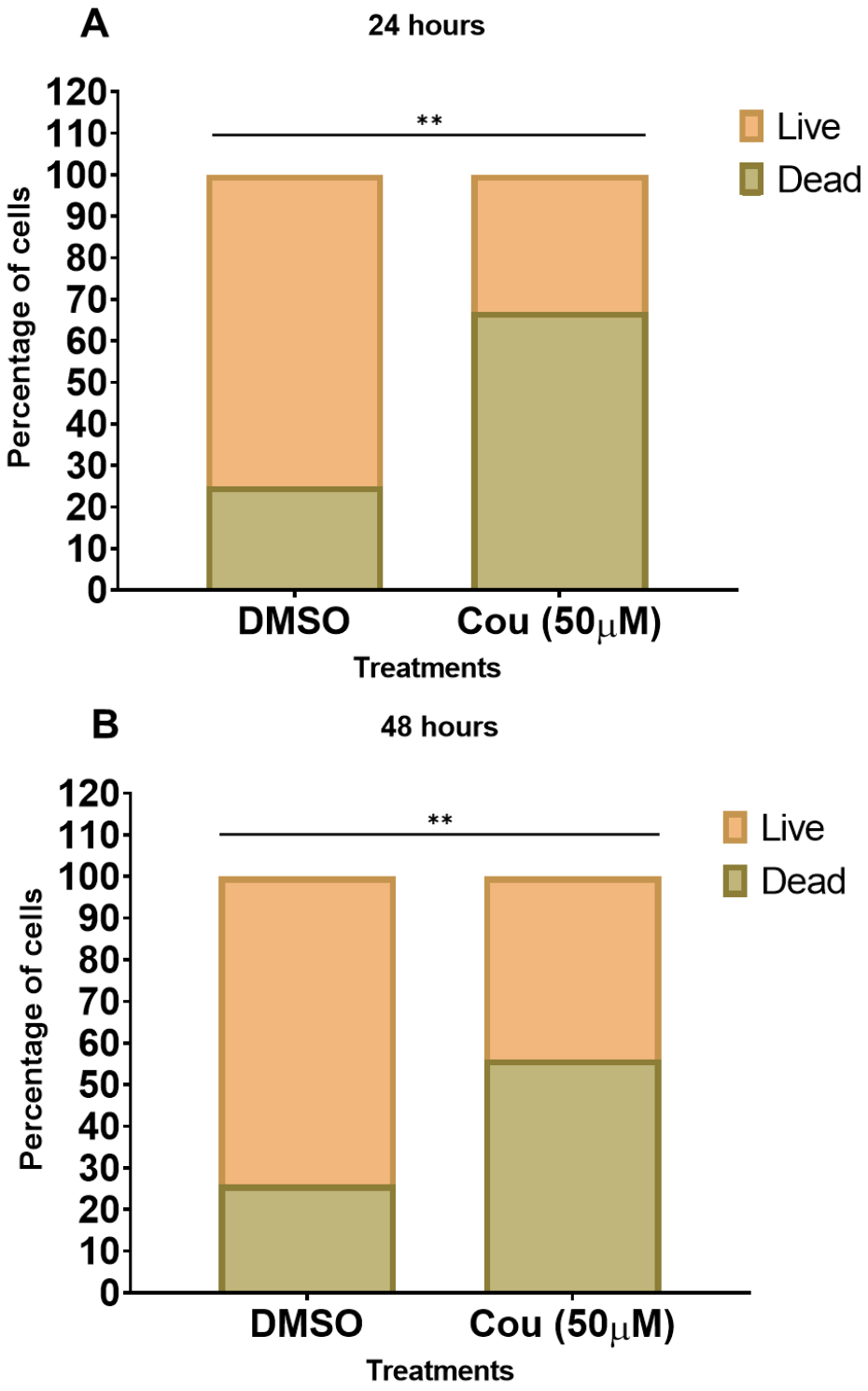

Figure 29. SUM149PT cells death induced upon coumestrol treatment. A trypan blue assay after twenty-four **(A)** and forty-eight **(B)** hours of coumestrol (50 µM) treatment showed an increase in the percentage of cell death. Values are expressed as a mean of three independent experiments**.** ** = $p<0.01$

2.4 Discussion and conclusions

The natural compound, Cou, has been known for its benefits regarding breast cancer patients who base their diet on a high soy consumption in the Chinese population (Shu et al., 2009). Our study presents that this phytoestrogen shows remarkable potential as an anti-cancer agent, particularly in TN-IBC. Our data show that Cou decreases ER-positive, non-IBC triple-negative, and TN-IBC cells viability but is more effective against TNBC and TN-IBC cells lines (Figure 21-23). A recent study performed in a 2D culture model showed that Cou decreases cell viability of ER-positive (MCF-7) breast cancer cell line with an IC_{50} value of 50.0 ± 2.1 µM after 72 hours of treatment (Zafar et al., 2017). Also, 45.2 ± 1.3 µM at 72 hours of treatment is the half-maximal inhibitory concentration of Cou against the TNBC cell line MDA-MB-231 in the 2D culture model (Zafar et al., 2018). Interestingly, the effect of Cou in our experiments differs from the one obtained in the literature for the MCF-7 cell lines. Our data shows a slight decrease (32%) in MCF-7 viability after 72 hours with 50 µM of Cou treatment (Figure 23B). In addition, in comparison with the IC_{50} reported in the literature, our relative cell viability assay showed a higher anti-proliferative effect with 50 µM of Cou treatment (68%) after 72 hours in MDA-MB-231 cells (Figure 23B). The differences in the half-maximal inhibitory concentration (IC_{50}) between our data and the reported literature could be explained since the experiments were carried out with different media conditions. The reported experiments were performed under complete growth medium (Zafar et al., 2017; Zafar et al., 2018). In contrast, our assays were

performed under a free-hormone medium which guarantees that the effects are due to the addition of coumestrol.

Surprisingly, our data showed that HER2 amplified IBC (SUM190PT) cell line showed resistance to increasing doses of Cou (Figure 22). Likewise, treatment with Cou at 50 µM shows a minor effect in cell viability inhibition in SUM190PT, suggesting that this subtype of IBC might be resistant to Cou (Figure 23 and 24). Interestingly, a study showed that SUM190PT cells have resistance to trastuzumab (Herceptin), targeted therapy to HER2 amplified breast cancer cell lines (Ginestier et al., 2007). A study showed that NF-kB activation leads to resistance to breast cancer therapy such as chemotherapy, radiotherapy, and endocrine therapy (Wang et al., 2015). Also, HER2 is an epidermal growth factor receptor that activates NF-kB (Wang et al., 2015). Based on this, further studies are needed to determine if the constant activation of NF-kB due to HER2 amplification plays a role in the resistance of SUM190PT cells to Cou treatment.

Regardless of the type, all the cancer cells possess the capacity to sustain proliferative signaling and activate invasion and metastasis, hallmarks of cancer (Hanahan & Weinberg, 2011). Our results demonstrated that E2 induces SUM149PT proliferation, migration, and invasion (Figure 25-27). In contrast, Cou inhibits SUM149PT cell proliferation after 10 days of treatment and does not induce migration and invasion after 18 and 22 hours of treatment, respectively (Figure 25-27). Similar effects were seen in prostate and ovarian cancers, with the additional findings that Cou induced apoptosis (Lim et al., 2017; Lim et al., 2016). Also, various studies demonstrated that Cou induces apoptosis and G1/S cell cycle

arrest in ER-positive and triple-negative non-IBC cell lines, but the cytotoxic effect of Cou in TN-IBC is unknown (Zafar et al., 2017; Zafar et al., 2018). Despite this, our data showed that Cou increases the percentage of dead cells by affecting the membrane of the cells (Figure 29). This data opens the opportunity to characterize the cytotoxic effects of Cou in the most aggressive breast cancer subtype, IBC.

Our study considers the effects of Cou in the presence and absence of E2. The increased proliferation and migration in response to E2 are significantly inhibited under Cou treatment (Figure 25, 26 and 27A). Due to this, experimental approaches combining both estradiol and coumestrol treatment will help us, in the long term, to determine if Cou will be an effective therapy that will benefit pre- and/or postmenopausal women. Furthermore, we need to consider that TNBC and IBC cases are more common in women younger than 50 years (premenopausal women) who naturally have E2 in their bodies (Wingo et al., 2004). Based on these facts, our data suggest that Cou in the presence of E2, could have a role in attenuating the progression of breast cancer. However, the potential role of Cou as a therapeutic drug for IBC has not been characterized using an *in vivo* model. For that reason, further investigation using xenografts mouse models of IBC are needed to validate the effectiveness of Cou as an anti-cancer agent in preclinical studies.

IBC is a type of breast cancer that does not produce a palpable mass; however, the cancer cells block lymph vessels by forming diffuse tumor cell clusters called tumor emboli, one of the hallmarks of IBC (Dobiasova & Mego, 2020; Mohamed et al., 2014). Unfortunately, IBC symptoms can be easily

confused with a breast infection or mastitis, producing a delay in proper diagnosis. Consequently, there is evidence suggesting that tumor emboli are responsible for IBC's aggressive and rapid metastasis phenotype (Dobiasova & Mego, 2020; Mohamed et al., 2014). The presence of cell clusters or tumor emboli in the breast lymph nodes is a current barrier to successful treatment for IBC patients (Arora et al., 2017). It has been found that IBC tumor cells retain epithelial markers like high E-cadherin expression and gain mesenchymal and stem-like (aldehyde dehydrogenase [ALDH]-positivity) characteristics, unlike non-IBC cells (Arora et al., 2017). Therefore, the retention of these phenotypes can be contributing to progression and survival of IBC tumor cells (Arora et al., 2017). In a proactive approach toward inhibiting progression of this disease, we could arrest tumor emboli growth by utilizing a natural compound like Cou.

Our study is pivotal in elucidating the effect of Cou in SUM149PT tumor emboli growth rate and is the first study that demonstrates the impact of a phytoestrogen in tumor emboli. Cou inhibits tumor emboli growth after 72 and 96 hours of treatment (Figure 8). This data confirmed that Cou might play a role in cancer metastasis hallmark by inhibiting tumor emboli growth, migration and invasion induced by E2.

The literature showed that the anti-cancer effect of Cou has been only studied under 2D culture models. Growing cells in a 2D culture model imply that the cells were seeded in monolayer polystyrene plastic flasks that do not mimic the natural tumor microenvironment of the cells. Thus, cell morphology and physiology could change compared to 3D culture models since *in vivo* environments are

surrounded by other cells and extracellular matrix (ECM) (Edmondson et al., 2014). It has been demonstrated that cell responses in 3D cultures are more similar to *in vivo* behavior than in 2D cultures (Edmondson et al., 2014). Also, compared to 3D cultures, a study performed in ovarian cancer showed a higher reduction of cell proliferation in 2D culture models under paclitaxel treatment (Loessner et al., 2010). Interestingly, diverse studies have shown that 3D cell cultures are more resistant to anticancer drugs (Karlsson et al., 2012; Loessner et al., 2010). This shows that our study is pivotal in determine the effect of a coumestrol in 3D culture models of breast cancer cell lines. Also, its open the opportunity for scientists in the field to performed studies using mouse models since the screening of drugs in 3D models are more representative to the *in vivo* studies (Belfiore et al., 2021).

This study reports that coumestrol shows remarkable potential as an anti-cancer agent. The anti-cancer effects of Cou in TN-IBC cells occur by decreasing pro-oncogenic phenotypes such as proliferation, migration, invasion, and tumor emboli formation. Interestingly, our study is pivotal in demonstrating the impact of a phytoestrogen in the hallmark of IBC, tumor emboli. Thus, our data present that a phytoestrogen, Cou, might play a role in cancer metastasis hallmark, which is the principal cause of death in IBC patients. Furthermore, this research presents an opportunity for other scientists to study the effect of Cou *in vivo* models to improve knowledge of natural compounds as potential treatments.

Chapter III. Molecular mechanism by which coumestrol exerts its anti-cancer activity

3.1 Introduction

Recent studies have shown an important role of estrogen non-genomic effects in various tumors, including ERα-negative breast cancers and IBC cell lines (Ohshiro et al., 2012). Studying novel signaling pathways and molecules that can target them is crucial for developing targeted therapeutics. These data give us the opportunity to study the possible anti-cancer effects of compounds that are considered antagonists of estrogen signaling, such as Cou (Chen et al., 2004; Hopert et al., 1998). It has been shown that Cou is similar in structure to E2 and binds to estrogen receptors and function as an antagonist (Bilal et al., 2014; Chen et al., 2004; Hopert et al., 1998). However, coumestrol anti-cancer activity may also be independent of modulating the estrogen non-genomic signaling. Despite this, reported literature on prostate and ovarian cancers showed that Cou decreased pro-oncogenic phenotypes by regulating the activity of various kinases such as PI3K/AKT and MAPK/ERK (Lim et al., 2017; Lim et al., 2016). Interestingly, AKT and ERK1/2 are kinases involved in the non-genomic signaling pathway upon estrogen treatment in triple-negative breast cancer cells. Based on the similar structures between Cou and E2 and their opposite effects, we **hypothesize that Cou exerts its cytotoxicity effect by inhibiting the activation**

of PI3K/AKT and/or MAPK/ERK pathway and by affecting the expression of genes involved in tumor suppressive activity.

3.2 Materials and methods

Cell protein extracts

SUM149PT cells were seeded in their respective plate in 25-30% confluency under complete growth medium (Table 7). After 24 hours, cells were placed under a free hormone or starving medium (DMEM/F12 without phenol red, and 1% Charcoal Stripped Fetal Bovine Serum) for 48 hours. To prepare cell lysates, the cells in 80-85% of confluency were treated with DMSO, E2 (10nM), or Cou (50µM) and placed in a 5% CO2 incubator for the corresponding time. After each timepoint, cells were washed with 1,000µl of 1X Phosphate buffered saline (PBS) and lysed using 100µl of 1X Cell Lysis Buffer (9803S; Cell Signaling Technology) for 10 minutes on ice in a shaker. Then, the plate was scraped to collect the lysate and transferred to a microtube. The cell lysates were centrifuged at 10,000 rpm for 20 minutes at 4ºC. The supernatant was transferred in a new tube and storage at -20ºC.

Table 7: Treatments before cells lysate.

Experiments	Seeding plates	Cou and E2 treatment time
Protein lysates for Western blot	6-wells plate	Timepoints (5, 10, 15, 30, 45, and 60 minutes)
Protein lysates for Human Phospho-Kinase Array	100mm plate	5 minutes

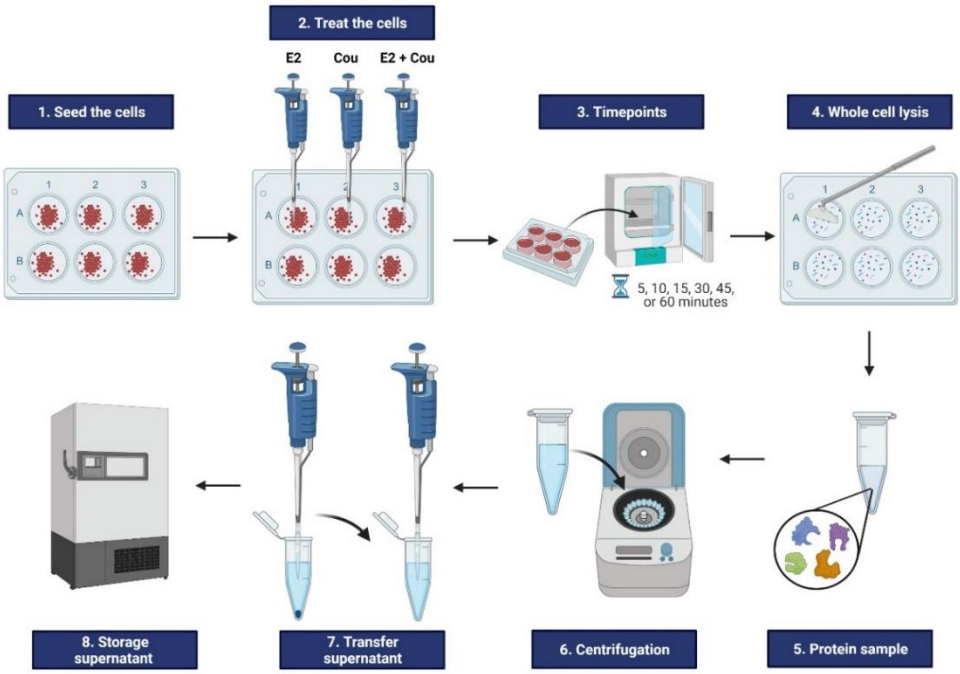

Figure 30. Summary of cell protein extracts protocol. (Created with BioRender.com)

Western blot analysis

First, we determined the concentration of protein in the cell lysate using the Pierce BCA Protein Assay Kit (Thermo Fisher Scientific). Then, an SDS-PAGE was run using 50µg of protein (cell lysate) in a 4–15% polyacrylamide gel (Mini-PROTEAN® TGX™ Gel; BioRad) and transferred to a PVDF membrane in a Trans-Blot Turbo Transfer System (BioRad) using mixed molecular weight protocol (1.3 amperage and 25 volts for 7 minutes). The membranes were blocked in 5% BSA in 1X Tris-buffered saline and 0.1% of Tween 20 (1X TBST) for 1 hour at room temperature in a shaker. Then, the membrane was incubated overnight at 4ºC with primary antibodies (Phospho-p44/42 MAPK (Erk1/2) (Thr202/Tyr204), p44/42 MAPK (ERK1/2), Phospho-Akt (Ser473) or GAPDH) diluted as manufacturer's instructions (Table 8). After the incubation, the membranes were

washed three times for 5 minutes in 1X TBST and incubated with corresponding secondary antibodies (Cell Signaling Technology) conjugated with HRP in 5% BSA in 1X TBST for 1 hour at room temperature. The membrane was developed using the ECL detection reagent (BioRad) in an Azure Sapphire™ Biomolecular Imager. A maximum of three strippings using mild stripping buffer (7.5g glycine, 0.5g SDS, 5mL Tween 20, pH 2.2, 500mL of water) was allowed per membrane.

Table 8: List of primary antibodies.

Antibodies	Dilution	Buffer	Catalog #	Manufacturers
Phospho-p44/42 MAPK (Erk1/2) (Thr202/Tyr204)	1:2000	2.5%BSA + 1X TBST	4370	Cell Signaling Technology
Phospho-Akt (Ser473) (D9E)	1:2000	2.5%BSA + 1X TBST	4060	Cell Signaling Technology
p44/42 MAPK (Erk1/2) (137F5)	1:1000	5%BSA + 1X TBST	4695	Cell Signaling Technology
AKT	1:1000	5%BSA + 1X TBST	9272	Cell Signaling Technology

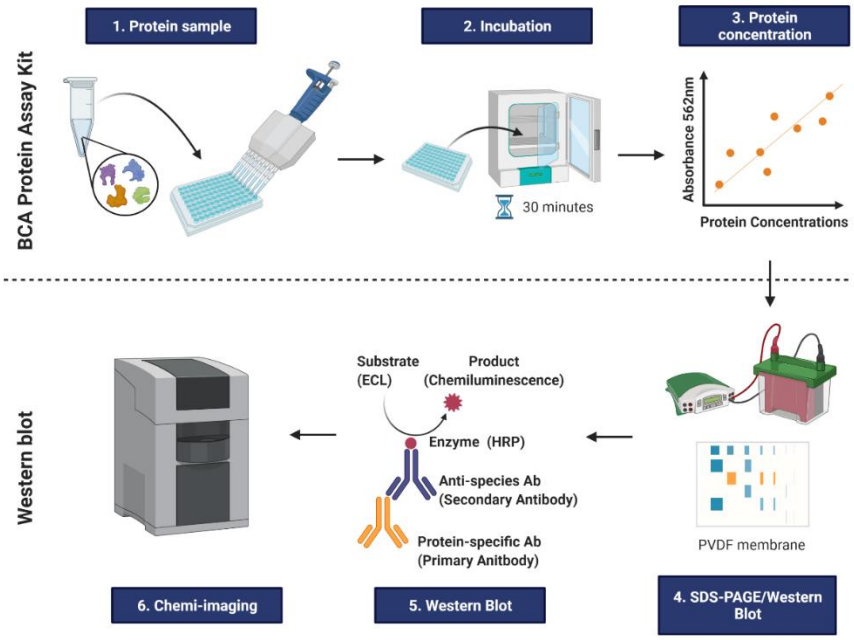

Figure 31. Summary of Western blot protocol. (Created with BioRender.com)

Human Phospho-Kinase Array

After collecting the cells lysates and determining the protein concentration, all the Human Phospho Kinase Array reagents were prepared per array set (A and B) as manufacturers instructions (R&D Systems). Each well of the 8-well multi-dish to be used was blocked with Array Buffer 1 and their respective membrane (part A or part B). After 1 hour of incubation at room temperature on a shaker, a total concentration of 450 µg of protein diluted with Array Buffer 1 was added to each membrane and incubated overnight at 4ºC on a shaker. Then, each set (A and B) was washed with 1X Wash Buffer. The diluted Detection Antibody Cocktail A was added into Part A membranes and the diluted Detection Antibody Cocktail B in Part B membranes. The membranes were placed into their appropriate wells and incubated for 2 hours on a rocking platform. Each set was washed with 1X Wash Buffer before adding diluted Streptavidin-HRP for 30 minutes. After washing with 1X Wash Buffer again, the membrane was developed using the ECL detection reagent (SuperSignal™ West Dura Extended Duration Substrate; Thermo Scientific) in the Azure Sapphire™ Biomolecular Imager for 10 minutes. We used ImageJ software for quantifying the mean gray value of every spot. Then, an average signal of the pair of duplicate spots representing each phosphorylated kinase protein was calculated. An average of the duplicate negative spot was subtracted from all measurements as a background. Using GraphPad Prism 9.0, a heatmap was generated after data normalization with DMSO. Finally, we analyzed the data using two-way ANOVA to determine the treatments' statistical significance difference (p-value).

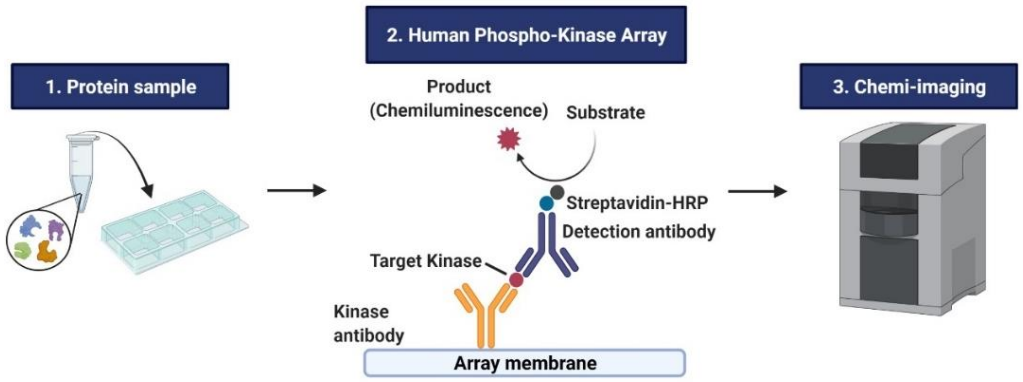

Figure 32. Summary of Human Phospho-Kinase Array protocol. (Created with BioRender.com)

RNA extraction

After two days of starving, we treated the SUM149PT cells for 1.5 hours with DMSO or Cou 50µM. Then, we removed the medium with the treatment and wash the cells with 1,000µl of 1X PBS. To lysate the cells, we added 350µl of RLT Buffer previously prepared with BME (1ml of RLT Buffer + 10µl of BME), followed by scrapping and collecting the lysates to transfer it to a QIAshredder Spin Columns (Qiagen, Cat.# 79656). Then, centrifuge at full speed for 2 minutes two times consecutively and measure the final collected volume. We added the same amount of volume of 70% ethanol. After mixing the sample with ethanol, we transferred 600µl to an RNeasy Mini Spin Columns (Qiagen, Cat.# 74104) and centrifuged it for 15 seconds at 8,000xg. We repeated the process until the total amount of volume was pass through the column. Then, we added 600µl of RW1 Buffer and centrifuged for 15 seconds at 8,000xg. Also, we added 500µl of RPE Buffer and centrifuged for 15 seconds at 8,000xg. We added 500µl of RPE Buffer again, centrifuged at 8,000xg for 2 minutes, and discarded the flow-through. Finally, the column was centrifuged for 1 minute at full speed, and we added 40µl

of RNAse free water. After 1 minute, the column was centrifuged for 1 minute at 8,000xg. The RNA was stored at -80C.

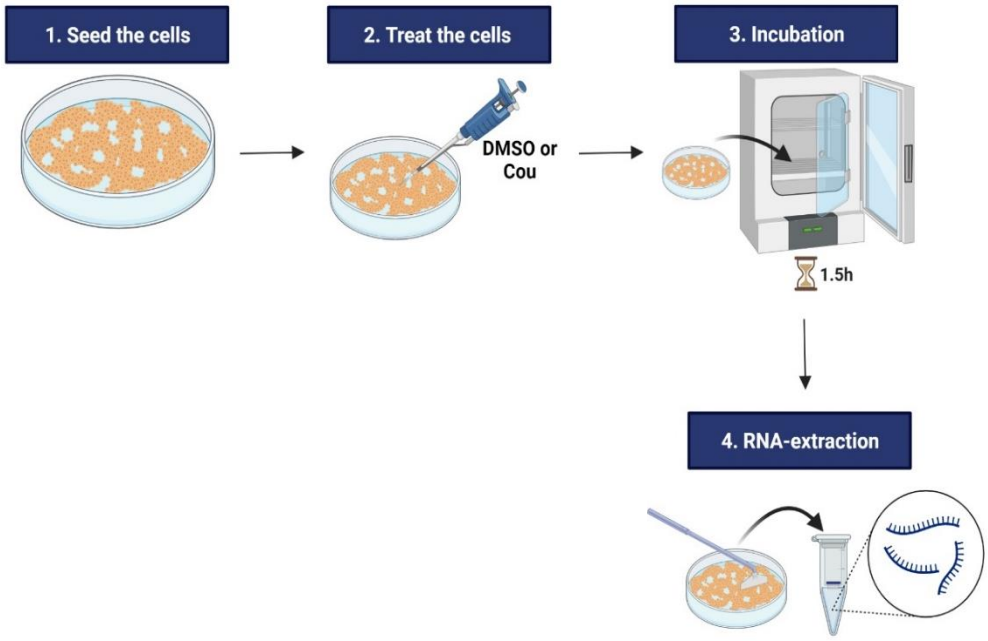

Figure 33. Summary of RNA extraction protocol. (Created with BioRender.com)

RNA sequencing

After performing the RNA extraction, the RNA concentrations were measured using NanoDrop and Qubit. We used a Truseq stranded mRNA Library with a polyA selection to prepare the cDNA. Also, to sequence the RNA, we use Hiseq High Output with 100 cycles (paired end). Raw RNA-seq reads will be quality assessed using fastQC (v0.11.9), and trimmed using fastp (v.0.20.0) and Trimmomatic (v0.39.0) prior to further analysis. Quality trimmed reads will be quantified using salmon (v1.4.0) by mapping to the GRCh38 human genome assembly. The R packages DESeq2 (v.1.32.0) and tidyverse (v1.3.1) were used to normalize and visualize counts (measured by TPM) for each experimental condition using a custom script available upon request.

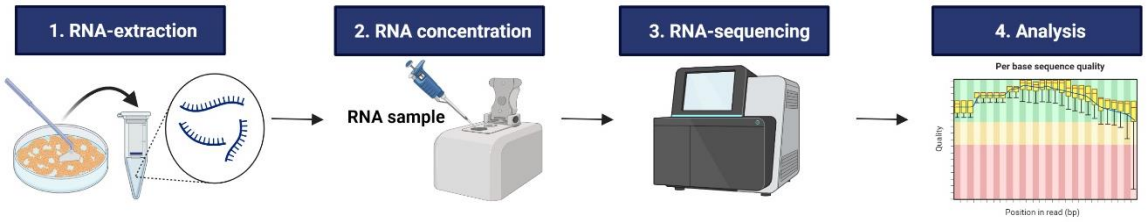

Figure 34. Summary of RNA sequencing protocol. (Created with BioRender.com)

qRT-PCR

After determined the concentration of the extracted RNA by a Nanodrop (Thermo Scientific), we performed a cDNA synthesis by using an iScript™ cDNA Synthesis Kit (Biorad, Cat.# 1708891). The method for RNA extraction We added in a PCR tube 4µl of 5X iScript Reaction Mix, 1µl of iScript Reverse Transcriptase, 1µg of the RNA template, and nuclease-free water for a total volume of 20µl as manufacturer's instructions (Table 9). The reaction mixture was incubated in the following thermal cycler conditions: 5 minutes at 25ºC, 20 minutes at 46º, 1 minute at 95ºC, and hold at 4ºC (Table 10). Then, iTaq™ Universal SYBR® Green Supermix (Biorad, Cat.# 1725121) and other reaction components were thawed at room temperature and stored on ice protected from light . All reactions were prepared by adding 10µl of iTaq™ Universal SYBR® Green Supermix, 400nM (final concentration from a 10µM working stock) of forward and reverse primers, and 7.4µl of nuclease-free water on ice as the manufacturer's instructions (Table 11). According to the sample number, a master mix was prepared with the mentioned reactions. After adding 19µl of the master mix to each well of the PCR plate, 1µl of cDNA (diluted by a factor of 1:8) was added to each well. A well with

the reaction components and without cDNA was used as a negative control. Finally, the plate was covered with a transparent film and incubated in the Biorad® CFX96™ Real-Time PCR System under the following conditions:30 seconds at 95ºC, 5 seconds at 95ºC, 30 seconds at 60 ºC, repeat the steps 40 cycles, melt curve at 95 ºC by 0.5 ºC increment and hold at 4 ºC (Table 12 and Figure 35). A column chart using GraphPad Prism 9.0 was generated using the three biological replicates per treatment calculated by the Pfaffl method.

$$Ratio = \frac{2^{\Delta Ct,target\ (calibrator-test)}}{2^{\Delta Ct,ref\ (calibrator-test)}}$$

$$=2^{-[(Ct,target\ (test)-Ct\ target\ (calibrator)]\ -[(Ct,ref\ (test)-Ct,ref\ (calibrator)]}$$

$$= 2^{-\Delta\Delta Ct}$$

Table 9: qRT-PCR reaction protocol.

COMPONENT	VOLUME PER 20µL REACTION	FINAL CONCENTRATION
ITAQ™ UNIVERSAL SYBR® GREEN SUPERMIX (2X)	10µl	1x
FORWARD AND REVERSE PRIMERS	Variable	400 nM each
DNA TEMPLATE	1 µl	cDNA: 1:8
H_2O	Variable	-

Table 10: cDNA synthesis reaction protocol.

STEP	TIME AND TEMPERATURE
PRIMING	5 minutes at 25ºC
REVERSE TRANSCRIPTION	20 minutes at 46º
RT INACTIVATION	1 minute at 95ºC
OPTIONAL STEP	Hold at 4ºC

Table 11: Primer sequences.

GENE	SEQUENCE
TIPARP	FW 5‘CCACTACATCCTCCACAATTC’3 RV 3‘CCCACCAAGTGTCTGTAAAT’5
GAPDH	FW 5‘CAAGAGCACAAGAGGAAGAGAG’3 RV 3‘CTACATGGCAACTGTGAGGAG’5

Table 12: qRT-PCR thermal cycling protocol.

STEPS		TIME AND TEMPERATURE
POLYMERASE ACTIVATION AND DNA DENATURATION		30 sec at 95ºC
AMPLIFICATION	Denaturation	5 sec at 95ºC
	Annealing/Extension + Plate Read	30 sec at 60 ºC
	Cycles	40
MELT-CURVE ANALYSIS		95 ºC by 0.5 ºC increment for 5 sec
OPTIONAL STEP		Hold at 4ºC

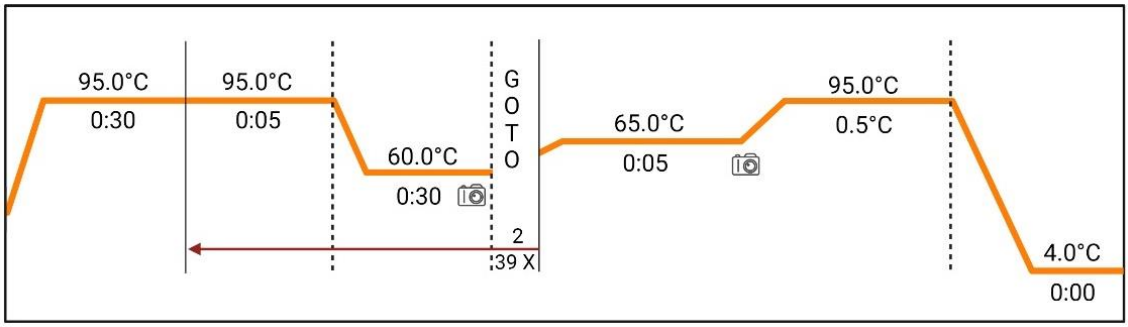

Figure 35. qRT-PCR thermal cycling protocol. (Created with BioRender.com)

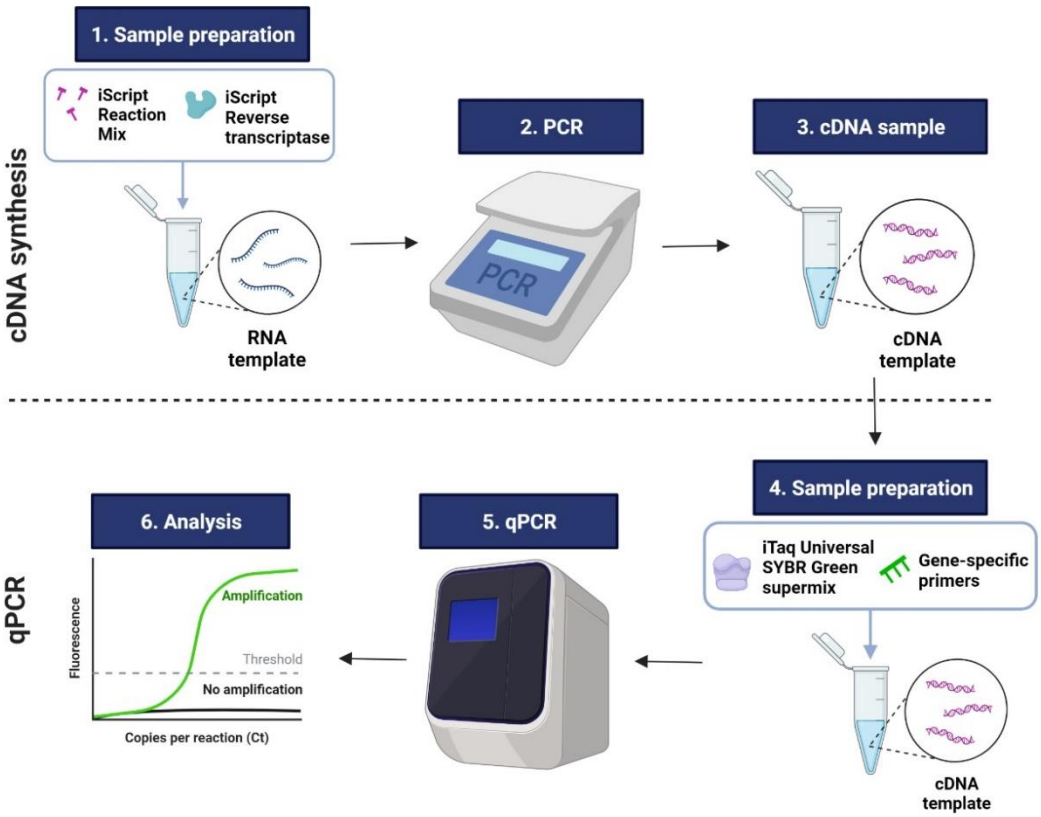

Figure 36. Summary of qPCR protocol. (Created with Biorender.com)

3.3 Results

Coumestrol inhibits phosphorylation of downstream kinases and other effector proteins of the oncogenic PI3K/AKT and MAPK/ERK pathways

Due to the effects on cell proliferation and migration of Cou shown in SUM149PT cells, a Proteome Profiler Human Phospho-Kinase Array was used to determine changes in phosphorylation levels of key kinases and effector proteins upon E2 and Cou treatment. Previous studies have shown including this thesis work that TN-IBC cells express alternate estrogen receptors that promote proliferation and migration via a non-genomic signaling pathway (phosphorylation of ERK1/2 and AKT) after E2 treatment (Ohshiro et al., 2012). This data shows that E2 can induce pro-oncogenic phenotypes in TN-IBC by the alternative

estrogen non-genomic signaling pathway. Interestingly, Cou reduces, and E2 increases the phosphorylation of protein kinases involved in the PI3K/AKT and MAPK/ERK oncogenic signaling pathway (Figure 37 and 38). Specifically, in comparison to E2, Cou decreases the phosphorylation of AKT at S473 residue (Figure 37 and 38). Also, ERK1/2 phosphorylation decreases after Cou treatment (Figure 37B and 38). Similar inhibition of ERK1/2 and AKT phosphorylation was observed after treating the cells with the combination of treatments suggesting that the effects of E2 on phosphorylation levels was inhibited by the presence of Cou (Figure 37). In comparison to E2, Cou decreases the phosphorylation of downstream kinases of the PI3K/AKT pathway such as PRAS40, p70 S6 residues T421/S424 and T389, among other kinases (Figure 38). It has been shown that PRAS40 promotes tumorigenesis by mediating cell proliferation, and metastasis, and p70 S6 is crucial for cell cycle progression (Dufner & Thomas, 1999; Lv et al., 2017; Pullen & Thomas, 1997). Similarly, Cou reduced the phosphorylation levels of p-STAT5a/b, which induces AKT transcription, and p-GSK-3α/β, a substrate of PI3K/AKT/mTOR pathway, by 36% and 28%, respectively (Figure 38) (Schmidt et al., 2014; Song et al., 2006). Similarly, HSP27 and β-catenin phosphorylation decrease after Cou treatment (Figure 38). Interestingly, the combination of treatments increases heat shock protein 27 (HSP27) phosphorylation associated with an induction in cell migration and drug resistance of breast cancer cells (Wei et al., 2011). Also, Cou decreases the phosphorylation of CREB which is a transcription factor that induces the expression of genes involved in the regulation of proliferation and apoptosis (H. Zhang et al., 2020). CREB can be

phosphorylated by AKT and ERK1/2 and Cou reduces the phosphorylation of these three kinases (Figure 38).

In addition, Cou affects the phosphorylation level of kinases involved in the MAPK/ERK pathway, such as Lck, Lyn, MSK1/2 among others. Cou decreases the phosphorylation of Lck, which promotes angiogenesis, and Lyn, which is involved in growth, motility, and invasion (Choi et al., 2010; Vahedi et al., 2015) (Figure 37). Also, Cou reduces the phosphorylation of kinases that plays a role in cell proliferation, such as MSK1/2 and PLC-γ1 (Emmanouilidi et al., 2017; Pu et al., 2018) (Figure 38). Interestingly, in comparison with E2, no change in phosphorylation levels of these kinases (Lck, Lyn, MSK1/2, and PLC-γ1) is observed in the combination of treatments (Figure 38). Nevertheless, this data suggests that the inhibition of phosphorylation levels shown by Cou was inhibited by E2 treatment. In comparison with E2, Cou reduces the phosphorylation of kinases involved in cancer cell proliferation, invasion, and migration like PYK2 and RSK1/2 (Shen & Guo, 2018; Zhao et al., 2016) (Figure 38).

.

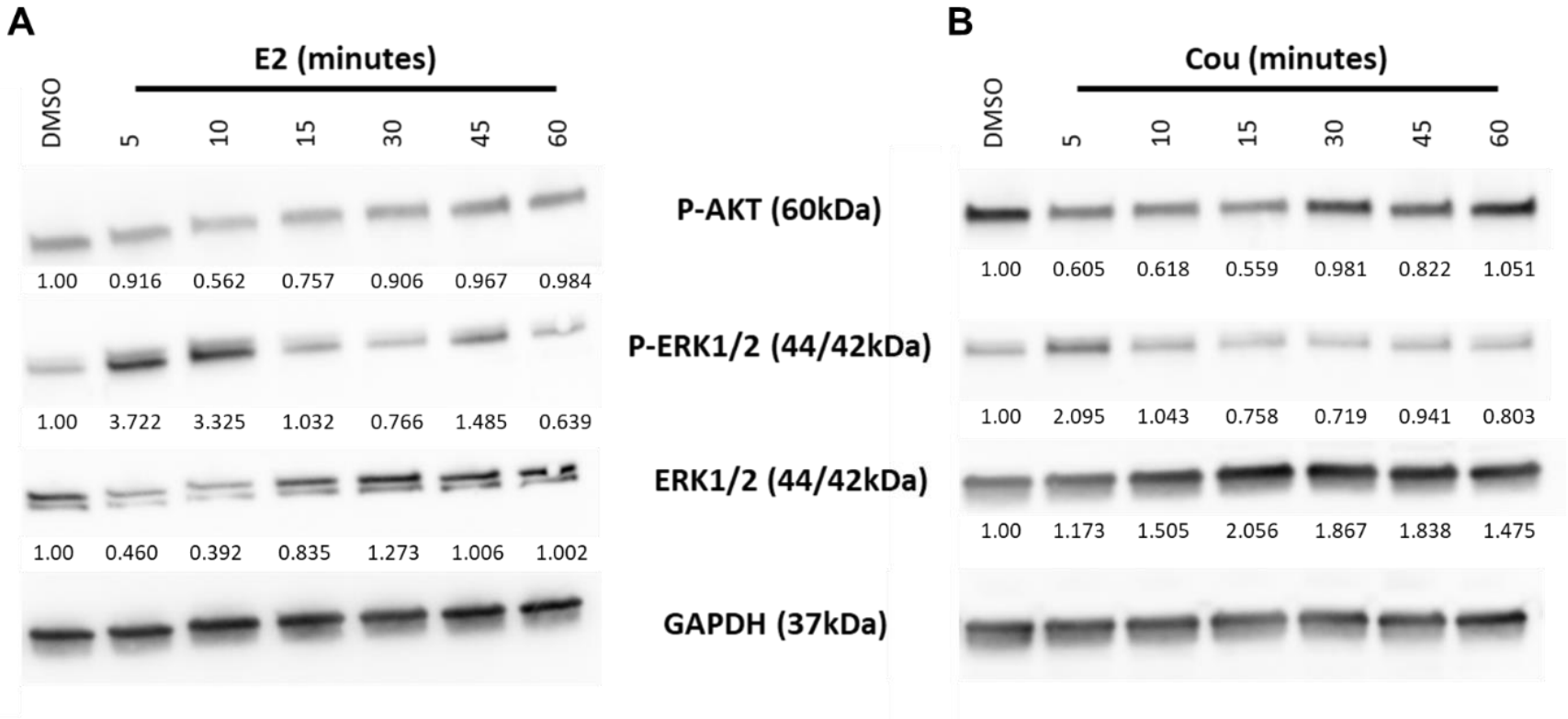

Figure 37. Activation of downstream kinases of the estrogen non-genomic signaling pathway in IBC cell lines. (A) Phosphorylation of p44/42 ERK was seen in the SUM149PT cell line after 5 minutes of estradiol treatment. Also, there is no phosphorylation in AKT upon estradiol treatment. **(B)** Coumestrol reduces the phosphorylation levels of AKT and p44/42 ERK after 5 to 15 and 15 to 30 minutes of treatment, respectively. GAPDH was used as a loading control.

Similarly, Cou decreases the phosphorylation of epidermal growth factor receptor (EGFR), a receptor that is overexpressed in triple-negative inflammatory breast cancer (Wang et al., 2017) (Figure 38). Interestingly, a study showed that inhibition of EGFR inhibited IBC tumor growth and metastasis (Wang et al., 2017). Also, Cou decreases the phosphorylation of src, which is a kinase involved in the signaling and crosstalk of estrogen receptors (ER) and EGFR (Finn, 2008) (Figure 38). In addition, src is involved in tumor angiogenesis similar to PDGF-Rβ, another tyrosine kinase receptor that Cou reduces its phosphorylation (Finn, 2008; Jansson et al., 2018) (Figure 38). Cou showed a decrease in phosphorylation of different kinases such as FGR, STAT2, and YES (Figure 38). YES is a kinase that acts as a tumor suppressor and an oncogene depending on its expression levels (Kim et al., 2015). STAT2 is involved in inflammatory response and cancer initiation (Lee et al., 2020). In summary, all these data allow us to hypothesize a pathway by which Cou exerts its anti-cancer effect in IBC (Figure 39). PDGF-Rβ can induce the phosphorylation of src, which can be involved in cross-activation of the EGFR receptor, our suggested pathway shows that Cou inhibits the phosphorylation of these three kinases. Also, the decrease in the phosphorylation levels of EGFR explained how Cou inhibits the activation of kinases involved in the ERK pathway. One explanation for the reduction in the AKT pathway's phosphorylation is that Cou decreases the phosphorylation levels of PDGF Rβ. Also, Cou reduces the expression AKT by lowering the STAT5 phosphorylation, which is a transcription factor involved in the transcription of AKT.

Based on the similar structures between Cou and E2, our hypothesis was to observe an inverse effect on kinase phosphorylation levels. That is, if an increase in the phosphorylation of a kinase occurs under E2 treatment, a decrease in phosphorylation levels should occur when treated with Cou. Despite this, we saw that some effects of Cou are independent of E2 because the phosphorylation levels of src, JNK1/2/3, MSK1/2, and EGFR decreased under Cou's treatment without any changes when cells were treated with E2 (Figure 38). Our data reveal that Cou can alter E2-independent signaling cascades in IBC cells.

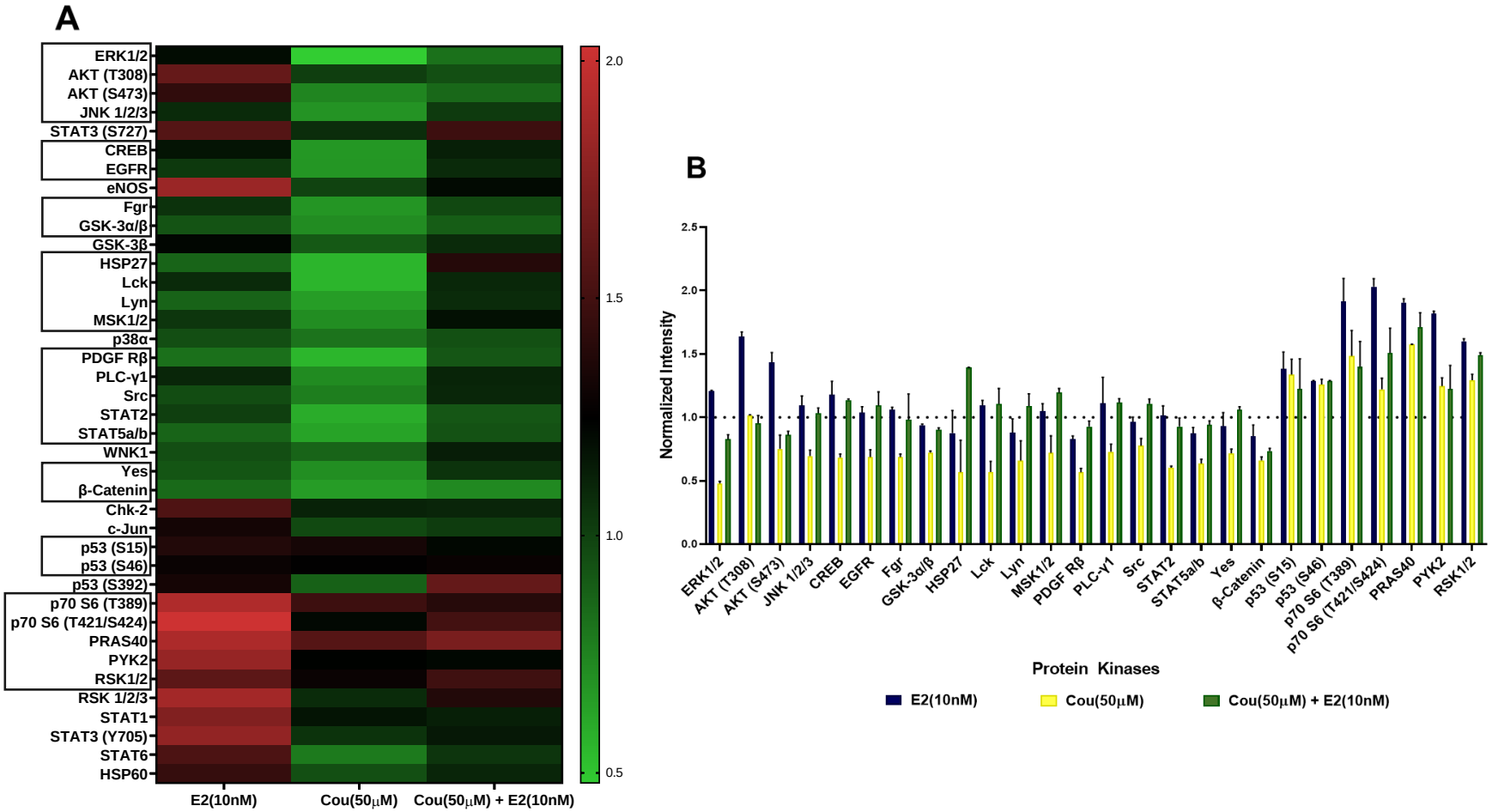

Figure 38. Reduction in the phosphorylation levels of downstream kinases in IBC cell lines. (A) Human Phospho-Kinase Array showed the phosphorylation levels of 39 kinases after 5 minutes of estradiol, coumestrol, or a combination of treatments in SUM149PT cells. The boxes show 26 kinases that have a significant difference with DMSO. **(B)** Bar graph of the 26 kinases that have significant differences with DMSO. Coumestrol decreases, and estradiol induces the phosphorylation of downstream kinases involved in the estrogen non-genomic signaling pathway, such as ERK1/2 and AKT.

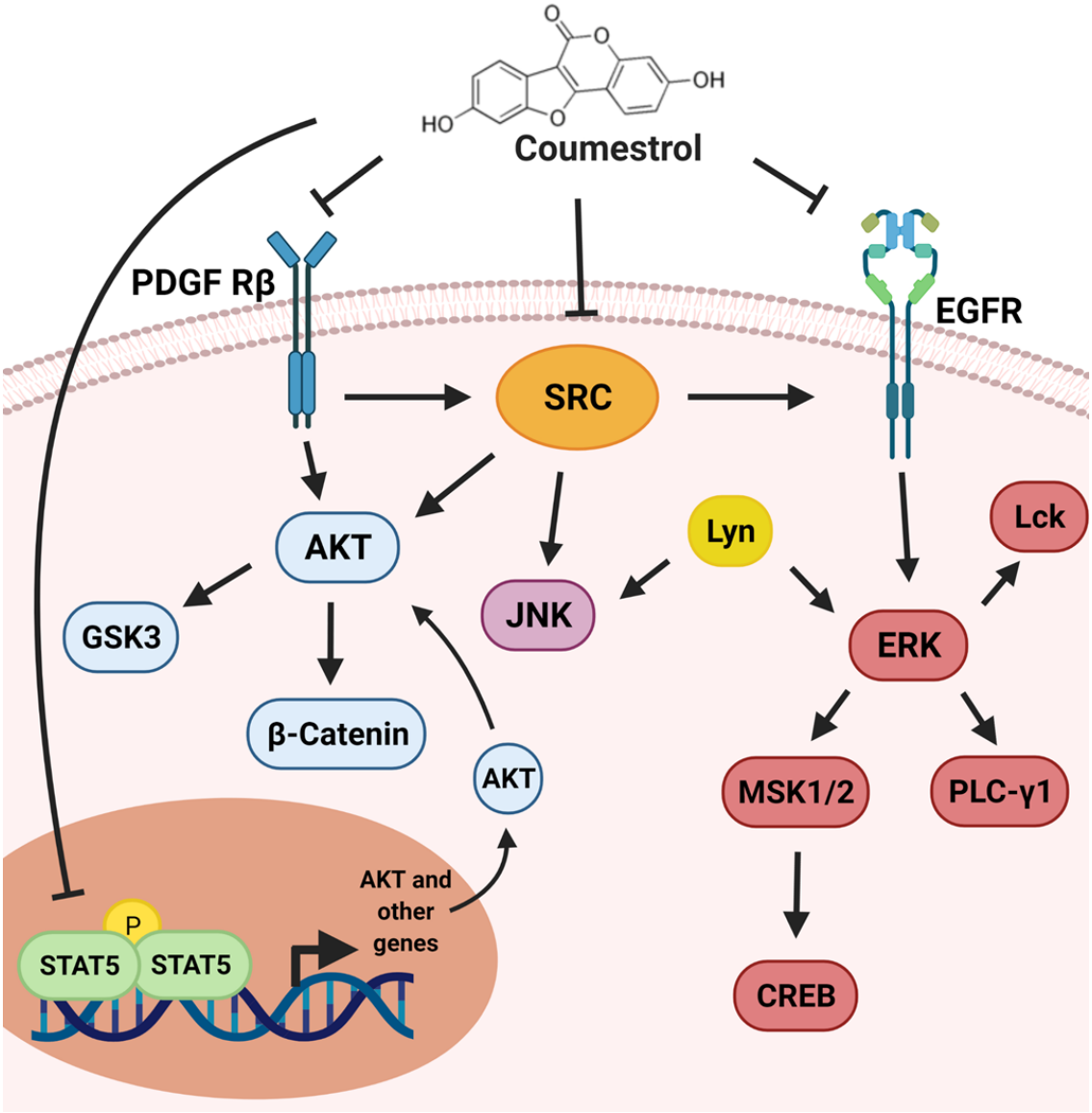

Figure 39. Proposed signaling pathway by which coumestrol exerts its anti-cancer effects. The proposed coumestrol signaling pathway was designed using the data obtained in the Human Phospho-Kinase Array. (Created with Biorender.com)

Coumestrol up-regulate the expression of TIPARP

Coumestrol has an anti-cancer effect by regulating the phosphorylation levels of multiple kinases (Lim et al., 2017; Lim et al., 2016). However, the effect that Cou can exert on the transcription levels of genes involved in oncogenic pathways remains unknown. Differentially expressed genes (DEGs) were identified by RNA-seq analysis after treated SUM149PT cells with Cou (Figure 40). Eleven and fourteen genes were down and up-regulated upon Cou treatment, respectively (Figure 40B). The top 5 most significant DEGs upon Cou treatment were TIPARP, ARRDC3, FAM43A, EGR3, and FOXS1 (Table 13). Particularly, TIPARP, ARRDC3, and FAM43A were up-regulated, while EGR3 and FOXS1 were down-regulated (Figure 40A and Table 13). Notably, TIPARP up-regulation upon Cou treatment was confirmed in qPCR analysis (Figure 41). TCDD Inducible Poly (ADP-Ribose) Polymerase (TIPARP) is the gene with the most significant difference with a p-value of 1.77E-252 (Table 13). Interestingly, TIPARP is a tumor suppressor gene identified as a novel therapeutic target in breast cancer involved in the hallmark of angiogenesis (Cheng et al., 2019; L. Zhang et al., 2020).

To estimate the biological functions of the DEGs and confirm that they were highly enriched in processes related to angiogenesis, we performed a Gene Ontology (GO) enrichment analysis (Figure 42). Notably, the GO enrichment analyses demonstrated that DEGs identified by RNA-sequencing were highly enriched in functions related to blood vessel development or angiogenesis (Figure 42). Also, the DEGs were involved in gonad development and the steroid metabolic process. Based on all the data obtained in the Human Phospho-Kinase Array, RNA

sequencing, and GO we suggest a possible pathway by which Cou could exert an anti-angiogenic effect (Figure 43). The suggested pathway showed that Cou reduces the phosphorylation levels of PDGF Rβ, an activator of AKT, which caused a decrease in the AKT/mTOR signaling pathway activation. Consequently, AKT/mTOR signaling pathway does not induce the transcription of HIF-1α producing a reduction in angiogenesis by inhibiting VEGF. Similarly, Cou reduces the phosphorylation of β-catenin and Lck, which are involved in VEGF transcription. VEGF is a molecule involved in blood vessel development, angiogenesis. In other words, the reduction in VEGF transcription inhibits the angiogenesis processes. Likewise, Cou up-regulates the expression of TIPARP, which is involved in the degradation of HIF-1α and, consequently, induces an anti-angiogenic effect,

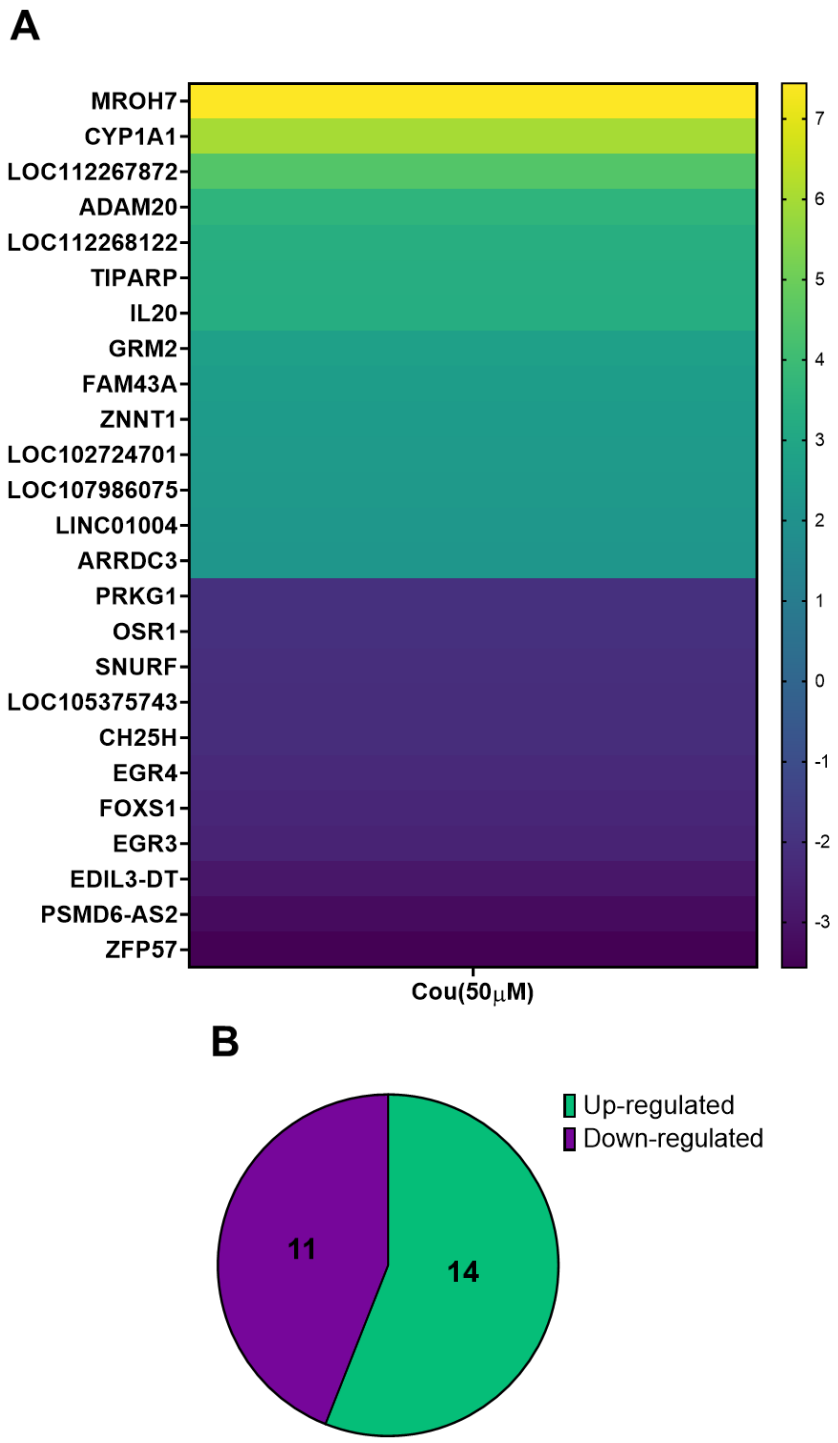

Figure 40. RNA-sequencing in IBC in cell lines treated with coumestrol for an hour and a half. Heatmap shows twenty-five differential expressed genes with a log fold change higher than 2 (**A**). After treating SUM149PT cells with coumestrol (50µM). Eleven and fourteen of these genes (**B**) were up and down-regulated, respectively.

Table 13: Top 5 regulated genes by coumestrol treatment in IBC cells lines.

Genes	p-value	Coumestrol response	Functions	References
TIPARP	1.77E-252	Up-regulated	In breast cancer patients, inhibits: • Cells growth • Suppresses tumorigenesis in xenograft models TIPARP could be considered a potential therapeutic target for breast cancer	(L. Zhang et al., 2020) (Cheng et al., 2019)
ARRDC3	4.42E-94	Up-regulated	In the MDA-MB-231 cell line (TNBC), represses: • Proliferation • Migration • Invasion • I*n vivo* tumorigenicity	(Arakaki et al., 2018) (Draheim et al., 2010)
FAM43A	6.82E-29	Up-regulated	Remains unclear	(Chen et al., 2011)
EGR3	2.9E-09	Down-regulated	In breast cancer, down regulation of EGR3 is related to: • Tumor stage In human umbilical vein endothelial cells, down regulation of EGR3 inhibits: • Migration • Vascular endothelial growth factor (VEGF) mediated angiogenesis	(Zhou et al., 2021) (Liu et al., 2008)
FOXS1	4.67E-06	Down-regulated	In gastric cancer, down regulation of FOXS1 inhibits: • Proliferation • Cell colony formation In breast cancer, high expression of FOXS1: • Correlated to improved relapse-free survival FOXS1 can be an oncogene or tumor suppressor gene depending on the cancer type.	(Wang et al., 2019) (Koch, 2021)

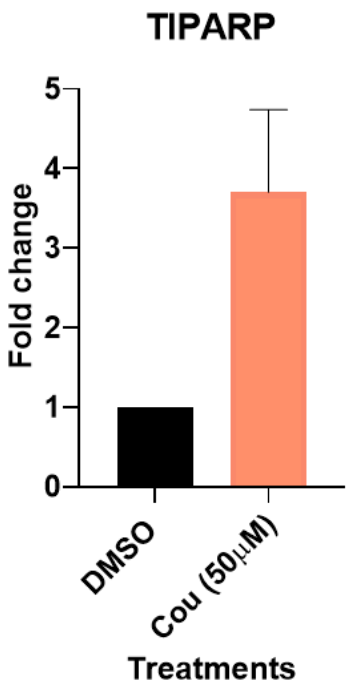

Figure 41. TIPARP is up-regulated upon coumestrol treatment in SUM149PT cells. qRT-PCR confirms the RNA-sequencing analysis. Coumestrol up-regulated the expression of TIPARP after 1.5 hours of treatment by a fold change of 3.70.

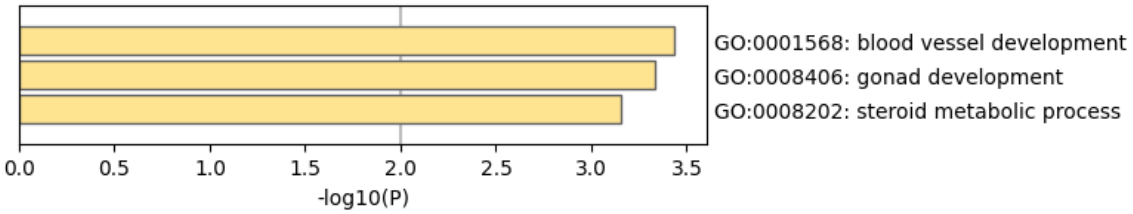

Figure 42. Meta-analysis in IBC cell lines treated with coumestrol. Coumestrol affects genes involved in blood vessel development, angiogenesis.

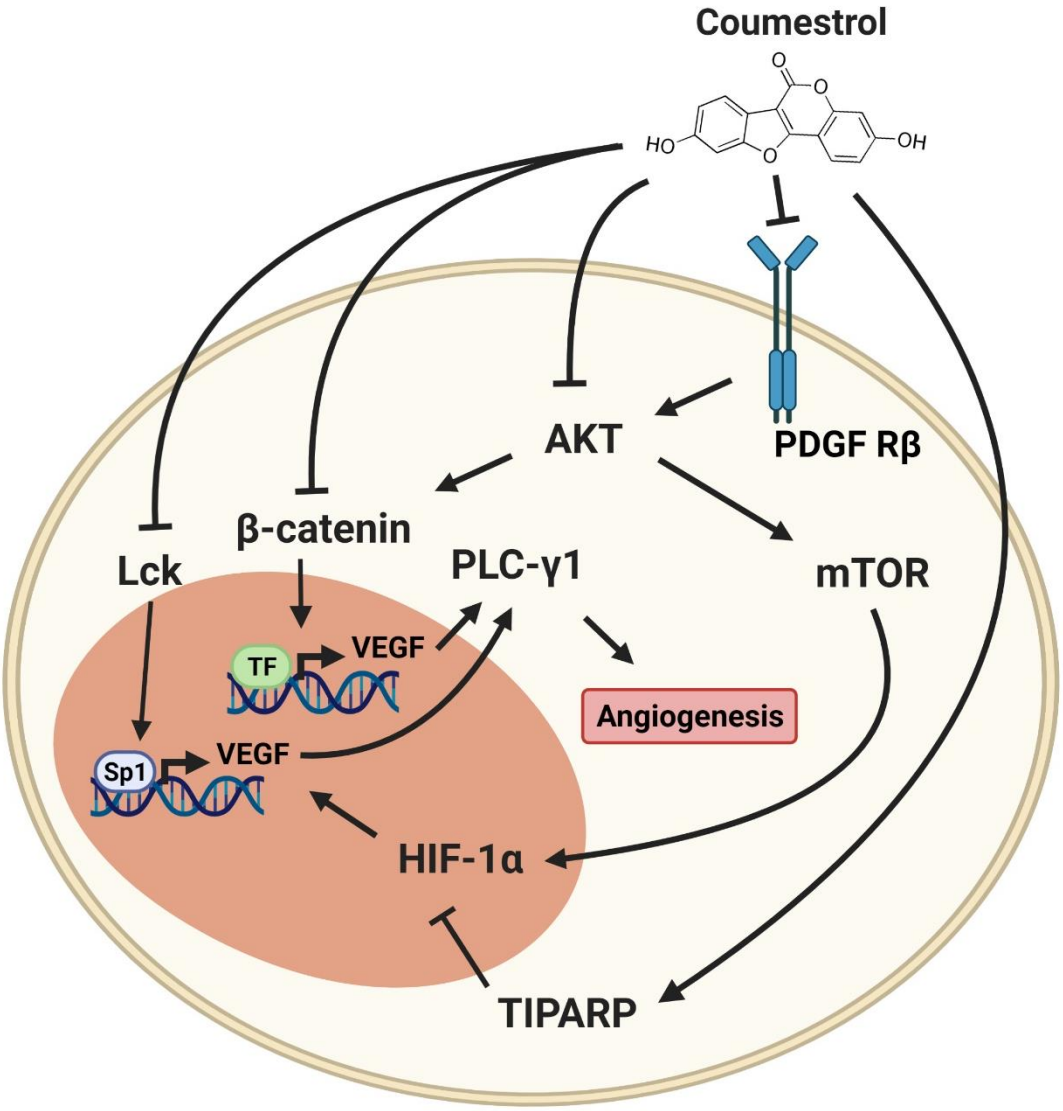

Figure 43. Proposed signaling pathway by which coumestrol induces an anti-angiogenic effect. The proposed coumestrol signaling pathway was designed using the data obtained in the Human Phospho-Kinase Array and RNA-sequencing. (Created with Biorender.com)

3.4 Discussion and conclusions

IBC patient's treatment consists in trimodality therapy with upfront systemic therapy, including chemotherapy, total mastectomy, axillary lymph node dissection, radiation to the chest wall, and regional draining lymph nodes (Rosenbluth & Overmoyer, 2019). Despite this, there are no effective targeted therapeutics for TN-IBC patients (Dawood et al., 2011; Li et al., 2011; Masuda et al., 2013). Tamoxifen, a targeted therapy for ER-positive breast cancer cell lines, has an agonist effect in TNBC cell lines which express alternative estrogen receptors (Gu et al., 2014; Wang et al., 2018). ICI182,780 (Fulvestrant), a targeted therapy for ER-positive breast cancer lines, accelerates the degradation of ER-α66, but it fails to induce degradation of ER-α36 (Gu et al., 2014; Su et al., 2014). Therefore, TN-IBC patients have a significantly worse prognosis and a greater 5-year recurrence rate (Wei et al., 2014). Given the lack of efficiency in TN-IBC targeted treatments, there is an urgent need to explore the underlying mechanism in TN-IBC cells in order to develop new targeted approaches for its treatment.

Triple-Negative Inflammatory Breast Cancer expresses alternate estrogen receptors that promote proliferation, migration, and invasion via a non-genomic signaling pathway (ERK and AKT kinases) upon estrogen treatment (Ohshiro et al., 2012). Interestingly, in prostate and ovarian cancers, Cou decreased proliferation and migration by regulating the activity of PI3K/AKT, ERK1/2, and JNK/MAPK signaling pathways (Lim et al., 2017; Lim et al., 2016). Particularly, Cou decreases the phosphorylation of AKT and activates ERK1/2 and JNK signaling pathways to reduce prostate cancer cell progression (Lim et al., 2017).

However, in ovarian cancer, Cou reduces the phosphorylation of ERK1/2, AKT, and JNK (Lim et al., 2016). This data suggests that the effects of Cou on the phosphorylation levels of tyrosine kinases such as ERK and JNK/MAPK signaling pathways varies depending on the cancer type. Nonetheless, similarly to ovarian cancer, Cou decreases the phosphorylation of ERK1/2, AKT, and JNK in SUM149PT cells (TN-IBC) (Figure 31 and 32). These similarities on breast and ovarian cancer were expected since both cancers share many genetic and epigenetic parallelism, changes in hormone regulation, and similar tumor suppressors (Longacre et al., 2016). Also, Cou decreases the phosphorylation of downstream kinases of the ERK and AKT signaling pathway involved in cell proliferation such as PRAS40, CREB, MSK1/2, PLC-γ1 and others, suggesting the possible mechanism by which Cou exerts its anti-proliferative effect (Figure 32). The anti-migration effects of Cou could be exerted by the reduction in the phosphorylation of ERK and AKT signaling pathway downstream kinases such HSP27, Lyn, PYK2, RSK1/2, EGFR, and other kinases (Figure 32). Also, Cou showed a decrease in the phosphorylation of kinases that play a role in angiogenesis, such as Lck, Src, and PDGF-Rβ, suggesting a role in this hallmark (Figure 32). Interestingly, gene ontology showed that coumestrol disrupted the expression of genes involved in blood vessel development, angiogenesis (Figure 41). Also, coumestrol upregulated TIPARP which promotes the degradation of a regulator of angiogenesis, HIF-1α (Figure 40 and Figure 41). In addition, we suggest that the inhibition of tumor emboli growth by Cou treatment could be mediated by the reduction of NF-kB phosphorylation. NF-kB is a transcription

factor that plays a role in inflammation and tumor emboli formation and its activation occurs downstream of EGFR and AKT pathways (Arora et al., 2017; Bai et al., 2009; Wang et al., 2015). Our data showed a reduction in EGFR and AKT phosphorylation, activators of NF-kB. Despite this, additional studies are needed to determine the effects of Cou regarding NF-kB activation and if this activation is mediated by the inhibition of EGFR and AKT phosphorylation upon Cou treatment.

Our study demonstrated that Cou induces an effect on the phosphorylation levels of various kinases and affects the expression levels of genes involved in suppressing pro-oncogenic phenotypes (Figure 40). DEGs analysis showed that Cou affects the expression levels of 25 genes. The most significant DEGs included three up-regulated genes (TIPARP, ARRDC3, and FAM43A) and two down-regulated genes (EGR3 and FOXS1). In fact, overexpression of TIPARP was found to decrease the ligand-dependent estrogen receptor α (ERα) signaling (Rasmussen et al., 2021). Increase in cell proliferation and expression of ERα target genes was observed after treating ER-positive breast cancer cells with TIPARP-knockdown and E2 (Rasmussen et al., 2021). Another study demonstrated that TIPARP forms distinct nuclear condensates in an ADP ribosylation-dependent manner, recruiting both HIF-1α and an E3 ubiquitin ligase, promoting the degradation of hypoxia-inducible factor one alpha (HIF-1α) (Balfour, 2020; L. Zhang et al., 2020). HIF-1α is a transcription factor that regulates one of the hallmarks of cancer, angiogenesis. Interestingly, studies shown that AKT pathway (kinase that decreases its phosphorylation upon Cou treatment) enhances HIF-1α signaling and expression (Stegeman et al., 2016). In summary,

all this data suggests that TIPARP activation should be the target of future cancer drugs (Balfour, 2020). Also, studies have shown upregulation of ARRDC3 represses proliferation, migration, and invasion in TNBC cell lines (Arakaki et al., 2018; Draheim et al., 2010). Interestingly, the upregulation of FAM43A remains unclear, suggesting that new studies are needed to elucidate its effect (Chen et al., 2011). Early growth response proteins (EGR) are rarely studied in breast cancer cases, which implies a gap in knowledge on whether or not this protein have a role in breast tumorigenesis (Zhou et al., 2021). Despite this, a study analyzed a database of breast cancer patients and determined that downregulation of EGR3 is related to a higher tumor stage (Zhou et al., 2021). Also, an *in vitro* study performed in human umbilical vein endothelial cells (HUVEC) showed that downregulation of EGR3 inhibits migration and angiogenesis mediated by vascular endothelial growth factor (VEGF) (Liu et al., 2008). A study demonstrated that downregulation of FOXS1 inhibits proliferation and cell colony formation of gastric cancer (Wang et al., 2019). On the contrary, upregulation of FOXS1 in breast cancer was correlated to improved relapse-free survival (Koch, 2021). Thus, FOXS1 can be an oncogene or tumor suppressor gene depending on the cancer type (Wang et al., 2019).

This study reports the potential that coumestrol has as a novel hormonal targeted therapeutic for TN-IBC cells. While uncovering the inhibition of the different hallmarks in cancer mentioned in this project, we can propose a mechanism of action for this phytoestrogen. Furthermore, these research findings present an opportunity for other scientists in the field to test and identify other

natural compounds that may antagonize the estrogen non-genomic signaling pathway. In other words, this research has the potential to bring new advantages in the discovery of natural compounds that inhibit the downstream effects of the ERK and AKT signaling pathway. The data gathered from this work is pivotal to achieving the long-term goal of developing effective targeted therapies for IBC to improve patients' prognosis, survival rates, and quality of life.

Chapter IV: Future directions

Our data demonstrated that Cou increases the cell death in TN-IBC cells, but the specific mechanism by which Cou exerts its cytotoxic effects is unknown. The literature reported that Cou increases the expression or activation of pro-apoptotic proteins and reduces the expression of anti-apoptotic and cell cycle progression proteins. Based on this, Annexin V, TUNEL assay, ApoTox-Glo™, cell cycle analysis, and Western blots could be performed to determine the possible mechanism by which Cou induces a cytotoxic effect. Western blots analysis will be used to determine the expression and/or activation of apoptotic markers (caspases 3/7/9, Bax, Bcl-2, and phospho-histone H2A.X) and cell cycle regulators (cyclin E, and CDK2).

Our finding shows that Cou decreases the tumor emboli growth, but the molecular mechanism remains unknown. Based on this, studying the impact of Cou on the expression of NF-kB and E-cadherin is crucial for suggesting a mechanism since the literature reported that NF-kB and E-cadherin are involved in the tumor emboli formation (Arora et al., 2017; Ye et al., 2010). An experiment that could bring insight regarding the mechasnism of tumor emboli formation and how Coumestrol might be affecting this procress will be to perform a RNAseq. RNA could be extracted from tumor emboli to determine DEGs under Coumestrol treatment as compared to vehicle control. This could give us potential candidate genes that are involved in tumor emboli and also which of those might be affected by coumestrol treatment.

Cou treatment did not reduce SUM190PT (HER2 amplified) viability. One possible explanation is that HER2 confers resistance to therapies in this cell line,

but further studies are needed to confirm this. Based on this, knockout of HER2 in SUM190PT cells could be performed to generate a SUM190PT subline the overexpression of HER2. Then, a dose-response curve could be generated to determine if Cou has an effect on the SUM190PT HER2-knockout cells suggesting that the anti-cancer effects of Cou hindered by the amplification of HER2.

Our study considers the anti-cancer effects of Cou in four different breast cancer cell lines, but the effect of Cou in non-tumorigenic breast epithelial cell lines is unknown. We proposed to perform an dose response curve and a RCV analysis in a non-tumorigenic human mammary epithelial cell line (MCF10A); it's crucial to demonstrate that the anti-cancer effects of Cou only occur in breast cancer cells. In the long term, this data could determine the feasibility of designing clinical trials with coumestrol on breast cancer patients with the warranty that normal mammary epithelial cells will not be affected by the treatment. To accomplish this, and since the potential role of Cou as a therapeutic drug for IBC has not been characterized in an *in vivo* model, we will propose to validate the role of Cou as an anti-cancer agent in different xenograft mouse models of IBC.

In addition, if overexpression of TIPARP in SUM149PT cells confirms its suppressive role, we would like to identify therapeutic strategies to increase the expression of TIPARP *in vitro* and *in vivo* models. Overexpression of TIPARP in SUM149PT cells and evaluating its effects in pro-oncogenic phenotypes is essential for elucidating the role of TIPARP in TN-IBC cells. Angiogenesis functional assays are needed to confirm the GO enrichment analysis and the suggested role of TIPARP in this hallmark. In addition, we propose to perform a

qRT-PCR for at least 20 DEGs reported in the RNA-seq to validate the obtained data. Also, performing an RNA-seq in SUM149PT cells treated with different timepoints could help us identify other DEGs affected by Cou treatment and help establish if the up-regulation of TIPARP occurs in a time-dependent manner.

Our long-term goal is to suggest the combination of coumestrol with chemotherapy to increase the survival rate of breast cancer patients. To accomplish this goal is fundamental to study the combination of Cou with other phytoestrogens such as Genistein, Daidzein, and others. Also, it is crucial to study the synergistic effects or combinations of drugs of phytoestrogens and cancer therapies such as Tamoxifen, Paclitaxel, EGFR inhibitors, and others. This data obtained by this analysis opens an opportunity for medical doctors to explore the soy, lettuce, clover sprouts, and beans as part of breast cancer patients' diet.

Chapter V: Appendix

Appendix 1. Supplementary data

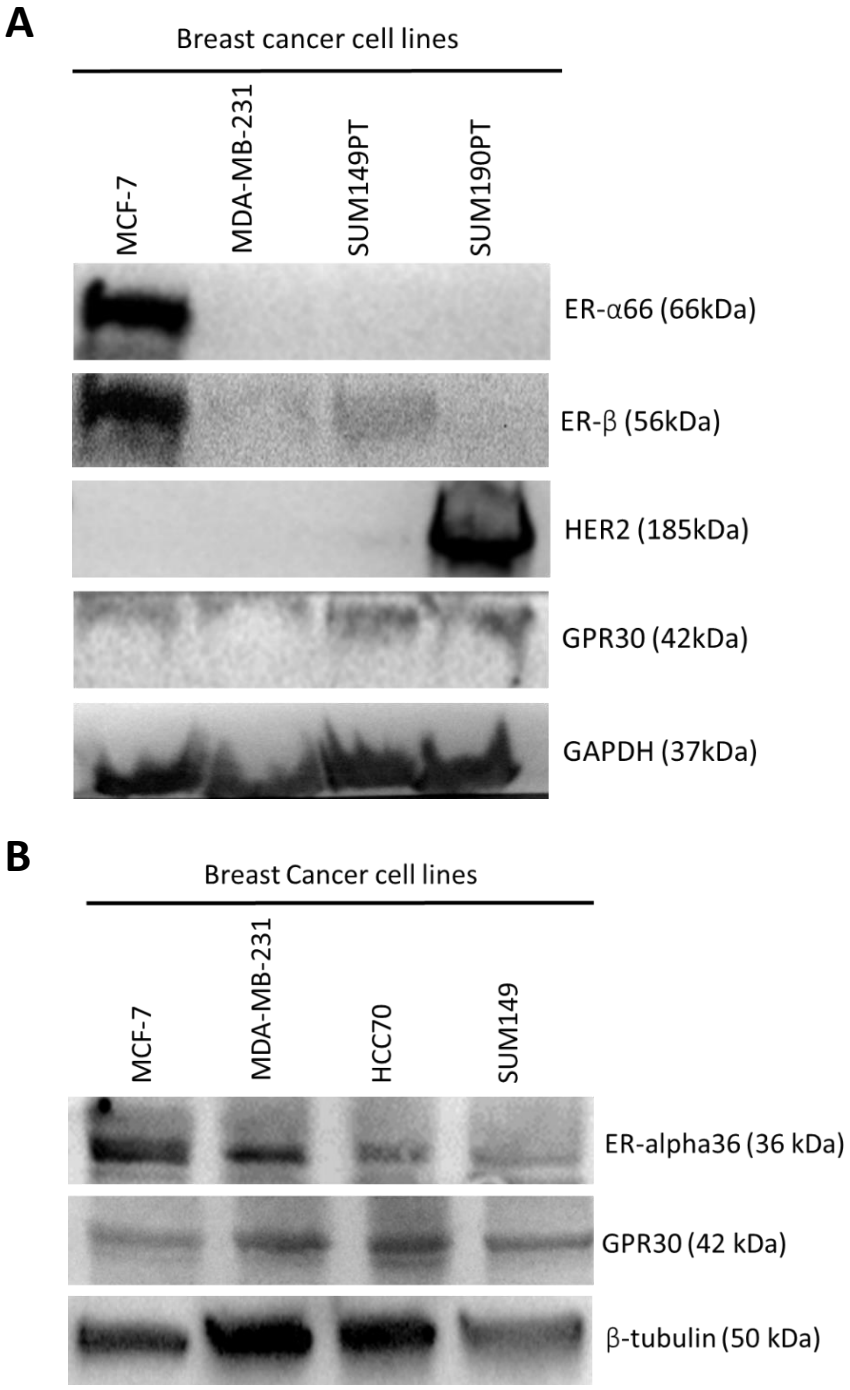

Figure 44: Expression of receptors in breast cancer cell lines. MCF-7 cell lines showed the expression of ER-alpha66, ER-alpha36, and ER-beta (**A and B**). Also, triple-negative breast cancer cell lines (MDA-MB-231 and SUM149) express ER-alpha36 (**B**). MDA-MB-231, SUM149 and SUM190 didn't express ER-alpha66 (**A**). Based in the expression of HER2 amplification in SUM190, this cell lines could not be classified as a triple negative breast cancer (**B**).

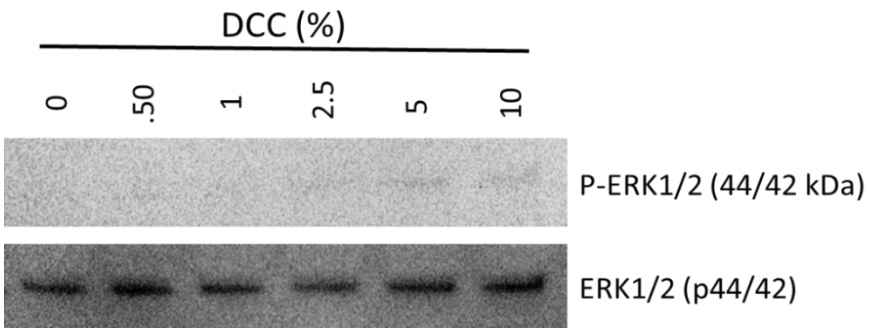

Figure 45: Free-hormone medium does not induce the activation of the estrogen non-genomic signaling pathway. The concentration or percentage of DCC in the free-hormone medium does not increase the phosphorylation levels of ERK1/2.

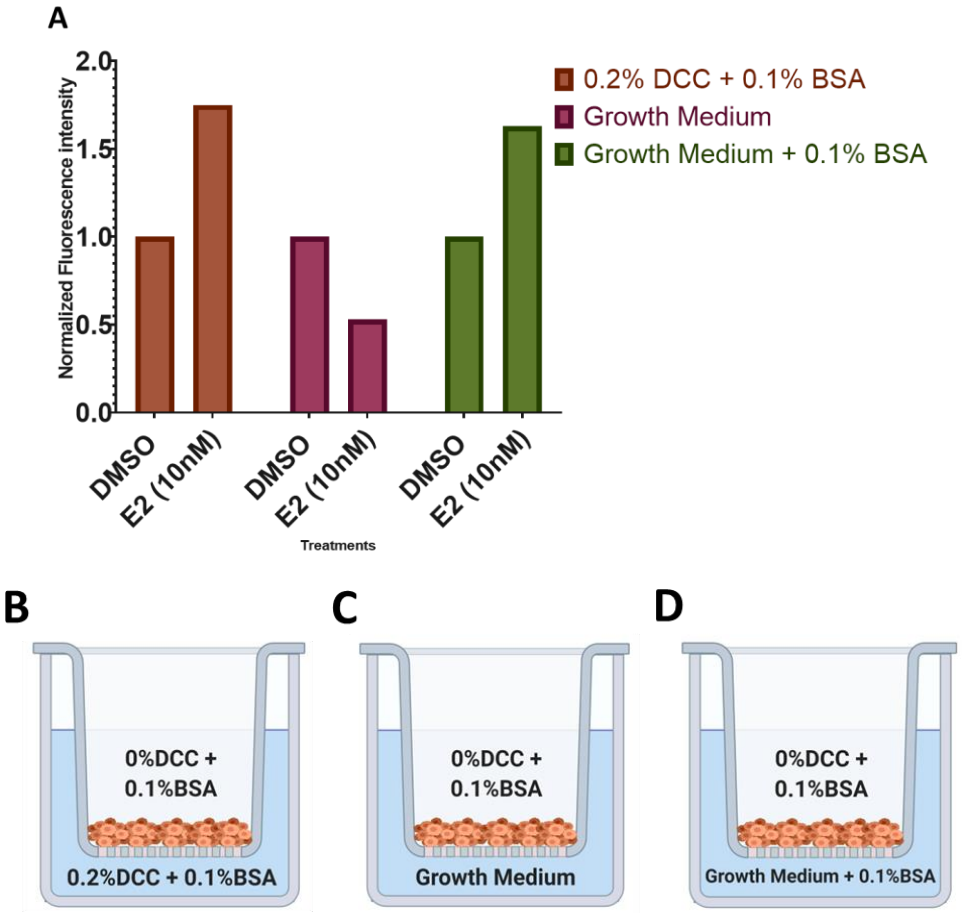

Figure 46: Boyden Chamber Assay in IBC cell line treated for fourteen hours with DMSO or estradiol using different chemoattractants. (A) SUM149 cell line showed increased migration when 0.2%DCC+0.1%BSA or growth medium+0.1%BSA were used as chemoattractants. Illustrations of the three different chemoattracts used in the experiments: **(B)** 0.2%DCC+0.1%BSA, **(C)** growth medium, and **(D)** growth medium+0.1%BSA.

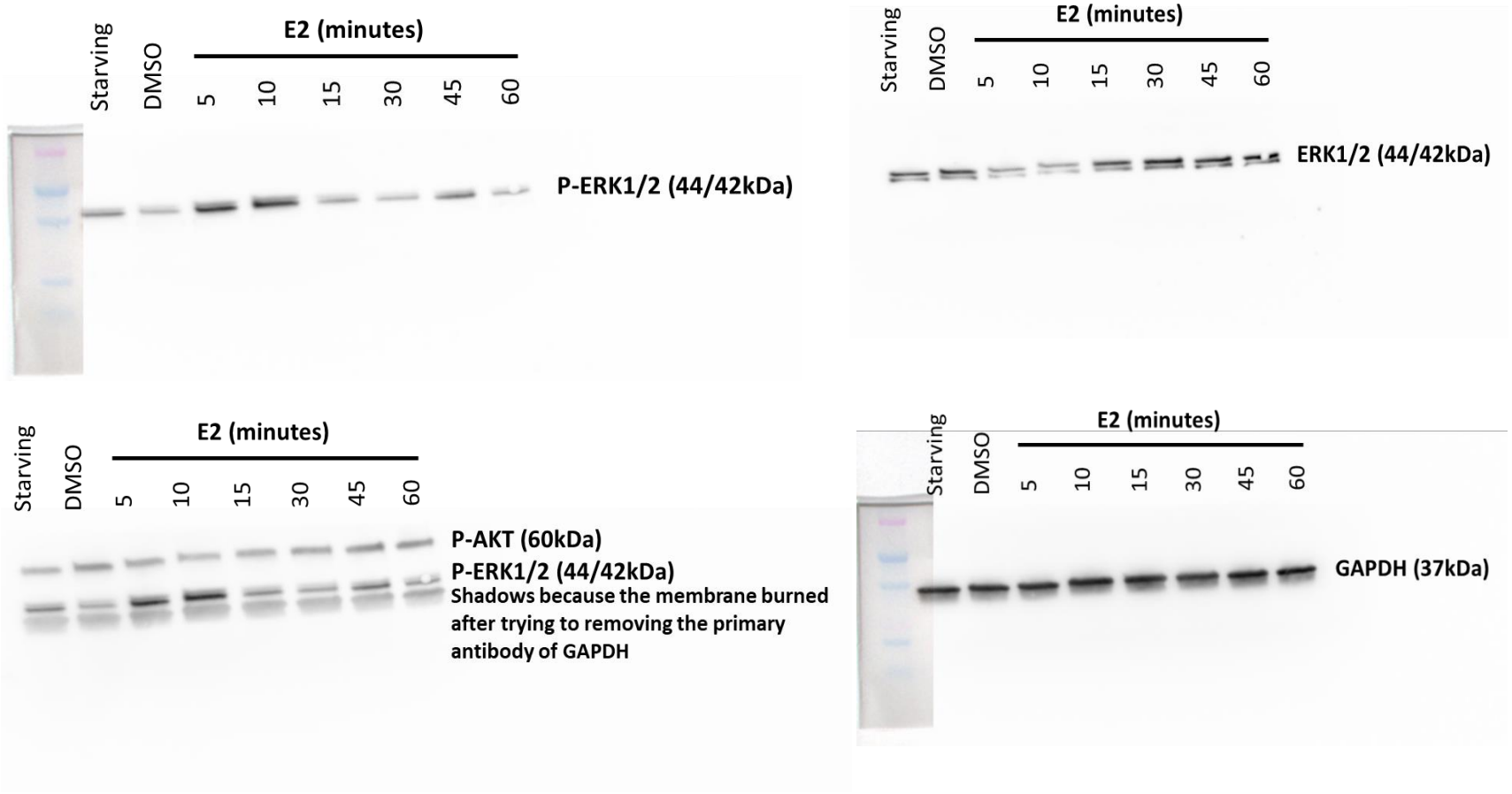

Figure 47: Uncropped membranes of Western Blots after treating the SUM149PT cells with estradiol.

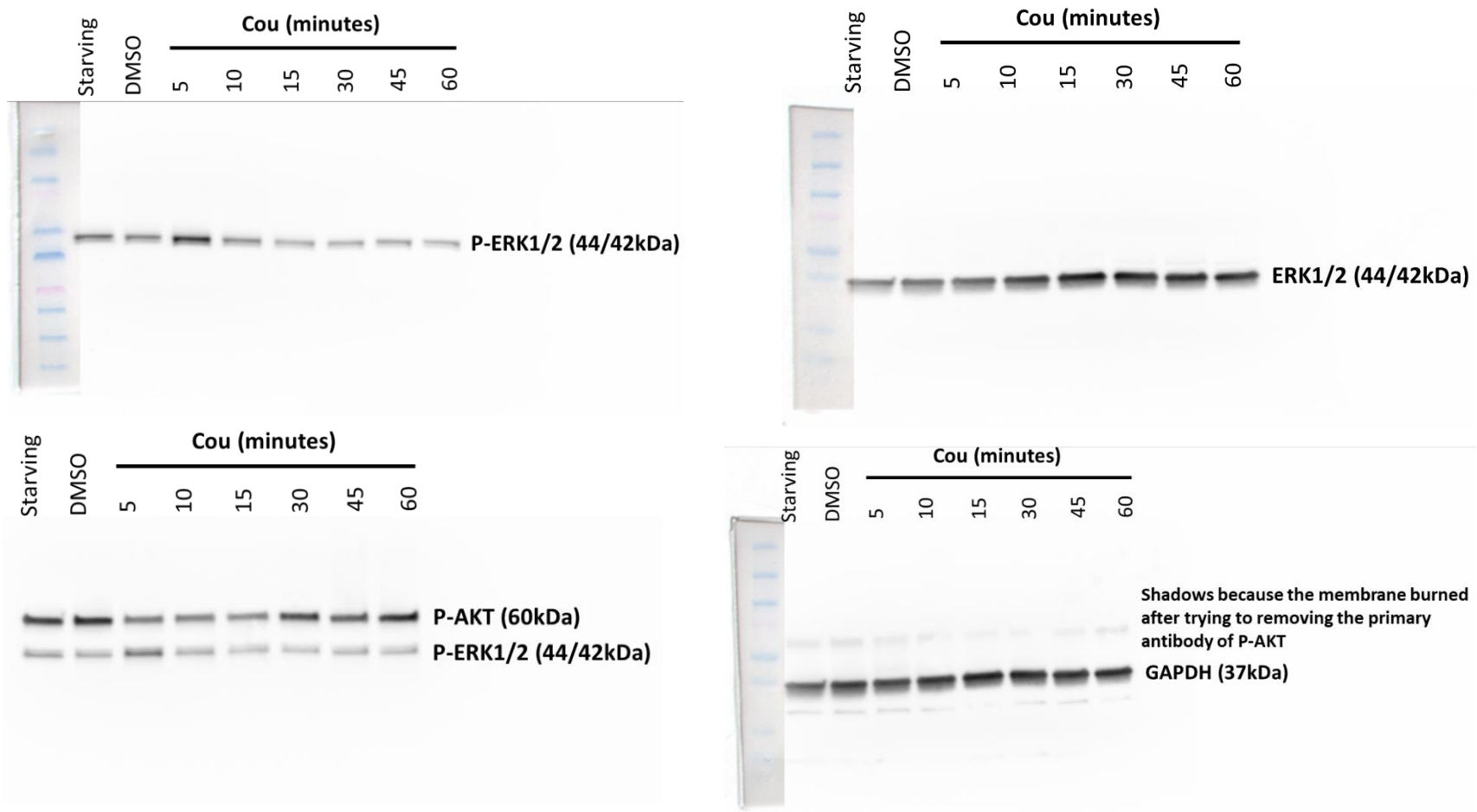

Figure 48: Membranes of Western Blots (uncropped) upon Cou treatment in SUM149PT.

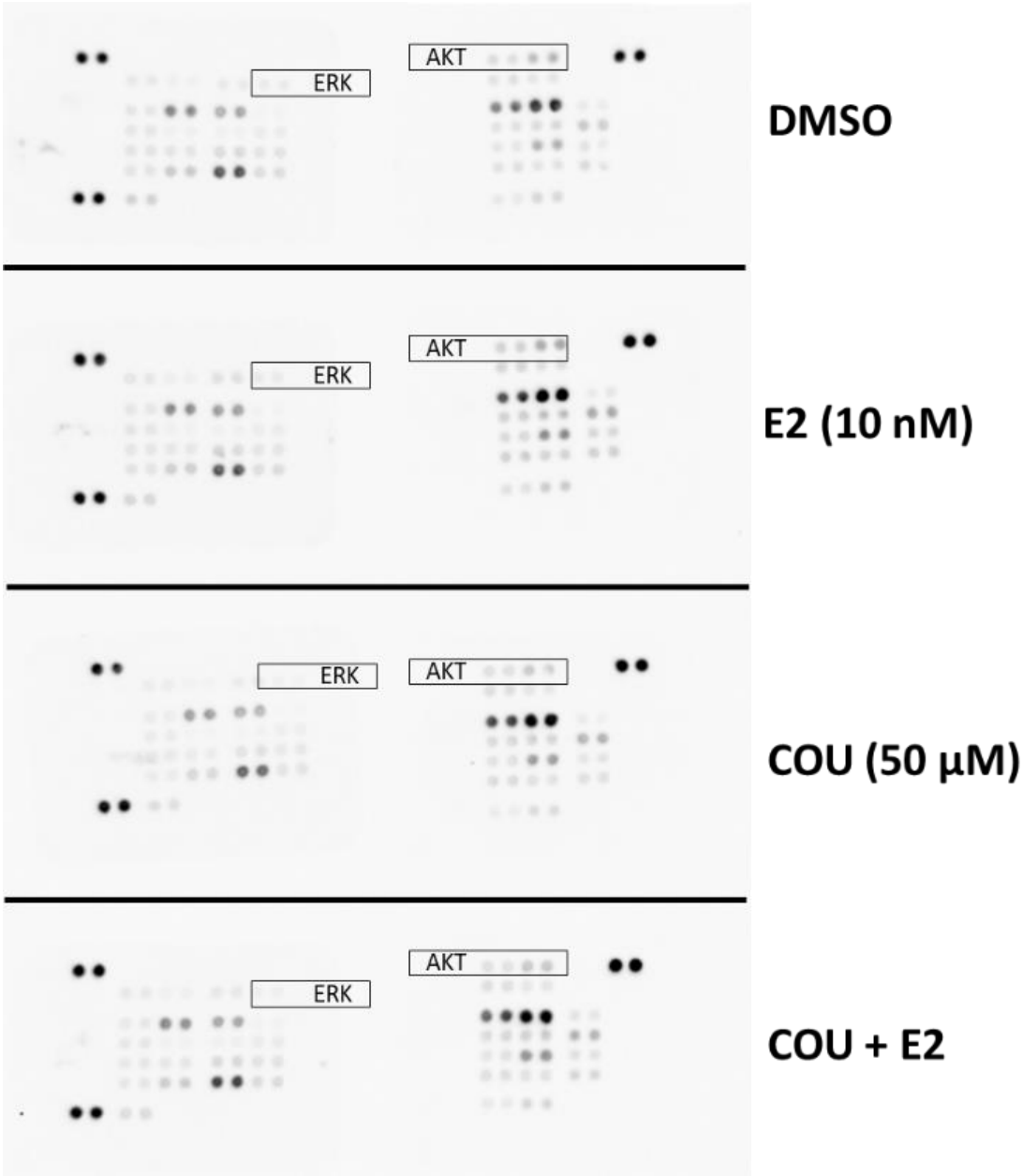

Figure 49: Illustration of Human Phosho-Kinase Array membranes. The membranes show the levels of phosphorylation of 39 kinases upon treating the SUM149PT cells for 5 minutes with estrogen, coumestrol, or a combination of treatments. The boxes at the left illustrate the spots that show the phosphorylation level of ERK1/2. Also, the spots that show the phosphorylation of AKT were represented in the boxes at the right.

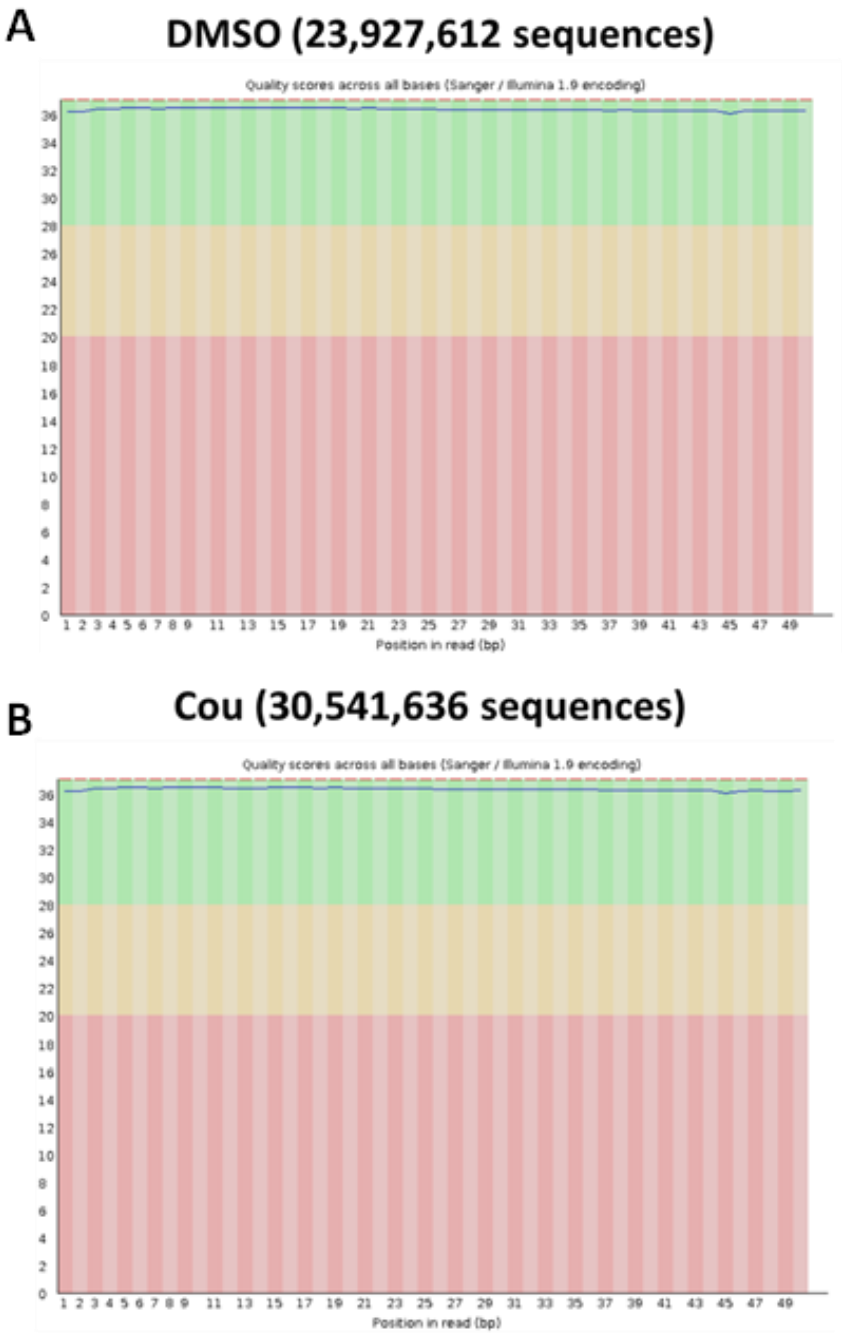

Figure 50: Fast QC analysis of the RNA sequencing. All the sequences have an average quality score of over 30, surpassing established thresholds.

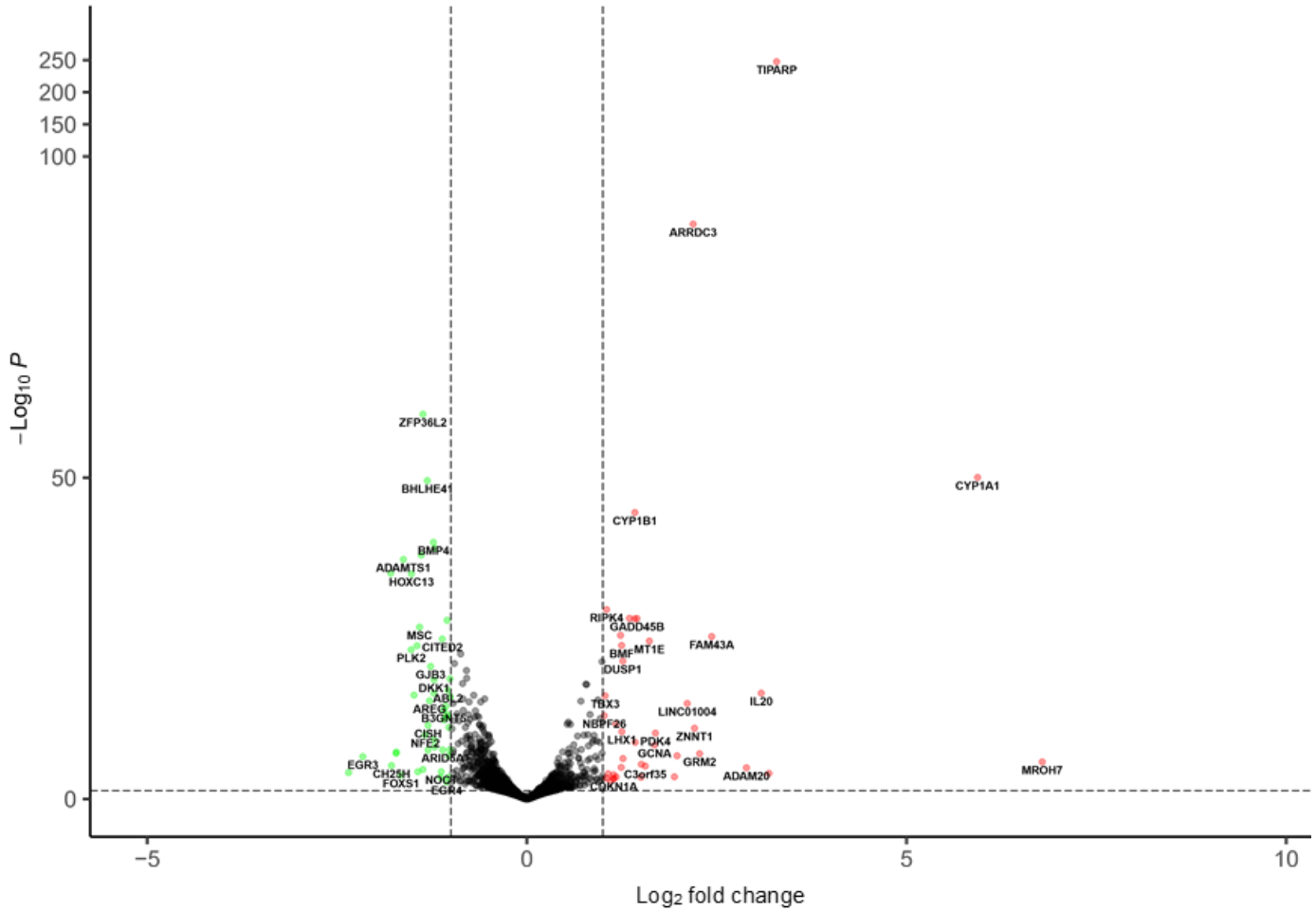

Figure 51: Differential expressed genes identified in RNA-sequencing. Volcano plot shows the DEGs with a log fold changer higher than 1 after treat the SUM149PT cell with coumestrol for an hour and a half.

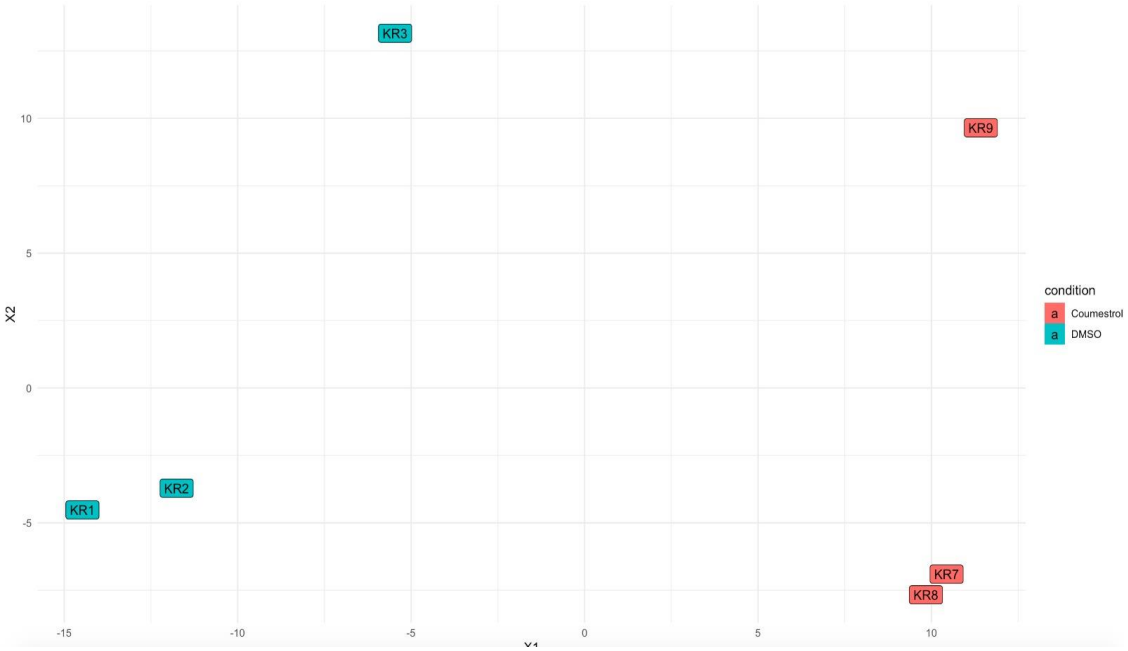

Figure 52: Principal component analysis (PCA) of the RNA sequencing. Biological replicates cluster together suggesting global RNA expression levels.

Appendix 2. Permission for publication of figure 1

ELSEVIER LICENSE
TERMS AND CONDITIONS

May 19, 2022

This Agreement between Ms. Keishla Rodriguez ("You") and Elsevier ("Elsevier") consists of your license details and the terms and conditions provided by Elsevier and Copyright Clearance Center.

License Number	5312500219279
License date	May 19, 2022
Licensed Content Publisher	Elsevier
Licensed Content Publication	The American Journal of Pathology
Licensed Content Title	Molecular and Cellular Heterogeneity in Breast Cancer Challenges for Personalized Medicine
Licensed Content Author	Ashley G. Rivenbark,Siobhan M. O'Connor,William B. Coleman
Licensed Content Date	Oct 1, 2013
Licensed Content Volume	183
Licensed Content Issue	4
Licensed Content Pages	12
Start Page	1113

End Page	1124
Type of Use	reuse in a thesis/dissertation
Portion	figures/tables/illustrations
Number of figures/tables/illustrations	4
Format	both print and electronic
Are you the author of this Elsevier article?	No
Will you be translating?	Yes, including English rights
Number of languages	1
Title	Graduate Student
Institution name	University of Puerto Rico at Rio Piedras Campus
Expected presentation date	May 2022
Portions	Figure 3, Figure 4
Specific Languages	English
Requestor Location	Ms. Keishla Rodriguez 2526 Av. Universidad #601 San Juan, 00925 Puerto Rico Attn: Ms. Keishla Rodriguez
Publisher Tax ID	GB 494 6272 12

Total 0.00 USD

Terms and Conditions

INTRODUCTION

1. The publisher for this copyrighted material is Elsevier. By clicking "accept" in connection with completing this licensing transaction, you agree that the following terms and conditions apply to this transaction (along with the Billing and Payment terms and conditions established by Copyright Clearance Center, Inc. ("CCC"), at the time that you opened your Rightslink account and that are available at any time at http://myaccount.copyright.com).

GENERAL TERMS

2. Elsevier hereby grants you permission to reproduce the aforementioned material subject to the terms and conditions indicated.

3. Acknowledgement: If any part of the material to be used (for example, figures) has appeared in our publication with credit or acknowledgement to another source, permission must also be sought from that source. If such permission is not obtained then that material may not be included in your publication/copies. Suitable acknowledgement to the source must be made, either as a footnote or in a reference list at the end of your publication, as follows:

"Reprinted from Publication title, Vol /edition number, Author(s), Title of article / title of chapter, Pages No., Copyright (Year), with permission from Elsevier [OR APPLICABLE SOCIETY COPYRIGHT OWNER]." Also Lancet special credit - "Reprinted from The Lancet, Vol. number, Author(s), Title of article, Pages No., Copyright (Year), with permission from Elsevier."

4. Reproduction of this material is confined to the purpose and/or media for which permission is hereby given.

5. Altering/Modifying Material: Not Permitted. However figures and illustrations may be altered/adapted minimally to serve your work. Any other abbreviations, additions, deletions and/or any other alterations shall be made only with prior written authorization of Elsevier Ltd. (Please contact Elsevier's permissions helpdesk here). No modifications can be made to any Lancet figures/tables and they must be reproduced in full.

6. If the permission fee for the requested use of our material is waived in this instance, please be advised that your future requests for Elsevier materials may attract a fee.

7. Reservation of Rights: Publisher reserves all rights not specifically granted in the combination of (i) the license details provided by you and accepted in the course of this licensing transaction, (ii) these terms and conditions and (iii) CCC's Billing and Payment terms and conditions.

8. License Contingent Upon Payment: While you may exercise the rights licensed immediately upon issuance of the license at the end of the licensing process for the transaction, provided that you have disclosed complete and accurate details of your proposed use, no license is finally effective unless and until full payment is received from you (either

by publisher or by CCC) as provided in CCC's Billing and Payment terms and conditions. If full payment is not received on a timely basis, then any license preliminarily granted shall be deemed automatically revoked and shall be void as if never granted. Further, in the event that you breach any of these terms and conditions or any of CCC's Billing and Payment terms and conditions, the license is automatically revoked and shall be void as if never granted. Use of materials as described in a revoked license, as well as any use of the materials beyond the scope of an unrevoked license, may constitute copyright infringement and publisher reserves the right to take any and all action to protect its copyright in the materials.

9. Warranties: Publisher makes no representations or warranties with respect to the licensed material.

10. Indemnity: You hereby indemnify and agree to hold harmless publisher and CCC, and their respective officers, directors, employees and agents, from and against any and all claims arising out of your use of the licensed material other than as specifically authorized pursuant to this license.

11. No Transfer of License: This license is personal to you and may not be sublicensed, assigned, or transferred by you to any other person without publisher's written permission.

12. No Amendment Except in Writing: This license may not be amended except in a writing signed by both parties (or, in the case of publisher, by CCC on publisher's behalf).

13. Objection to Contrary Terms: Publisher hereby objects to any terms contained in any purchase order, acknowledgment, check endorsement or other writing prepared by you, which terms are inconsistent with these terms and conditions or CCC's Billing and Payment terms and conditions. These terms and conditions, together with CCC's Billing and Payment terms and conditions (which are incorporated herein), comprise the entire agreement between you and publisher (and CCC) concerning this licensing transaction. In the event of any conflict between your obligations established by these terms and conditions and those established by CCC's Billing and Payment terms and conditions, these terms and conditions shall control.

14. Revocation: Elsevier or Copyright Clearance Center may deny the permissions described in this License at their sole discretion, for any reason or no reason, with a full refund payable to you. Notice of such denial will be made using the contact information provided by you. Failure to receive such notice will not alter or invalidate the denial. In no event will Elsevier or Copyright Clearance Center be responsible or liable for any costs, expenses or damage incurred by you as a result of a denial of your permission request, other than a refund of the amount(s) paid by you to Elsevier and/or Copyright Clearance Center for denied permissions.

LIMITED LICENSE

The following terms and conditions apply only to specific license types:

15. **Translation**: This permission is granted for non-exclusive world **English** rights only unless your license was granted for translation rights. If you licensed translation rights you may only translate this content into the languages you requested. A professional translator must perform all translations and reproduce the content word for word preserving the integrity of the article.

16. **Posting licensed content on any Website**: The following terms and conditions apply as follows: Licensing material from an Elsevier journal: All content posted to the web site must maintain the copyright information line on the bottom of each image; A hyper-text must be included to the Homepage of the journal from which you are licensing at http://www.sciencedirect.com/science/journal/xxxxx or the Elsevier homepage for books at http://www.elsevier.com; Central Storage: This license does not include permission for a scanned version of the material to be stored in a central repository such as that provided by Heron/XanEdu.

Licensing material from an Elsevier book: A hyper-text link must be included to the Elsevier homepage at http://www.elsevier.com . All content posted to the web site must maintain the copyright information line on the bottom of each image.

Posting licensed content on Electronic reserve: In addition to the above the following clauses are applicable: The web site must be password-protected and made available only to bona fide students registered on a relevant course. This permission is granted for 1 year only. You may obtain a new license for future website posting.

17. **For journal authors:** the following clauses are applicable in addition to the above:

Preprints:

A preprint is an author's own write-up of research results and analysis, it has not been peer-reviewed, nor has it had any other value added to it by a publisher (such as formatting, copyright, technical enhancement etc.).

Authors can share their preprints anywhere at any time. Preprints should not be added to or enhanced in any way in order to appear more like, or to substitute for, the final versions of articles however authors can update their preprints on arXiv or RePEc with their Accepted Author Manuscript (see below).

If accepted for publication, we encourage authors to link from the preprint to their formal publication via its DOI. Millions of researchers have access to the formal publications on ScienceDirect, and so links will help users to find, access, cite and use the best available version. Please note that Cell Press, The Lancet and some society-owned have different preprint policies. Information on these policies is available on the journal homepage.

Accepted Author Manuscripts: An accepted author manuscript is the manuscript of an article that has been accepted for publication and which typically includes author-incorporated changes suggested during submission, peer review and editor-author communications.

Authors can share their accepted author manuscript:

- immediately
  - via their non-commercial person homepage or blog
  - by updating a preprint in arXiv or RePEc with the accepted manuscript
  - via their research institute or institutional repository for internal institutional uses or as part of an invitation-only research collaboration work-group
  - directly by providing copies to their students or to research collaborators for their personal use

- for private scholarly sharing as part of an invitation-only work group on commercial sites with which Elsevier has an agreement
- After the embargo period
  - via non-commercial hosting platforms such as their institutional repository
  - via commercial sites with which Elsevier has an agreement

In all cases accepted manuscripts should:

- link to the formal publication via its DOI
- bear a CC-BY-NC-ND license - this is easy to do
- if aggregated with other manuscripts, for example in a repository or other site, be shared in alignment with our hosting policy not be added to or enhanced in any way to appear more like, or to substitute for, the published journal article.

Published journal article (JPA): A published journal article (PJA) is the definitive final record of published research that appears or will appear in the journal and embodies all value-adding publishing activities including peer review co-ordination, copy-editing, formatting, (if relevant) pagination and online enrichment.

Policies for sharing publishing journal articles differ for subscription and gold open access articles:

Subscription Articles: If you are an author, please share a link to your article rather than the full-text. Millions of researchers have access to the formal publications on ScienceDirect, and so links will help your users to find, access, cite, and use the best available version.

Theses and dissertations which contain embedded PJAs as part of the formal submission can be posted publicly by the awarding institution with DOI links back to the formal publications on ScienceDirect.

If you are affiliated with a library that subscribes to ScienceDirect you have additional private sharing rights for others' research accessed under that agreement. This includes use for classroom teaching and internal training at the institution (including use in course packs and courseware programs), and inclusion of the article for grant funding purposes.

Gold Open Access Articles: May be shared according to the author-selected end-user license and should contain a CrossMark logo, the end user license, and a DOI link to the formal publication on ScienceDirect.

Please refer to Elsevier's posting policy for further information.

18. **For book authors** the following clauses are applicable in addition to the above: Authors are permitted to place a brief summary of their work online only. You are not allowed to download and post the published electronic version of your chapter, nor may you scan the printed edition to create an electronic version. **Posting to a repository:** Authors are permitted to post a summary of their chapter only in their institution's repository.

19. **Thesis/Dissertation**: If your license is for use in a thesis/dissertation your thesis may be submitted to your institution in either print or electronic form. Should your thesis be published commercially, please reapply for permission. These requirements include permission for the Library and Archives of Canada to supply single copies, on demand, of the complete thesis and include permission for Proquest/UMI to supply single copies, on demand, of the complete thesis. Should your thesis be published commercially, please

---

Appendix 3. Permission for publication of figure 2

bio RENDER

49 Spadina Ave. Suite 200
Toronto ON M5V 2J1 Canada
www.biorender.com

Confirmation of Publication and Licensing Rights

May 19th, 2022
Science Suite Inc.

Subscription:	*Student Plan*
Agreement number:	*OZ23XQ13M3*
Journal name:	*Thesis Keishla M Rodriguez Martir*

To whom this may concern,

This document is to confirm that Keishla Rodriguez Martir has been granted a license to use the BioRender content, including icons, templates and other original artwork, appearing in the attached completed graphic pursuant to BioRender's Academic License Terms. This license permits BioRender content to be sublicensed for use in journal publications.

All rights and ownership of BioRender content are reserved by BioRender. All completed graphics must be accompanied by the following citation: "Created with BioRender.com".

BioRender content included in the completed graphic is not licensed for any commercial uses beyond publication in a journal. For any commercial use of this figure, users may, if allowed, recreate it in BioRender under an Industry BioRender Plan.

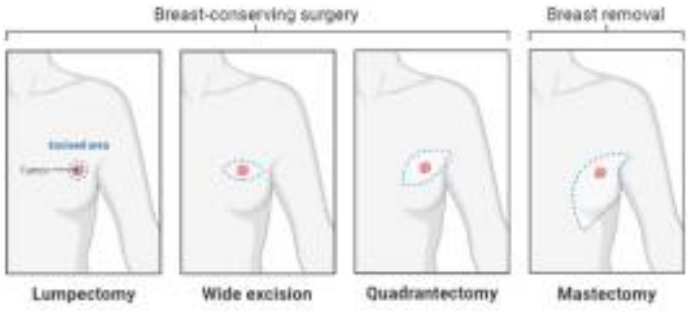

For any questions regarding this document, or other questions about publishing with BioRender refer to our BioRender Publication Guide, or contact BioRender Support at support@biorender.com.

Appendix 4. Permission for publication of figure 3

OXFORD UNIVERSITY PRESS LICENSE
TERMS AND CONDITIONS

May 19, 2022

This Agreement between Ms. Keishla Rodriguez ("You") and Oxford University Press ("Oxford University Press") consists of your license details and the terms and conditions provided by Oxford University Press and Copyright Clearance Center.

License Number	5312650204460
License date	May 19, 2022
Licensed content publisher	Oxford University Press
Licensed content publication	The Oncologist
Licensed content title	Inflammatory Breast Cancer: What We Know and What We Need to Learn
Licensed content author	Yamauchi, Hideko; Woodward, Wendy A.
Licensed content date	May 14, 2012
Type of Use	Thesis/Dissertation
Institution name	
Title of your work	Graduate Student
Publisher of your work	University of Puerto Rico at Rio Piedras Campus

Expected publication date	May 2022
Permissions cost	0.00 USD
Value added tax	0.00 USD
Total	0.00 USD
Title	Graduate Student
Institution name	University of Puerto Rico at Rio Piedras Campus
Expected presentation date	May 2022
Portions	Figure 1
Requestor Location	Ms. Keishla Rodriguez 2526 Av. Universidad #601 San Juan, 00925 Puerto Rico Attn: Ms. Keishla Rodriguez
Publisher Tax ID	GB125506730
Total	0.00 USD

Terms and Conditions

STANDARD TERMS AND CONDITIONS FOR REPRODUCTION OF MATERIAL FROM AN OXFORD UNIVERSITY PRESS JOURNAL

1. Use of the material is restricted to the type of use specified in your order details.

2. This permission covers the use of the material in the English language in the following territory: world. If you have requested additional permission to translate this material, the terms and conditions of this reuse will be set out in clause 12.

3. This permission is limited to the particular use authorized in (1) above and does not allow you to sanction its use elsewhere in any other format other than specified above, nor does it apply to quotations, images, artistic works etc that have been reproduced from other sources which may be part of the material to be used.

4. No alteration, omission or addition is made to the material without our written consent. Permission must be re-cleared with Oxford University Press if/when you decide to reprint.

5. The following credit line appears wherever the material is used: author, title, journal, year, volume, issue number, pagination, by permission of Oxford University Press or the sponsoring society if the journal is a society journal. Where a journal is being published on behalf of a learned society, the details of that society must be included in the credit line.

6. For the reproduction of a full article from an Oxford University Press journal for whatever purpose, the corresponding author of the material concerned should be informed of the proposed use. Contact details for the corresponding authors of all Oxford University Press journal contact can be found alongside either the abstract or full text of the article concerned, accessible from www.oxfordjournals.org Should there be a problem clearing these rights, please contact journals.permissions@oup.com

7. If the credit line or acknowledgement in our publication indicates that any of the figures, images or photos was reproduced, drawn or modified from an earlier source it will be necessary for you to clear this permission with the original publisher as well. If this permission has not been obtained, please note that this material cannot be included in your publication/photocopies.

8. While you may exercise the rights licensed immediately upon issuance of the license at the end of the licensing process for the transaction, provided that you have disclosed complete and accurate details of your proposed use, no license is finally effective unless and until full payment is received from you (either by Oxford University Press or by Copyright Clearance Center (CCC)) as provided in CCC's Billing and Payment terms and conditions. If full payment is not received on a timely basis, then any license preliminarily granted shall be deemed automatically revoked and shall be void as if never granted. Further, in the event that you breach any of these terms and conditions or any of CCC's Billing and Payment terms and conditions, the license is automatically revoked and shall be void as if never granted. Use of materials as described in a revoked license, as well as any use of the materials beyond the scope of an unrevoked license, may constitute copyright infringement and Oxford University Press reserves the right to take any and all action to protect its copyright in the materials.

9. This license is personal to you and may not be sublicensed, assigned or transferred by you to any other person without Oxford University Press's written permission.

10. Oxford University Press reserves all rights not specifically granted in the combination of (i) the license details provided by you and accepted in the course of this licensing transaction, (ii) these terms and conditions and (iii) CCC's Billing and Payment terms and conditions.

Appendix 5. Permission for publication of figure 5

49 Spadina Ave. Suite 200
Toronto ON M5V 2J1 Canada
www.biorender.com

Confirmation of Publication and Licensing Rights

May 19th, 2022
Science Suite Inc.

Subscription:	*Student Plan*
Agreement number:	*WJ23XQ0TJG*
Journal name:	*Thesis Keishla M Rodriguez Martir*

To whom this may concern,

This document is to confirm that Keishla Rodriguez Martir has been granted a license to use the BioRender content, including icons, templates and other original artwork, appearing in the attached completed graphic pursuant to BioRender's Academic License Terms. This license permits BioRender content to be sublicensed for use in journal publications.

All rights and ownership of BioRender content are reserved by BioRender. All completed graphics must be accompanied by the following citation: "Created with BioRender.com".

BioRender content included in the completed graphic is not licensed for any commercial uses beyond publication in a journal. For any commercial use of this figure, users may, if allowed, recreate it in BioRender under an Industry BioRender Plan.

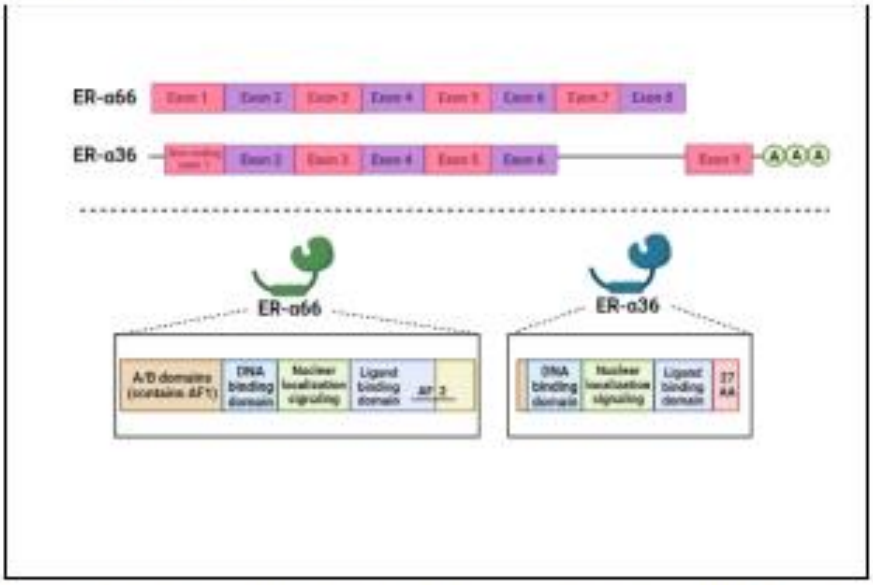

For any questions regarding this document, or other questions about publishing with BioRender refer to our BioRender Publication Guide, or contact BioRender Support at support@biorender.com.

Appendix 6. Permission for publication of figure 6

49 Spadina Ave. Suite 200
Toronto ON M5V 2J1 Canada
www.biorender.com

Confirmation of Publication and Licensing Rights

May 19th, 2022
Science Suite Inc.

Subscription:	*Student Plan*
Agreement number:	*NA23XQ0MU7*
Journal name:	*Thesis Keishla M Rodriguez Martir*

To whom this may concern,

This document is to confirm that Keishla Rodriguez Martir has been granted a license to use the BioRender content, including icons, templates and other original artwork, appearing in the attached completed graphic pursuant to BioRender's Academic License Terms. This license permits BioRender content to be sublicensed for use in journal publications.

All rights and ownership of BioRender content are reserved by BioRender. All completed graphics must be accompanied by the following citation: "Created with BioRender.com".

BioRender content included in the completed graphic is not licensed for any commercial uses beyond publication in a journal. For any commercial use of this figure, users may, if allowed, recreate it in BioRender under an Industry BioRender Plan.

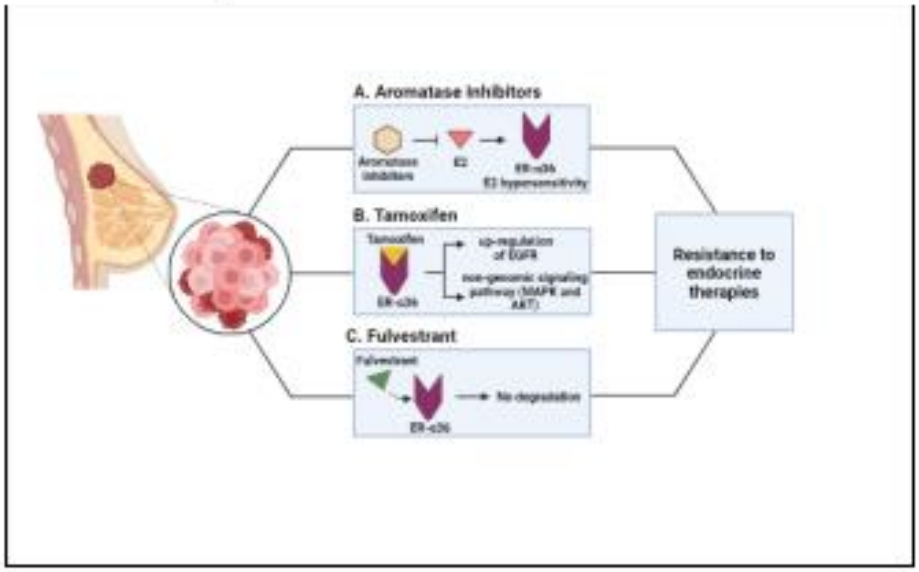

For any questions regarding this document, or other questions about publishing with BioRender refer to our BioRender Publication Guide, or contact BioRender Support at support@biorender.com.

Appendix 7. Permission for publication of figure 7

49 Spadina Ave. Suite 200
Toronto ON M5V 2J1 Canada
www.biorender.com

Confirmation of Publication and Licensing Rights

May 19th, 2022
Science Suite Inc.

Subscription:	*Student Plan*
Agreement number:	*AM23XQ1A4O*
Journal name:	*Thesis Keishla M Rodriguez Martir*

To whom this may concern,

This document is to confirm that Keishla Rodriguez Martir has been granted a license to use the BioRender content, including icons, templates and other original artwork, appearing in the attached completed graphic pursuant to BioRender's Academic License Terms. This license permits BioRender content to be sublicensed for use in journal publications.

All rights and ownership of BioRender content are reserved by BioRender. All completed graphics must be accompanied by the following citation: "Created with BioRender.com".

BioRender content included in the completed graphic is not licensed for any commercial uses beyond publication in a journal. For any commercial use of this figure, users may, if allowed, recreate it in BioRender under an Industry BioRender Plan.

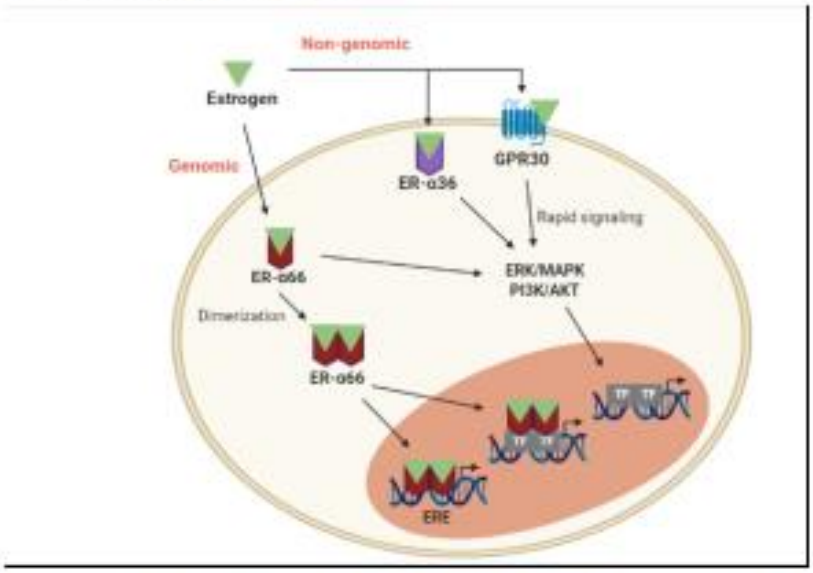

For any questions regarding this document, or other questions about publishing with BioRender refer to our BioRender Publication Guide, or contact BioRender Support at support@biorender.com.

Appendix 8. Permission for publication of figure 8

49 Spadina Ave. Suite 200
Toronto ON M5V 2J1 Canada
www.biorender.com

Confirmation of Publication and Licensing Rights

May 19th, 2022
Science Suite Inc.

Subscription:	*Student Plan*
Agreement number:	*WN23XQ1LUE*
Journal name:	*Thesis Keishla M Rodriguez Martir*

To whom this may concern,

This document is to confirm that Keishla Rodriguez Martir has been granted a license to use the BioRender content, including icons, templates and other original artwork, appearing in the attached completed graphic pursuant to BioRender's Academic License Terms. This license permits BioRender content to be sublicensed for use in journal publications.

All rights and ownership of BioRender content are reserved by BioRender. All completed graphics must be accompanied by the following citation: "Created with BioRender.com".

BioRender content included in the completed graphic is not licensed for any commercial uses beyond publication in a journal. For any commercial use of this figure, users may, if allowed, recreate it in BioRender under an Industry BioRender Plan.

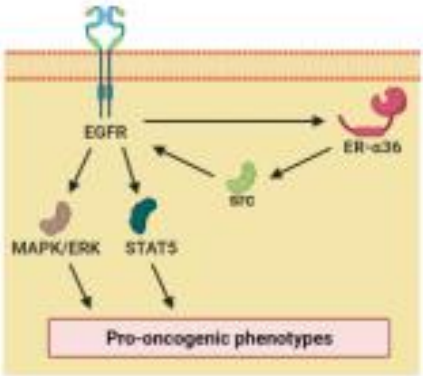

For any questions regarding this document, or other questions about publishing with BioRender refer to our BioRender Publication Guide, or contact BioRender Support at support@biorender.com.

Appendix 9. Permission for publication of figure 9

49 Spadina Ave. Suite 200
Toronto ON M5V 2J1 Canada
www.biorender.com

Confirmation of Publication and Licensing Rights

May 19th, 2022
Science Suite Inc.

Subscription:	*Student Plan*
Agreement number:	*VR23XQ1T7R*
Journal name:	*Thesis Keishla M Rodriguez Martir*

To whom this may concern,

This document is to confirm that Keishla Rodriguez Martir has been granted a license to use the BioRender content, including icons, templates and other original artwork, appearing in the attached completed graphic pursuant to BioRender's Academic License Terms. This license permits BioRender content to be sublicensed for use in journal publications.

All rights and ownership of BioRender content are reserved by BioRender. All completed graphics must be accompanied by the following citation: "Created with BioRender.com".

BioRender content included in the completed graphic is not licensed for any commercial uses beyond publication in a journal. For any commercial use of this figure, users may, if allowed, recreate it in BioRender under an Industry BioRender Plan.

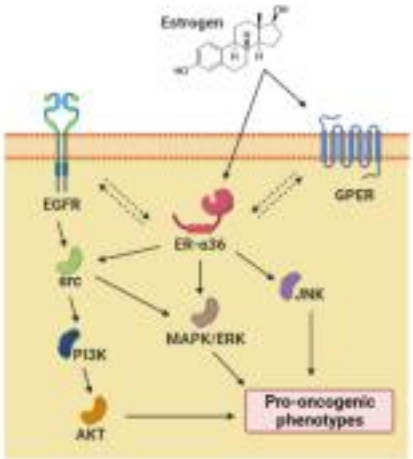

For any questions regarding this document, or other questions about publishing with BioRender refer to our BioRender Publication Guide, or contact BioRender Support at support@biorender.com.

Appendix 10. Permission for publication of figure 10

49 Spadina Ave. Suite 200
Toronto ON M5V 2J1 Canada
www.biorender.com

Confirmation of Publication and Licensing Rights

May 19th, 2022
Science Suite Inc.

Subscription:	*Student Plan*
Agreement number:	*NL23XQ0EO0*
Journal name:	*Thesis Keishla M Rodriguez Martir*

To whom this may concern,

This document is to confirm that Keishla Rodriguez Martir has been granted a license to use the BioRender content, including icons, templates and other original artwork, appearing in the attached completed graphic pursuant to BioRender's Academic License Terms. This license permits BioRender content to be sublicensed for use in journal publications.

All rights and ownership of BioRender content are reserved by BioRender. All completed graphics must be accompanied by the following citation: "Created with BioRender.com".

BioRender content included in the completed graphic is not licensed for any commercial uses beyond publication in a journal. For any commercial use of this figure, users may, if allowed, recreate it in BioRender under an Industry BioRender Plan.

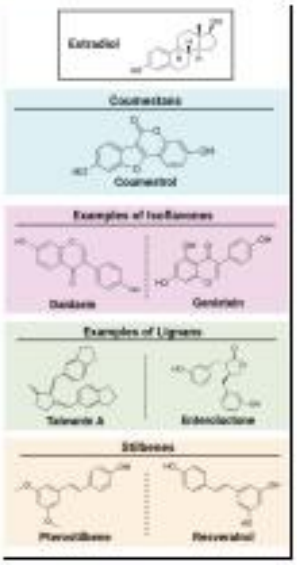

For any questions regarding this document, or other questions about publishing with BioRender refer to our BioRender Publication Guide, or contact BioRender Support at support@biorender.com.

Appendix 11. Permission for publication of figure 11

bio RENDER

49 Spadina Ave. Suite 200
Toronto ON M5V 2J1 Canada
www.biorender.com

Confirmation of Publication and Licensing Rights

May 23rd, 2022
Science Suite Inc.

Subscription:	*Student Plan*
Agreement number:	*OU23YB4S5J*
Journal name:	*Thesis Keishla M Rodriguez Martir*

To whom this may concern,

This document is to confirm that Keishla Rodriguez Martir has been granted a license to use the BioRender content, including icons, templates and other original artwork, appearing in the attached completed graphic pursuant to BioRender's Academic License Terms. This license permits BioRender content to be sublicensed for use in journal publications.

All rights and ownership of BioRender content are reserved by BioRender. All completed graphics must be accompanied by the following citation: "Created with BioRender.com".

BioRender content included in the completed graphic is not licensed for any commercial uses beyond publication in a journal. For any commercial use of this figure, users may, if allowed, recreate it in BioRender under an Industry BioRender Plan.

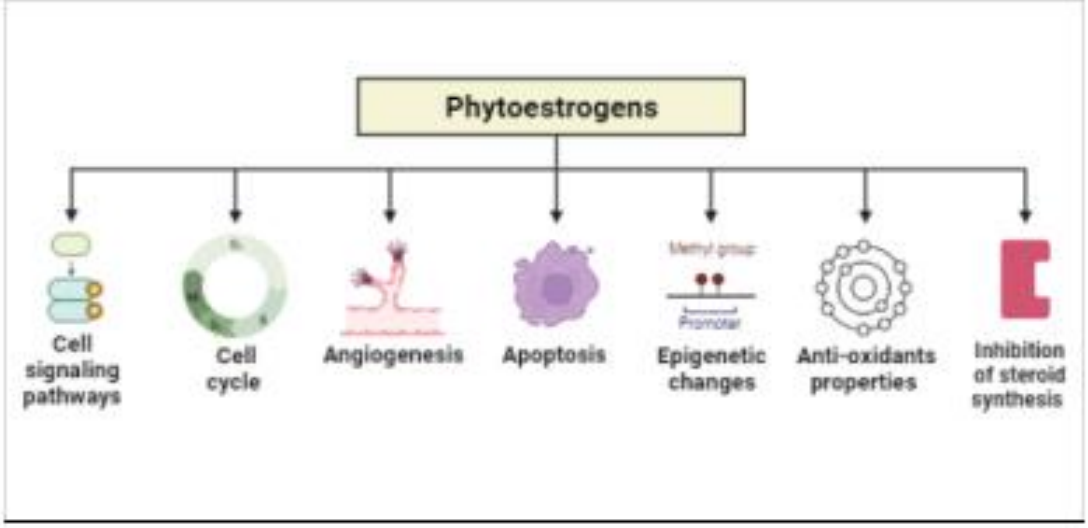

For any questions regarding this document, or other questions about publishing with BioRender refer to our BioRender Publication Guide, or contact BioRender Support at support@biorender.com.

Appendi x 12. Permission for publication of figure 12

49 Spadina Ave. Suite 200
Toronto ON M5V 2J1 Canada
www.biorender.com

Confirmation of Publication and Licensing Rights

May 19th, 2022
Science Suite Inc.

Subscription:	*Student Plan*
Agreement number:	*AV23XQEWDP*
Journal name:	*Thesis Keishla M Rodriguez Martir*

To whom this may concern,

This document is to confirm that Keishla Rodriguez Martir has been granted a license to use the BioRender content, including icons, templates and other original artwork, appearing in the attached completed graphic pursuant to BioRender's Academic License Terms. This license permits BioRender content to be sublicensed for use in journal publications.

All rights and ownership of BioRender content are reserved by BioRender. All completed graphics must be accompanied by the following citation: "Created with BioRender.com".

BioRender content included in the completed graphic is not licensed for any commercial uses beyond publication in a journal. For any commercial use of this figure, users may, if allowed, recreate it in BioRender under an Industry BioRender Plan.

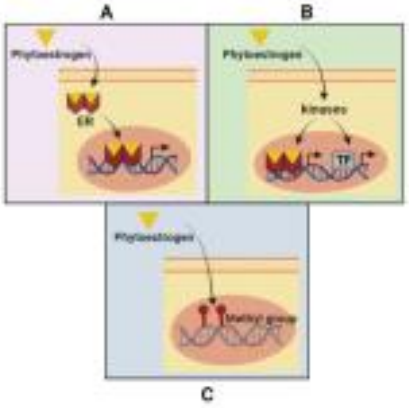

For any questions regarding this document, or other questions about publishing with BioRender refer to our BioRender Publication Guide, or contact BioRender Support at support@biorender.com.

Appendix 13. Permission for publicatio n of figure 13

49 Spadina Ave. Suite 200
Toronto ON M5V 2J1 Canada
www.biorender.com

Confirmation of Publication and Licensing Rights

May 19th, 2022
Science Suite Inc.

Subscription:	*Student Plan*
Agreement number:	*RF23XQ7KN9*
Journal name:	*Thesis Keishla M Rodriguez Martir*

To whom this may concern,

This document is to confirm that Keishla Rodriguez Martir has been granted a license to use the BioRender content, including icons, templates and other original artwork, appearing in the attached completed graphic pursuant to BioRender's Academic License Terms. This license permits BioRender content to be sublicensed for use in journal publications.

All rights and ownership of BioRender content are reserved by BioRender. All completed graphics must be accompanied by the following citation: "Created with BioRender.com".

BioRender content included in the completed graphic is not licensed for any commercial uses beyond publication in a journal. For any commercial use of this figure, users may, if allowed, recreate it in BioRender under an Industry BioRender Plan.

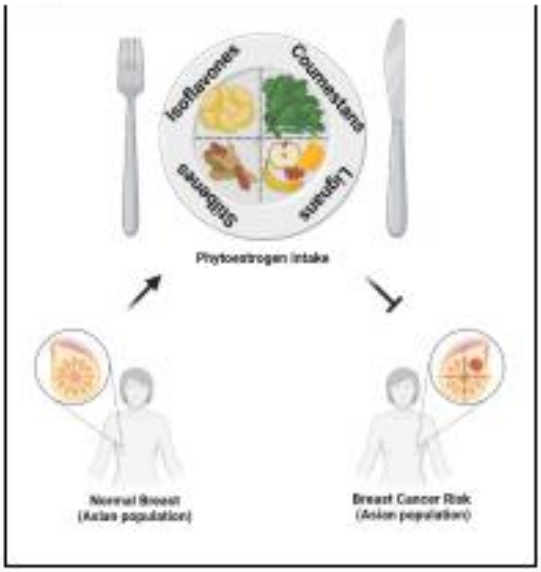

For any questions regarding this document, or other questions about publishing with BioRender refer to our BioRender Publication Guide, or contact BioRender Support at support@biorender.com.

Appendix 14. Permis sion for publication of figure 14

bio RENDER

49 Spadina Ave. Suite 200
Toronto ON M5V 2J1 Canada
www.biorender.com

Confirmation of Publication and Licensing Rights

May 19th, 2022
Science Suite Inc.

Subscription:	*Student Plan*
Agreement number:	*XY23XQFOHS*
Journal name:	*Thesis Keishla M Rodriguez Martir*

To whom this may concern,

This document is to confirm that Keishla Rodriguez Martir has been granted a license to use the BioRender content, including icons, templates and other original artwork, appearing in the attached completed graphic pursuant to BioRender's Academic License Terms. This license permits BioRender content to be sublicensed for use in journal publications.

All rights and ownership of BioRender content are reserved by BioRender. All completed graphics must be accompanied by the following citation: "Created with BioRender.com".

BioRender content included in the completed graphic is not licensed for any commercial uses beyond publication in a journal. For any commercial use of this figure, users may, if allowed, recreate it in BioRender under an Industry BioRender Plan.

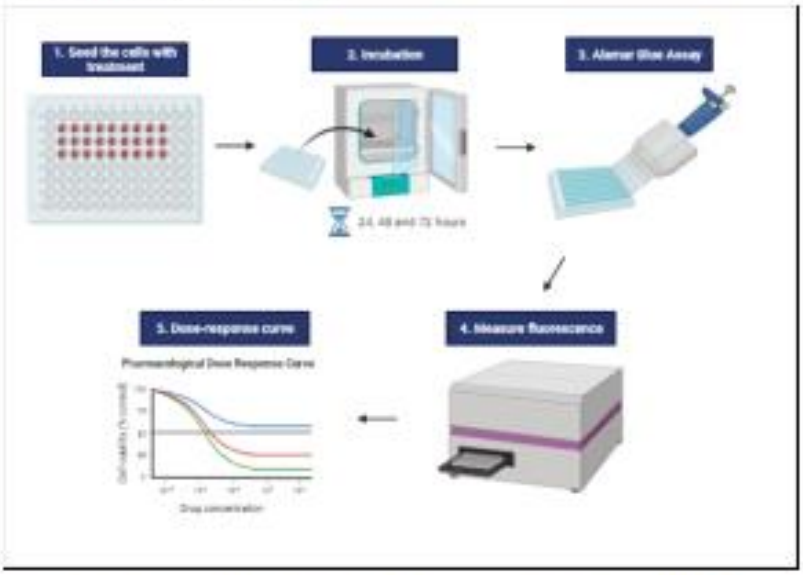

For any questions regarding this document, or other questions about publishing with BioRender refer to our BioRender Publication Guide, or contact BioRender Support at support@biorender.com.

Appendix 15. Permission for publication of figure 15

49 Spadina Ave. Suite 200
Toronto ON M5V 2J1 Canada
www.biorender.com

Confirmation of Publication and Licensing Rights

May 19th, 2022
Science Suite Inc.

Subscription:	*Student Plan*
Agreement number:	*IJ23XQFU4C*
Journal name:	*Thesis Keishla M Rodriguez Martir*

To whom this may concern,

This document is to confirm that Keishla Rodriguez Martir has been granted a license to use the BioRender content, including icons, templates and other original artwork, appearing in the attached completed graphic pursuant to BioRender's Academic License Terms. This license permits BioRender content to be sublicensed for use in journal publications.

All rights and ownership of BioRender content are reserved by BioRender. All completed graphics must be accompanied by the following citation: "Created with BioRender.com".

BioRender content included in the completed graphic is not licensed for any commercial uses beyond publication in a journal. For any commercial use of this figure, users may, if allowed, recreate it in BioRender under an Industry BioRender Plan.

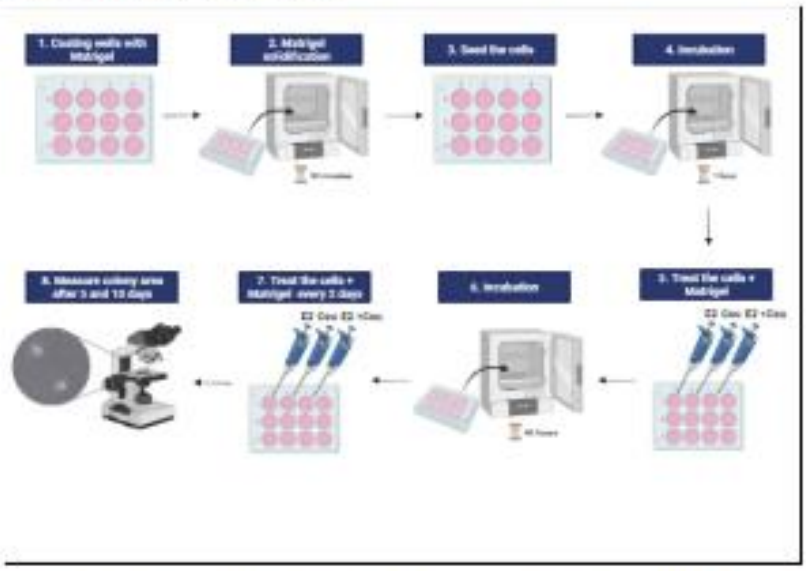

For any questions regarding this document, or other questions about publishing with BioRender refer to our BioRender Publication Guide, or contact BioRender Support at support@biorender.com.

Appendix 16. Permission for publication of figure 16

49 Spadina Ave. Suite 200
Toronto ON M5V 2J1 Canada
www.biorender.com

Confirmation of Publication and Licensing Rights

May 23rd, 2022
Science Suite Inc.

Subscription:	*Student Plan*
Agreement number:	*LQ23YB8S90*
Journal name:	*Thesis Keishla M Rodriguez Martir*

To whom this may concern,

This document is to confirm that Keishla Rodriguez Martir has been granted a license to use the BioRender content, including icons, templates and other original artwork, appearing in the attached completed graphic pursuant to BioRender's Academic License Terms. This license permits BioRender content to be sublicensed for use in journal publications.

All rights and ownership of BioRender content are reserved by BioRender. All completed graphics must be accompanied by the following citation: "Created with BioRender.com".

BioRender content included in the completed graphic is not licensed for any commercial uses beyond publication in a journal. For any commercial use of this figure, users may, if allowed, recreate it in BioRender under an Industry BioRender Plan.

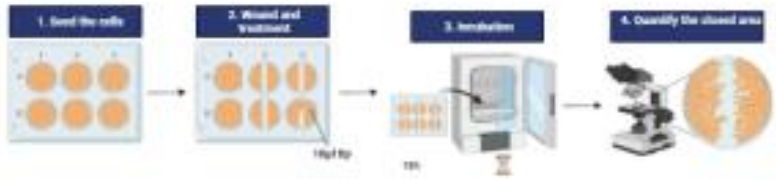

For any questions regarding this document, or other questions about publishing with BioRender refer to our BioRender Publication Guide, or contact BioRender Support at support@biorender.com.

Appendix 17. Permission for publication of figure 17

49 Spadina Ave. Suite 200
Toronto ON M5V 2J1 Canada
www.biorender.com

Confirmation of Publication and Licensing Rights

May 23rd, 2022
Science Suite Inc.

Subscription:	*Student Plan*
Agreement number:	*ZE23YBAAH2*
Journal name:	*Thesis Keishla M Rodriguez Martir*

To whom this may concern,

This document is to confirm that Keishla Rodriguez Martir has been granted a license to use the BioRender content, including icons, templates and other original artwork, appearing in the attached completed graphic pursuant to BioRender's Academic License Terms. This license permits BioRender content to be sublicensed for use in journal publications.

All rights and ownership of BioRender content are reserved by BioRender. All completed graphics must be accompanied by the following citation: "Created with BioRender.com".

BioRender content included in the completed graphic is not licensed for any commercial uses beyond publication in a journal. For any commercial use of this figure, users may, if allowed, recreate it in BioRender under an Industry BioRender Plan.

For any questions regarding this document, or other questions about publishing with BioRender refer to our BioRender Publication Guide, or contact BioRender Support at support@biorender.com.

Appendix 18. Permission for publication of figure 18

49 Spadina Ave. Suite 200
Toronto ON M5V 2J1 Canada
www.biorender.com

Confirmation of Publication and Licensing Rights

May 23rd, 2022
Science Suite Inc.

Subscription:	*Student Plan*
Agreement number:	*JT23YBAHWU*
Journal name:	*Thesis Keishla M Rodriguez Martir*

To whom this may concern,

This document is to confirm that Keishla Rodriguez Martir has been granted a license to use the BioRender content, including icons, templates and other original artwork, appearing in the attached completed graphic pursuant to BioRender's Academic License Terms. This license permits BioRender content to be sublicensed for use in journal publications.

All rights and ownership of BioRender content are reserved by BioRender. All completed graphics must be accompanied by the following citation: "Created with BioRender.com".

BioRender content included in the completed graphic is not licensed for any commercial uses beyond publication in a journal. For any commercial use of this figure, users may, if allowed, recreate it in BioRender under an Industry BioRender Plan.

For any questions regarding this document, or other questions about publishing with BioRender refer to our BioRender Publication Guide, or contact BioRender Support at support@biorender.com.

Appendix 19. Permission for publication of figure 19

49 Spadina Ave. Suite 200
Toronto ON M5V 2J1 Canada
www.biorender.com

Confirmation of Publication and Licensing Rights

May 23rd, 2022
Science Suite Inc.

Subscription:	*Student Plan*
Agreement number:	*SY23YB7SPP*
Journal name:	*Thesis Keishla M Rodriguez Martir*

To whom this may concern,

This document is to confirm that Keishla Rodriguez Martir has been granted a license to use the BioRender content, including icons, templates and other original artwork, appearing in the attached completed graphic pursuant to BioRender's Academic License Terms. This license permits BioRender content to be sublicensed for use in journal publications.

All rights and ownership of BioRender content are reserved by BioRender. All completed graphics must be accompanied by the following citation: "Created with BioRender.com".

BioRender content included in the completed graphic is not licensed for any commercial uses beyond publication in a journal. For any commercial use of this figure, users may, if allowed, recreate it in BioRender under an Industry BioRender Plan.

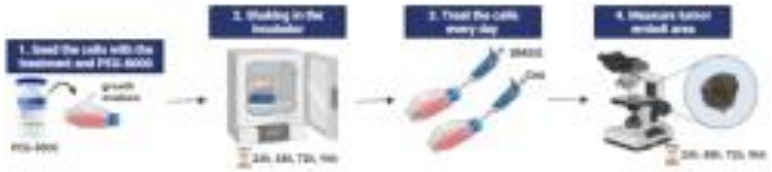

For any questions regarding this document, or other questions about publishing with BioRender refer to our BioRender Publication Guide, or contact BioRender Support at support@biorender.com.

Appendix 20. Permission for publication of figure 20

49 Spadina Ave. Suite 200
Toronto ON M5V 2J1 Canada
www.biorender.com

Confirmation of Publication and Licensing Rights

May 19th, 2022
Science Suite Inc.

Subscription:	*Student Plan*
Agreement number:	*PY23XQHGG4*
Journal name:	*Thesis Keishla M Rodriguez Martir*

To whom this may concern,

This document is to confirm that Keishla Rodriguez Martir has been granted a license to use the BioRender content, including icons, templates and other original artwork, appearing in the attached completed graphic pursuant to BioRender's Academic License Terms. This license permits BioRender content to be sublicensed for use in journal publications.

All rights and ownership of BioRender content are reserved by BioRender. All completed graphics must be accompanied by the following citation: "Created with BioRender.com".

BioRender content included in the completed graphic is not licensed for any commercial uses beyond publication in a journal. For any commercial use of this figure, users may, if allowed, recreate it in BioRender under an Industry BioRender Plan.

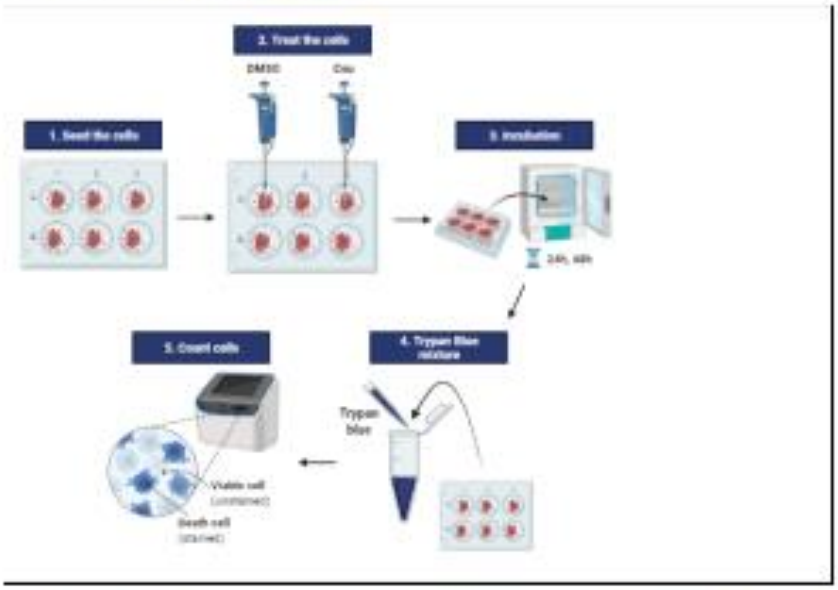

For any questions regarding this document, or other questions about publishing with BioRender refer to our BioRender Publication Guide, or contact BioRender Support at support@biorender.com.

Appendix 21. Permission for publication of figure 30

49 Spadina Ave. Suite 200
Toronto ON M5V 2J1 Canada
www.biorender.com

Confirmation of Publication and Licensing Rights

May 19th, 2022
Science Suite Inc.

Subscription:	*Student Plan*
Agreement number:	*EO23XQHPKB*
Journal name:	*Thesis Keishla M Rodriguez Martir*

To whom this may concern,

This document is to confirm that Keishla Rodriguez Martir has been granted a license to use the BioRender content, including icons, templates and other original artwork, appearing in the attached completed graphic pursuant to BioRender's Academic License Terms. This license permits BioRender content to be sublicensed for use in journal publications.

All rights and ownership of BioRender content are reserved by BioRender. All completed graphics must be accompanied by the following citation: "Created with BioRender.com".

BioRender content included in the completed graphic is not licensed for any commercial uses beyond publication in a journal. For any commercial use of this figure, users may, if allowed, recreate it in BioRender under an Industry BioRender Plan.

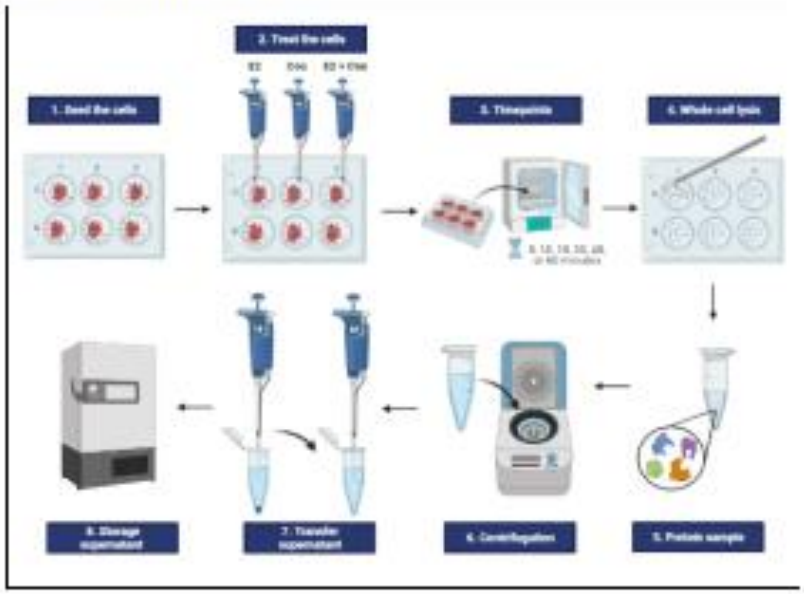

For any questions regarding this document, or other questions about publishing with BioRender refer to our BioRender Publication Guide, or contact BioRender Support at support@biorender.com.

Appendix 22. Permission for publication of figure 31

49 Spadina Ave. Suite 200
Toronto ON M5V 2J1 Canada
www.biorender.com

Confirmation of Publication and Licensing Rights

May 19th, 2022
Science Suite Inc.

Subscription:	*Student Plan*
Agreement number:	*EA23XQHYCV*
Journal name:	*Thesis Keishla M Rodriguez Martir*

To whom this may concern,

This document is to confirm that Keishla Rodriguez Martir has been granted a license to use the BioRender content, including icons, templates and other original artwork, appearing in the attached completed graphic pursuant to BioRender's Academic License Terms. This license permits BioRender content to be sublicensed for use in journal publications.

All rights and ownership of BioRender content are reserved by BioRender. All completed graphics must be accompanied by the following citation: "Created with BioRender.com".

BioRender content included in the completed graphic is not licensed for any commercial uses beyond publication in a journal. For any commercial use of this figure, users may, if allowed, recreate it in BioRender under an Industry BioRender Plan.

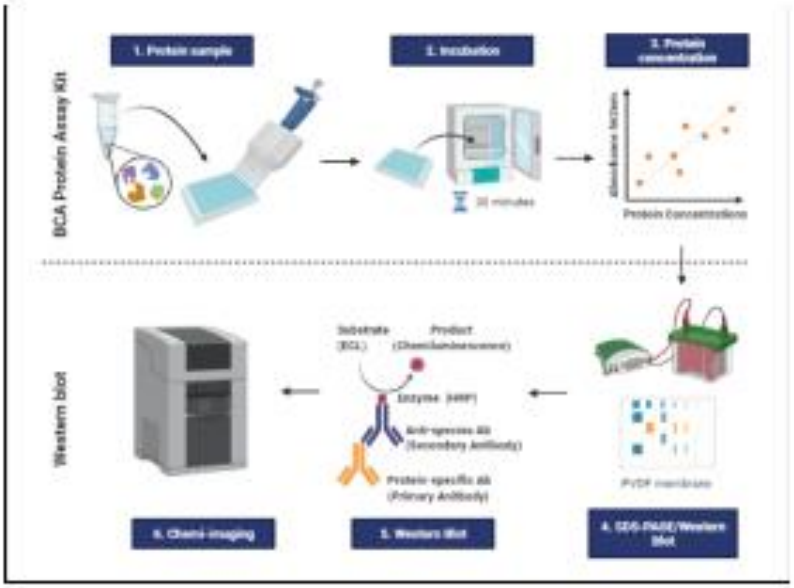

For any questions regarding this document, or other questions about publishing with BioRender refer to our BioRender Publication Guide, or contact BioRender Support at support@biorender.com.

Appendix 23. Permission for publication of figure 32

49 Spadina Ave. Suite 200
Toronto ON M5V 2J1 Canada
www.biorender.com

Confirmation of Publication and Licensing Rights

May 23rd, 2022
Science Suite Inc.

Subscription:	*Student Plan*
Agreement number:	*UP23YB7IO1*
Journal name:	*Thesis Keishla M Rodriguez Martir*

To whom this may concern,

This document is to confirm that Keishla Rodriguez Martir has been granted a license to use the BioRender content, including icons, templates and other original artwork, appearing in the attached completed graphic pursuant to BioRender's Academic License Terms. This license permits BioRender content to be sublicensed for use in journal publications.

All rights and ownership of BioRender content are reserved by BioRender. All completed graphics must be accompanied by the following citation: "Created with BioRender.com".

BioRender content included in the completed graphic is not licensed for any commercial uses beyond publication in a journal. For any commercial use of this figure, users may, if allowed, recreate it in BioRender under an Industry BioRender Plan.

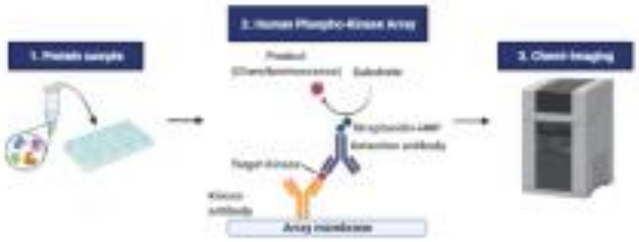

For any questions regarding this document, or other questions about publishing with BioRender refer to our BioRender Publication Guide, or contact BioRender Support at support@biorender.com.

Appendix 24. Permission for publication of figure 33

bio RENDER

49 Spadina Ave. Suite 200
Toronto ON M5V 2J1 Canada
www.biorender.com

Confirmation of Publication and Licensing Rights

May 23rd, 2022
Science Suite Inc.

Subscription:	*Student Plan*
Agreement number:	*YX23YB9BIV*
Journal name:	*Thesis Keishla M Rodriguez Martir*

To whom this may concern,

This document is to confirm that Keishla Rodriguez Martir has been granted a license to use the BioRender content, including icons, templates and other original artwork, appearing in the attached completed graphic pursuant to BioRender's Academic License Terms. This license permits BioRender content to be sublicensed for use in journal publications.

All rights and ownership of BioRender content are reserved by BioRender. All completed graphics must be accompanied by the following citation: "Created with BioRender.com".

BioRender content included in the completed graphic is not licensed for any commercial uses beyond publication in a journal. For any commercial use of this figure, users may, if allowed, recreate it in BioRender under an Industry BioRender Plan.

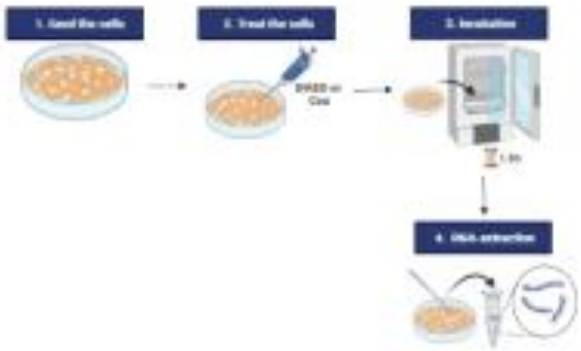

For any questions regarding this document, or other questions about publishing with BioRender refer to our BioRender Publication Guide, or contact BioRender Support at support@biorender.com.

Appendix 25. Permission for publication of figure 34

49 Spadina Ave. Suite 200
Toronto ON M5V 2J1 Canada
www.biorender.com

Confirmation of Publication and Licensing Rights

May 23rd, 2022
Science Suite Inc.

Subscription:	*Student Plan*
Agreement number:	*HQ23YB9HYM*
Journal name:	*Thesis Keishla M Rodriguez Martir*

To whom this may concern,

This document is to confirm that Keishla Rodriguez Martir has been granted a license to use the BioRender content, including icons, templates and other original artwork, appearing in the attached completed graphic pursuant to BioRender's Academic License Terms. This license permits BioRender content to be sublicensed for use in journal publications.

All rights and ownership of BioRender content are reserved by BioRender. All completed graphics must be accompanied by the following citation: "Created with BioRender.com".

BioRender content included in the completed graphic is not licensed for any commercial uses beyond publication in a journal. For any commercial use of this figure, users may, if allowed, recreate it in BioRender under an Industry BioRender Plan.

For any questions regarding this document, or other questions about publishing with BioRender refer to our BioRender Publication Guide, or contact BioRender Support at support@biorender.com.

Appendix 26. Permission for publication of figure 35

49 Spadina Ave. Suite 200
Toronto ON M5V 2J1 Canada
www.biorender.com

Confirmation of Publication and Licensing Rights

May 19th, 2022
Science Suite Inc.

Subscription:	*Student Plan*
Agreement number:	*PF23XQI6Y0*
Journal name:	*Thesis Keishla M Rodriguez Martir*

To whom this may concern,

This document is to confirm that Keishla Rodriguez Martir has been granted a license to use the BioRender content, including icons, templates and other original artwork, appearing in the attached completed graphic pursuant to BioRender's Academic License Terms. This license permits BioRender content to be sublicensed for use in journal publications.

All rights and ownership of BioRender content are reserved by BioRender. All completed graphics must be accompanied by the following citation: "Created with BioRender.com".

BioRender content included in the completed graphic is not licensed for any commercial uses beyond publication in a journal. For any commercial use of this figure, users may, if allowed, recreate it in BioRender under an Industry BioRender Plan.

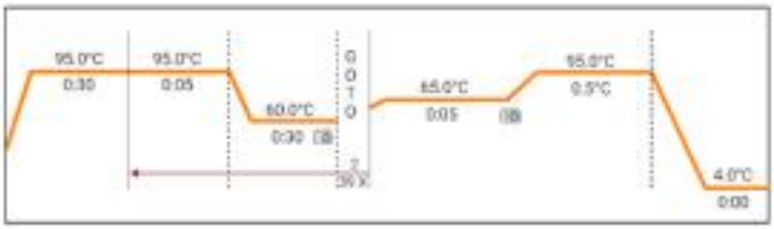

For any questions regarding this document, or other questions about publishing with BioRender refer to our BioRender Publication Guide, or contact BioRender Support at support@biorender.com.

Appendix 27. Permission for publication of figure 36

49 Spadina Ave. Suite 200
Toronto ON M5V 2J1 Canada
www.biorender.com

Confirmation of Publication and Licensing Rights

May 19th, 2022
Science Suite Inc.

Subscription:	*Student Plan*
Agreement number:	*FO23XQIEE1*
Journal name:	*Thesis Keishla M Rodriguez Martir*

To whom this may concern,

This document is to confirm that Keishla Rodriguez Martir has been granted a license to use the BioRender content, including icons, templates and other original artwork, appearing in the attached completed graphic pursuant to BioRender's Academic License Terms. This license permits BioRender content to be sublicensed for use in journal publications.

All rights and ownership of BioRender content are reserved by BioRender. All completed graphics must be accompanied by the following citation: "Created with BioRender.com".

BioRender content included in the completed graphic is not licensed for any commercial uses beyond publication in a journal. For any commercial use of this figure, users may, if allowed, recreate it in BioRender under an Industry BioRender Plan.

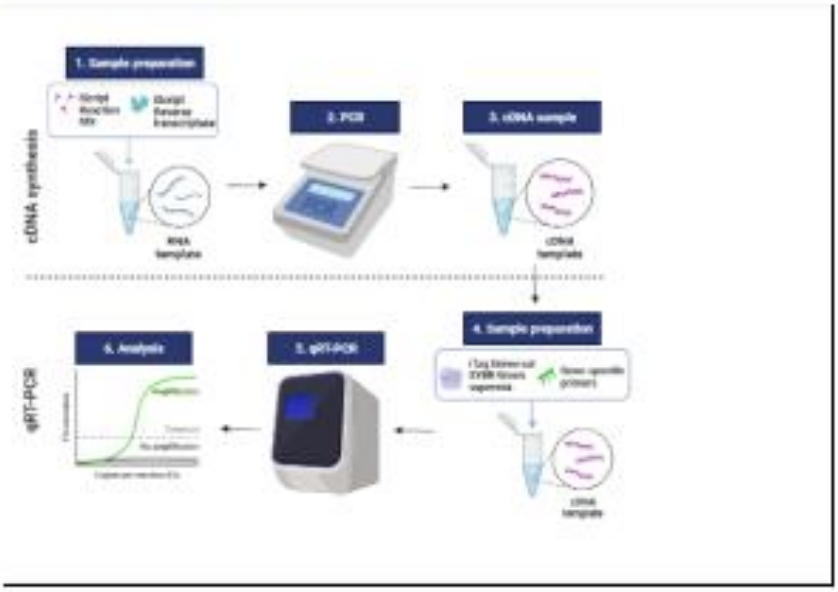

For any questions regarding this document, or other questions about publishing with BioRender refer to our BioRender Publication Guide, or contact BioRender Support at support@biorender.com.

Appendix 28. Permission for publication of figure 39

49 Spadina Ave. Suite 200
Toronto ON M5V 2J1 Canada
www.biorender.com

Confirmation of Publication and Licensing Rights

May 19th, 2022
Science Suite Inc.

Subscription:	*Student Plan*
Agreement number:	*KI23XQIM5M*
Journal name:	*Thesis Keishla M Rodriguez Martir*

To whom this may concern,

This document is to confirm that Keishla Rodriguez Martir has been granted a license to use the BioRender content, including icons, templates and other original artwork, appearing in the attached completed graphic pursuant to BioRender's Academic License Terms. This license permits BioRender content to be sublicensed for use in journal publications.

All rights and ownership of BioRender content are reserved by BioRender. All completed graphics must be accompanied by the following citation: "Created with BioRender.com".

BioRender content included in the completed graphic is not licensed for any commercial uses beyond publication in a journal. For any commercial use of this figure, users may, if allowed, recreate it in BioRender under an Industry BioRender Plan.

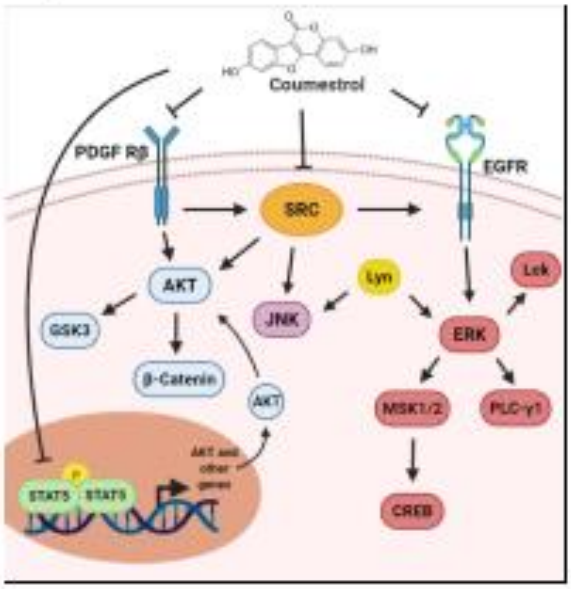

For any questions regarding this document, or other questions about publishing with BioRender refer to our BioRender Publication Guide, or contact BioRender Support at support@biorender.com.

Appendix 29. Permission for publication of figure 43

49 Spadina Ave. Suite 200
Toronto ON M5V 2J1 Canada
www.biorender.com

Confirmation of Publication and Licensing Rights

May 19th, 2022
Science Suite Inc.

Subscription:	*Student Plan*
Agreement number:	*YL23XQJ4Y8*
Journal name:	*Thesis Keishla M Rodriguez Martir*

To whom this may concern,

This document is to confirm that Keishla Rodriguez Martir has been granted a license to use the BioRender content, including icons, templates and other original artwork, appearing in the attached completed graphic pursuant to BioRender's Academic License Terms. This license permits BioRender content to be sublicensed for use in journal publications.

All rights and ownership of BioRender content are reserved by BioRender. All completed graphics must be accompanied by the following citation: "Created with BioRender.com".

BioRender content included in the completed graphic is not licensed for any commercial uses beyond publication in a journal. For any commercial use of this figure, users may, if allowed, recreate it in BioRender under an Industry BioRender Plan.

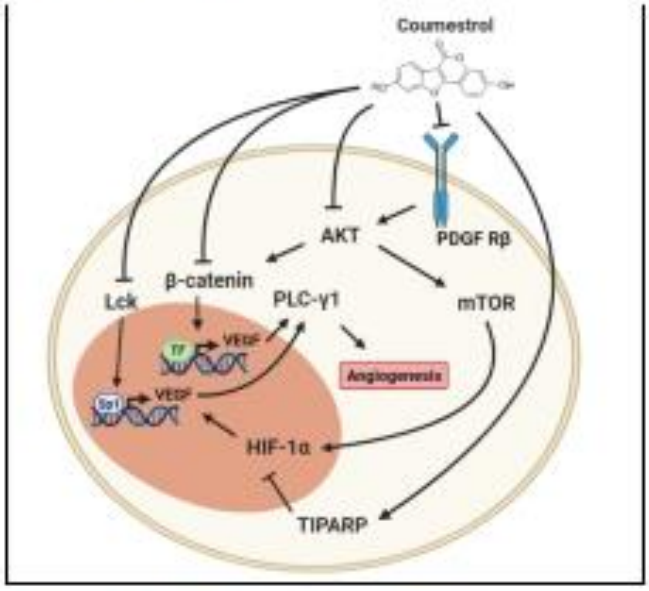

For any questions regarding this document, or other questions about publishing with BioRender refer to our BioRender Publication Guide, or contact BioRender Support at support@biorender.com.

Appendix 30. Permission for publication of figure 46

49 Spadina Ave. Suite 200
Toronto ON M5V 2J1 Canada
www.biorender.com

Confirmation of Publication and Licensing Rights

May 23rd, 2022
Science Suite Inc.

Subscription:	*Student Plan*
Agreement number:	*JO23YBB7E3*
Journal name:	*Thesis Keishla M Rodriguez Martir*

To whom this may concern,

This document is to confirm that Keishla Rodriguez Martir has been granted a license to use the BioRender content, including icons, templates and other original artwork, appearing in the attached completed graphic pursuant to BioRender's Academic License Terms. This license permits BioRender content to be sublicensed for use in journal publications.

All rights and ownership of BioRender content are reserved by BioRender. All completed graphics must be accompanied by the following citation: "Created with BioRender.com".

BioRender content included in the completed graphic is not licensed for any commercial uses beyond publication in a journal. For any commercial use of this figure, users may, if allowed, recreate it in BioRender under an Industry BioRender Plan.

For any questions regarding this document, or other questions about publishing with BioRender refer to our BioRender Publication Guide, or contact BioRender Support at support@biorender.com

Chapter VI: References

Adapted from “Breast Cancer Surgery Types”, by BioRender.com (2020). Retrieved from https://app.biorender.com/biorender-templates

AmericanCancerSociety. (2021). *Treatment of Inflammatory Breast Cancer*. https://www.cancer.org/cancer/breast-cancer/treatment/treatment-of-inflammatory-breast-cancer.html#references

AmericanCancerSociety. (2022). *Cancer Facts and Figures*. https://www.cancer.org/research/cancer-facts-statistics/all-cancer-facts-figures/cancer-facts-figures-2022.html#:~:text=The%20Facts%20%26%20Figures%20annual%20report,deaths%20in%20the%20United%20States

Arakaki, A. K. S., Pan, W. A., Lin, H., & Trejo, J. (2018). The α-arrestin ARRDC3 suppresses breast carcinoma invasion by regulating G protein-coupled receptor lysosomal sorting and signaling. *J Biol Chem*, *293*(9), 3350-3362. https://doi.org/10.1074/jbc.RA117.001516

Arias-Pulido, H., Royce, M., Gong, Y., Joste, N., Lomo, L., Lee, S. J., Chaher, N., Verschraegen, C., Lara, J., Prossnitz, E. R., & Cristofanilli, M. (2010). GPR30 and estrogen receptor expression: new insights into hormone dependence of inflammatory breast cancer. *Breast Cancer Res Treat*, *123*(1), 51-58. https://doi.org/10.1007/s10549-009-0631-7

Arora, J., Sauer, S. J., Tarpley, M., Vermeulen, P., Rypens, C., Van Laere, S., Williams, K. P., Devi, G. R., & Dewhirst, M. W. (2017). Inflammatory breast cancer tumor emboli express high levels of anti-apoptotic proteins: use of a quantitative high content and high-throughput 3D IBC spheroid assay to

identify targeting strategies. *Oncotarget*, *8*(16), 25848-25863. https://doi.org/10.18632/oncotarget.15667

Bai, D., Ueno, L., & Vogt, P. K. (2009). Akt-mediated regulation of NFkappaB and the essentialness of NFkappaB for the oncogenicity of PI3K and Akt. *Int J Cancer*, *125*(12), 2863-2870. https://doi.org/10.1002/ijc.24748

Balfour, H. (2020). *TiPARP activation should be the target of future cancer drugs, says researcher*. https://www.drugtargetreview.com/news/62627/tiparp-activation-should-be-the-target-of-future-cancer-drugs-says-researcher/

Basu, P., & Maier, C. (2018). Phytoestrogens and breast cancer: In vitro anticancer activities of isoflavones, lignans, coumestans, stilbenes and their analogs and derivatives. *Biomed Pharmacother*, *107*, 1648-1666. https://doi.org/10.1016/j.biopha.2018.08.100

Belfiore, L., Aghaei, B., Law, A. M. K., Dobrowolski, J. C., Raftery, L. J., Tjandra, A. D., Yee, C., Piloni, A., Volkerling, A., Ferris, C. J., & Engel, M. (2021). Generation and analysis of 3D cell culture models for drug discovery. *European Journal of Pharmaceutical Sciences*, *163*. https://doi.org/https://doi.org/10.1016/j.ejps.2021.105876

Bilal, I., Chowdhury, A., Davidson, J., & Whitehead, S. (2014). Phytoestrogens and prevention of breast cancer: The contentious debate. *World J Clin Oncol*, *5*(4), 705-712. https://doi.org/10.5306/wjco.v5.i4.705

Breastcancer.org. (2021). *U.S. Breast Cancer Statistics*. https://www.breastcancer.org/symptoms/understand_bc/statistics

Britt, T. (2021). *History of breast cancer: Discovery, milestones, and modern treatment*. Medical News Today. https://www.medicalnewstoday.com/articles/history-of-breast-cancer#summary

Chen, H. Y., Dykstra, K. D., Birzin, E. T., Frisch, K., Chan, W., Yang, Y. T., Mosley, R. T., DiNinno, F., Rohrer, S. P., Schaeffer, J. M., & Hammond, M. L. (2004). Estrogen receptor ligands. Part 1: The discovery of flavanoids with subtype selectivity. *Bioorg Med Chem Lett*, *14*(6), 1417-1421. https://doi.org/10.1016/j.bmcl.2004.01.031

Chen, L. H., Kuo, W. H., Tsai, M. H., Chen, P. C., Hsiao, C. K., Chuang, E. Y., Chang, L. Y., Hsieh, F. J., Lai, L. C., & Chang, K. J. (2011). Identification of prognostic genes for recurrent risk prediction in triple negative breast cancer patients in Taiwan. *PLoS One*, *6*(11), e28222. https://doi.org/10.1371/journal.pone.0028222

Cheng, L., Li, Z., Huang, Y. Z., Zhang, X., Dai, X. Y., Shi, L., Xi, P. W., Wei, J. F., & Ding, Q. (2019). TCDD-Inducible Poly-ADP-Ribose Polymerase (TIPARP), A Novel Therapeutic Target Of Breast Cancer. *Cancer Manag Res*, *11*, 8991-9004. https://doi.org/10.2147/cmar.S219289

Choi, Y. L., Bocanegra, M., Kwon, M. J., Shin, Y. K., Nam, S. J., Yang, J. H., Kao, J., Godwin, A. K., & Pollack, J. R. (2010). LYN is a mediator of epithelial-mesenchymal transition and a target of dasatinib in breast cancer. *Cancer Res*, *70*(6), 2296-2306. https://doi.org/10.1158/0008-5472.Can-09-3141

Clinic, M. (2020). *Male breast cancer*. https://www.mayoclinic.org/diseases-conditions/male-breast-cancer/symptoms-causes/syc-20374740

Cos, P., De Bruyne, T., Apers, S., Vanden Berghe, D., Pieters, L., & Vlietinck, A. J. (2003). Phytoestrogens: recent developments. *Planta Med*, *69*(7), 589-599. https://doi.org/10.1055/s-2003-41122

Dagdemir, A., Durif, J., Ngollo, M., Bignon, Y. J., & Bernard-Gallon, D. (2013). Breast cancer: mechanisms involved in action of phytoestrogens and epigenetic changes. *In Vivo*, *27*(1), 1-9.

Dawood, S., Ueno, N. T., Valero, V., Woodward, W. A., Buchholz, T. A., Hortobagyi, G. N., Gonzalez-Angulo, A. M., & Cristofanilli, M. (2011). Differences in survival among women with stage III inflammatory and noninflammatory locally advanced breast cancer appear early: a large population-based study. *Cancer*, *117*(9), 1819-1826. https://doi.org/10.1002/cncr.25682

Di Bonito, M., Cantile, M., & Botti, G. (2019). Pathological and molecular characteristics of inflammatory breast cancer. *Transl Cancer Res*, *8*(Suppl 5), S449-s456. https://doi.org/10.21037/tcr.2019.03.24

Division of Cancer Prevention and Control, C. f. D. C. a. P. (2021). *Breast Cancer Statistics*. https://www.cdc.gov/cancer/breast/statistics/index.htm

Dixon-Shanies, D., & Shaikh, N. (1999). Growth inhibition of human breast cancer cells by herbs and phytoestrogens. *Oncol Rep*, *6*(6), 1383-1387. https://doi.org/10.3892/or.6.6.1383

Dobiasova, B., & Mego, M. (2020). Biomarkers for Inflammatory Breast Cancer: Diagnostic and Therapeutic Utility. *Breast Cancer (Dove Med Press)*, *12*, 153-163. https://doi.org/10.2147/bctt.S231502

Draheim, K. M., Chen, H. B., Tao, Q., Moore, N., Roche, M., & Lyle, S. (2010). ARRDC3 suppresses breast cancer progression by negatively regulating integrin beta4. *Oncogene*, *29*(36), 5032-5047. https://doi.org/10.1038/onc.2010.250

Dufner, A., & Thomas, G. (1999). Ribosomal S6 kinase signaling and the control of translation. *Exp Cell Res*, *253*(1), 100-109. https://doi.org/10.1006/excr.1999.4683

Dushkin, H., & Cristofanilli, M. (2011). Inflammatory breast cancer. *J Natl Compr Canc Netw*, *9*(2), 233-240; quiz 241. https://doi.org/10.6004/jnccn.2011.0018

Edmondson, R., Broglie, J. J., Adcock, A. F., & Yang, L. (2014). Three-dimensional cell culture systems and their applications in drug discovery and cell-based biosensors. *Assay Drug Dev Technol*, *12*(4), 207-218. https://doi.org/10.1089/adt.2014.573

Eliyatkın, N., Yalçın, E., Zengel, B., Aktaş, S., & Vardar, E. (2015). Molecular Classification of Breast Carcinoma: From Traditional, Old-Fashioned Way to A New Age, and A New Way. *J Breast Health*, *11*(2), 59-66. https://doi.org/10.5152/tjbh.2015.1669

Emmanouilidi, A., Lattanzio, R., Sala, G., Piantelli, M., & Falasca, M. (2017). The role of phospholipase Cγ1 in breast cancer and its clinical significance. *Future Oncol*, *13*(22), 1991-1997. https://doi.org/10.2217/fon-2017-0125

Feng, Y., Spezia, M., Huang, S., Yuan, C., Zeng, Z., Zhang, L., Ji, X., Liu, W., Huang, B., Luo, W., Liu, B., Lei, Y., Du, S., Vuppalapati, A., Luu, H. H., Haydon, R. C., He, T. C., & Ren, G. (2018). Breast cancer development and progression: Risk factors, cancer stem cells, signaling pathways, genomics, and molecular pathogenesis. *Genes Dis*, *5*(2), 77-106. https://doi.org/10.1016/j.gendis.2018.05.001

Ferrières, J. (2004). The French paradox: lessons for other countries. *Heart*, *90*(1), 107-111. https://doi.org/10.1136/heart.90.1.107

Finn, R. S. (2008). Targeting Src in breast cancer. *Ann Oncol*, *19*(8), 1379-1386. https://doi.org/10.1093/annonc/mdn291

George Somlo, V. J. (2018). *64 - Inflammatory Breast Cancer* (The Breast (Fifth Edition) ed.). Elsevier. https://doi.org/10.1016/B978-0-323-35955-9.00064-7

Ginestier, C., Adélaïde, J., Gonçalvès, A., Repellini, L., Sircoulomb, F., Letessier, A., Finetti, P., Geneix, J., Charafe-Jauffret, E., Bertucci, F., Jacquemier, J., Viens, P., & Birnbaum, D. (2007). ERBB2 phosphorylation and trastuzumab sensitivity of breast cancer cell lines. *Oncogene*, *26*(50), 7163-7169. https://doi.org/10.1038/sj.onc.1210528

Goldman, R. (2020). *History of Breast Cancer: Timeline*. https://www.healthline.com/health/history-of-breast-cancer#outlook

Gu, Y., Chen, T., López, E., Wu, W., Wang, X., Cao, J., & Teng, L. (2014). The therapeutic target of estrogen receptor-alpha36 in estrogen-dependent tumors. *J Transl Med*, *12*, 16. https://doi.org/10.1186/1479-5876-12-16

Hanahan, D., & Weinberg, R. A. (2011). Hallmarks of cancer: the next generation. *Cell*, *144*(5), 646-674. https://doi.org/10.1016/j.cell.2011.02.013

Harris, D. M., Besselink, E., Henning, S. M., Go, V. L., & Heber, D. (2005). Phytoestrogens induce differential estrogen receptor alpha- or Beta-mediated responses in transfected breast cancer cells. *Exp Biol Med (Maywood)*, *230*(8), 558-568. https://doi.org/10.1177/153537020523000807

Hess-Wilson, J. K., Boldison, J., Weaver, K. E., & Knudsen, K. E. (2006). Xenoestrogen action in breast cancer: impact on ER-dependent transcription and mitogenesis. *Breast Cancer Res Treat*, *96*(3), 279-292. https://doi.org/10.1007/s10549-005-9082-y

Hester, R. H., Hortobagyi, G. N., & Lim, B. (2021). Inflammatory breast cancer: early recognition and diagnosis is critical. *Am J Obstet Gynecol*, *225*(4), 392-396. https://doi.org/10.1016/j.ajog.2021.04.217

Hopert, A. C., Beyer, A., Frank, K., Strunck, E., Wünsche, W., & Vollmer, G. (1998). Characterization of estrogenicity of phytoestrogens in an endometrial-derived experimental model. *Environ Health Perspect*, *106*(9), 581-586. https://doi.org/10.1289/ehp.98106581

Hyakudomi, M., Inao, T., Minari, Y., Itakura, M., Maruyama, R., & Tajima, Y. (2013). A case of male inflammatory breast cancer. *International Cancer*

Conference Journal, *2*(3), 183-187. https://doi.org/10.1007/s13691-013-0087-9

Jansson, S., Aaltonen, K., Bendahl, P. O., Falck, A. K., Karlsson, M., Pietras, K., & Rydén, L. (2018). The PDGF pathway in breast cancer is linked to tumour aggressiveness, triple-negative subtype and early recurrence. *Breast Cancer Res Treat*, *169*(2), 231-241. https://doi.org/10.1007/s10549-018-4664-7

Kang, L., Zhang, X., Xie, Y., Tu, Y., Wang, D., Liu, Z., & Wang, Z. Y. (2010). Involvement of estrogen receptor variant ER-alpha36, not GPR30, in nongenomic estrogen signaling. *Mol Endocrinol*, *24*(4), 709-721. https://doi.org/10.1210/me.2009-0317

Karlsson, H., Fryknäs, M., Larsson, R., & Nygren, P. (2012). Loss of cancer drug activity in colon cancer HCT-116 cells during spheroid formation in a new 3-D spheroid cell culture system. *Exp Cell Res*, *318*(13), 1577-1585. https://doi.org/10.1016/j.yexcr.2012.03.026

Kim, H. M., Jung, W. H., & Koo, J. S. (2015). Expression of Yes-associated protein (YAP) in metastatic breast cancer. *Int J Clin Exp Pathol*, *8*(9), 11248-11257.

Kleer, C. G., Zhang, Y., Pan, Q., van Golen, K. L., Wu, Z. F., Livant, D., & Merajver, S. D. (2002). WISP3 is a novel tumor suppressor gene of inflammatory breast cancer. *Oncogene*, *21*(20), 3172-3180. https://doi.org/10.1038/sj.onc.1205462

Koch, S. (2021). Regulation of Wnt Signaling by FOX Transcription Factors in Cancer. *Cancers (Basel)*, *13*(14). https://doi.org/10.3390/cancers13143446

Kolak, A., Kamińska, M., Sygit, K., Budny, A., Surdyka, D., Kukiełka-Budny, B., & Burdan, F. (2017). Primary and secondary prevention of breast cancer. *Ann Agric Environ Med*, *24*(4), 549-553. https://doi.org/10.26444/aaem/75943

Lee, C. J., An, H. J., Cho, E. S., Kang, H. C., Lee, J. Y., Lee, H. S., & Cho, Y. Y. (2020). Stat2 stability regulation: an intersection between immunity and carcinogenesis. *Exp Mol Med*, *52*(9), 1526-1536. https://doi.org/10.1038/s12276-020-00506-6

Li, J., Gonzalez-Angulo, A. M., Allen, P. K., Yu, T. K., Woodward, W. A., Ueno, N. T., Lucci, A., Krishnamurthy, S., Gong, Y., Bondy, M. L., Yang, W., Willey, J. S., Cristofanilli, M., Valero, V., & Buchholz, T. A. (2011). Triple-negative subtype predicts poor overall survival and high locoregional relapse in inflammatory breast cancer. *Oncologist*, *16*(12), 1675-1683. https://doi.org/10.1634/theoncologist.2011-0196

Lim, W., Jeong, M., Bazer, F. W., & Song, G. (2017). Coumestrol Inhibits Proliferation and Migration of Prostate Cancer Cells by Regulating AKT, ERK1/2, and JNK MAPK Cell Signaling Cascades. *J Cell Physiol*, *232*(4), 862-871. https://doi.org/10.1002/jcp.25494

Lim, W., Jeong, W., & Song, G. (2016). Coumestrol suppresses proliferation of ES2 human epithelial ovarian cancer cells. *J Endocrinol*, *228*(3), 149-160. https://doi.org/10.1530/joe-15-0418

Liu, D., Evans, I., Britton, G., & Zachary, I. (2008). The zinc-finger transcription factor, early growth response 3, mediates VEGF-induced angiogenesis. *Oncogene*, *27*(21), 2989-2998. https://doi.org/10.1038/sj.onc.1210959

Loessner, D., Stok, K. S., Lutolf, M. P., Hutmacher, D. W., Clements, J. A., & Rizzi, S. C. (2010). Bioengineered 3D platform to explore cell-ECM interactions and drug resistance of epithelial ovarian cancer cells. *Biomaterials*, *31*(32), 8494-8506. https://doi.org/10.1016/j.biomaterials.2010.07.064

Longacre, M., Snyder, N. A., Housman, G., Leary, M., Lapinska, K., Heerboth, S., Willbanks, A., & Sarkar, S. (2016). A Comparative Analysis of Genetic and Epigenetic Events of Breast and Ovarian Cancer Related to Tumorigenesis. *International Journal of Molecular Sciences*, *17*(5), 759. https://www.mdpi.com/1422-0067/17/5/759

Lukong, K. E. (2017). Understanding breast cancer - The long and winding road. *BBA Clin*, *7*, 64-77. https://doi.org/10.1016/j.bbacli.2017.01.001

Lv, D., Guo, L., Zhang, T., & Huang, L. (2017). PRAS40 signaling in tumor. *Oncotarget*, *8*(40), 69076-69085. https://doi.org/10.18632/oncotarget.17299

Martin, P. M., Horwitz, K. B., Ryan, D. S., & McGuire, W. L. (1978). Phytoestrogen interaction with estrogen receptors in human breast cancer cells. *Endocrinology*, *103*(5), 1860-1867. https://doi.org/10.1210/endo-103-5-1860

Masuda, H., Baggerly, K. A., Wang, Y., Iwamoto, T., Brewer, T., Pusztai, L., Kai, K., Kogawa, T., Finetti, P., Birnbaum, D., Dirix, L., Woodward, W. A., Reuben, J. M., Krishnamurthy, S., Symmans, W., Van Laere, S. J., Bertucci, F., Hortobagyi, G. N., & Ueno, N. T. (2013). Comparison of molecular subtype distribution in triple-negative inflammatory and non-inflammatory

breast cancers. *Breast Cancer Res*, *15*(6), R112. https://doi.org/10.1186/bcr3579

Masuda, H., Zhang, D., Bartholomeusz, C., Doihara, H., Hortobagyi, G. N., & Ueno, N. T. (2012). Role of epidermal growth factor receptor in breast cancer. *Breast Cancer Res Treat*, *136*(2), 331-345. https://doi.org/10.1007/s10549-012-2289-9

Menta, A., Fouad, T. M., Lucci, A., Le-Petross, H., Stauder, M. C., Woodward, W. A., Ueno, N. T., & Lim, B. (2018). Inflammatory Breast Cancer: What to Know About This Unique, Aggressive Breast Cancer. *Surg Clin North Am*, *98*(4), 787-800. https://doi.org/10.1016/j.suc.2018.03.009

Mohamed, M. M., Al-Raawi, D., Sabet, S. F., & El-Shinawi, M. (2014). Inflammatory breast cancer: New factors contribute to disease etiology: A review. *J Adv Res*, *5*(5), 525-536. https://doi.org/10.1016/j.jare.2013.06.004

Nascimento, R., & Otoni, K. (2020). Histological and molecular classification of breast cancer: what do we know? *Mastology*, *30*. https://doi.org/10.29289/25945394202020200024

Obiorah, I. E., Fan, P., & Jordan, V. C. (2014). Breast cancer cell apoptosis with phytoestrogens is dependent on an estrogen-deprived state. *Cancer Prev Res (Phila)*, *7*(9), 939-949. https://doi.org/10.1158/1940-6207.Capr-14-0061

Ohshiro, K., Schwartz, A. M., Levine, P. H., & Kumar, R. (2012). Alternate estrogen receptors promote invasion of inflammatory breast cancer cells via non-

genomic signaling. *PLoS One*, *7*(1), e30725. https://doi.org/10.1371/journal.pone.0030725

Privat, M., Aubel, C., Arnould, S., Communal, Y., Ferrara, M., & Bignon, Y. J. (2010). AKT and p21 WAF1/CIP1 as potential genistein targets in BRCA1-mutant human breast cancer cell lines. *Anticancer Res*, *30*(6), 2049-2054.

Pu, X., Storr, S. J., Ahmad, N. S., Rakha, E. A., Green, A. R., Ellis, I. O., & Martin, S. G. (2018). High nuclear MSK1 is associated with longer survival in breast cancer patients. *J Cancer Res Clin Oncol*, *144*(3), 509-517. https://doi.org/10.1007/s00432-018-2579-7

Pullen, N., & Thomas, G. (1997). The modular phosphorylation and activation of p70s6k. *FEBS Lett*, *410*(1), 78-82. https://doi.org/10.1016/s0014-5793(97)00323-2

Rao, J., Jiang, X., Wang, Y., & Chen, B. (2011). Advances in the understanding of the structure and function of ER-α36,a novel variant of human estrogen receptor-alpha. *J Steroid Biochem Mol Biol*, *127*(3-5), 231-237. https://doi.org/10.1016/j.jsbmb.2011.08.004

Rasmussen, M., Tan, S., Somisetty, V. S., Hutin, D., Olafsen, N. E., Moen, A., Anonsen, J. H., Grant, D. M., & Matthews, J. (2021). PARP7 and Mono-ADP-Ribosylation Negatively Regulate Estrogen Receptor α Signaling in Human Breast Cancer Cells. *Cells*, *10*(3). https://doi.org/10.3390/cells10030623

Rivenbark, A. G., O'Connor, S. M., & Coleman, W. B. (2013). Molecular and cellular heterogeneity in breast cancer: challenges for personalized

medicine. *Am J Pathol*, *183*(4), 1113-1124. https://doi.org/10.1016/j.ajpath.2013.08.002

Rosenbluth, J. M., & Overmoyer, B. A. (2019). Inflammatory Breast Cancer: a Separate Entity. *Curr Oncol Rep*, *21*(10), 86. https://doi.org/10.1007/s11912-019-0842-y

Schmidt, J. W., Wehde, B. L., Sakamoto, K., Triplett, A. A., Anderson, S. M., Tsichlis, P. N., Leone, G., & Wagner, K. U. (2014). Stat5 regulates the phosphatidylinositol 3-kinase/Akt1 pathway during mammary gland development and tumorigenesis. *Mol Cell Biol*, *34*(7), 1363-1377. https://doi.org/10.1128/mcb.01220-13

Schmidt, S., Michna, H., & Diel, P. (2005). Combinatory effects of phytoestrogens and 17beta-estradiol on proliferation and apoptosis in MCF-7 breast cancer cells. *J Steroid Biochem Mol Biol*, *94*(5), 445-449. https://doi.org/10.1016/j.jsbmb.2004.12.042

Selli, C., & Sims, A. H. (2019). Neoadjuvant Therapy for Breast Cancer as a Model for Translational Research. *Breast Cancer (Auckl)*, *13*, 1178223419829072. https://doi.org/10.1177/1178223419829072

Shen, T., & Guo, Q. (2018). Role of Pyk2 in Human Cancers. *Med Sci Monit*, *24*, 8172-8182. https://doi.org/10.12659/msm.913479

Shu, X. O., Zheng, Y., Cai, H., Gu, K., Chen, Z., Zheng, W., & Lu, W. (2009). Soy food intake and breast cancer survival. *Jama*, *302*(22), 2437-2443. https://doi.org/10.1001/jama.2009.1783

Słowikowski, B. K., Lianeri, M., & Jagodziński, P. P. (2017). Exploring estrogenic activity in lung cancer. *Mol Biol Rep*, *44*(1), 35-50. https://doi.org/10.1007/s11033-016-4086-8

Song, K., Wang, H., Krebs, T. L., & Danielpour, D. (2006). Novel roles of Akt and mTOR in suppressing TGF-beta/ALK5-mediated Smad3 activation. *Embo j*, *25*(1), 58-69. https://doi.org/10.1038/sj.emboj.7600917

Stegeman, H., Span, P. N., Peeters, W. J., Verheijen, M. M., Grénman, R., Meijer, T. W., Kaanders, J. H., & Bussink, J. (2016). Interaction between hypoxia, AKT and HIF-1 signaling in HNSCC and NSCLC: implications for future treatment strategies. *Future Sci OA*, *2*(1), Fso84. https://doi.org/10.4155/fso.15.84

Su, X., Xu, X., Li, G., Lin, B., Cao, J., & Teng, L. (2014). ER-α36: a novel biomarker and potential therapeutic target in breast cancer. *Onco Targets Ther*, *7*, 1525-1533. https://doi.org/10.2147/ott.S65345

Sun, Y. S., Zhao, Z., Yang, Z. N., Xu, F., Lu, H. J., Zhu, Z. Y., Shi, W., Jiang, J., Yao, P. P., & Zhu, H. P. (2017). Risk Factors and Preventions of Breast Cancer. *Int J Biol Sci*, *13*(11), 1387-1397. https://doi.org/10.7150/ijbs.21635

Tanhueco, A., & Youssef, M. M. G. (2021). Inflammatory Breast Cancer in Men: A rare clinical case report and a literature review. *Int J Surg Case Rep*, *80*, 105696. https://doi.org/10.1016/j.ijscr.2021.105696

Vahedi, S., Chueh, F. Y., Chandran, B., & Yu, C. L. (2015). Lymphocyte-specific protein tyrosine kinase (Lck) interacts with CR6-interacting factor 1 (CRIF1)

in mitochondria to repress oxidative phosphorylation. *BMC Cancer*, *15*, 551. https://doi.org/10.1186/s12885-015-1520-6

Van der Auwera, I., Van den Eynden, G., Van Hummelen, P., Van Dam, P., Van Marck, E., Vermeulen, P. B., & Dirix, L. (2007). Distinct molecular phenotype of inflammatory breast cancer compared to non-inflammatory breast cancer using Affymetrix-based genome-wide gene-expression analysis. *Br J Cancer*, *97*, 8. https://doi.org/10.1038/sj.bjc.6603967

van Golen, K. L., Davies, S., Wu, Z. F., Wang, Y., Bucana, C. D., Root, H., Chandrasekharappa, S., Strawderman, M., Ethier, S. P., & Merajver, S. D. (1999). A novel putative low-affinity insulin-like growth factor-binding protein, LIBC (lost in inflammatory breast cancer), and RhoC GTPase correlate with the inflammatory breast cancer phenotype. *Clin Cancer Res*, *5*(9), 2511-2519.

Van Laere, S., Van der Auwera, I., Van den Eynden, G. G., Fox, S. B., Bianchi, F., Harris, A. L., van Dam, P., Van Marck, E. A., Vermeulen, P. B., & Dirix, L. Y. (2005). Distinct molecular signature of inflammatory breast cancer by cDNA microarray analysis. *Breast Cancer Res Treat*, *93*(3), 237-246. https://doi.org/10.1007/s10549-005-5157-z

van Uden, D. J., van Laarhoven, H. W., Westenberg, A. H., de Wilt, J. H., & Blanken-Peeters, C. F. (2015). Inflammatory breast cancer: an overview. *Crit Rev Oncol Hematol*, *93*(2), 116-126. https://doi.org/10.1016/j.critrevonc.2014.09.003

Verdeal, K., Brown, R. R., Richardson, T., & Ryan, D. S. (1980). Affinity of phytoestrogens for estradiol-binding proteins and effect of coumestrol on growth of 7,12-dimethylbenz[a]anthracene-induced rat mammary tumors. *J Natl Cancer Inst*, *64*(2), 285-290. https://doi.org/10.1093/jnci/64.2.285

Vermeulen, P. B., van Golen, K. L., & Dirix, L. Y. (2010). Angiogenesis, lymphangiogenesis, growth pattern, and tumor emboli in inflammatory breast cancer: a review of the current knowledge. *Cancer*, *116*(11 Suppl), 2748-2754. https://doi.org/10.1002/cncr.25169

Vrtačnik, P., Ostanek, B., Mencej-Bedrač, S., & Marc, J. (2014). The many faces of estrogen signaling. *Biochem Med (Zagreb)*, *24*(3), 329-342. https://doi.org/10.11613/bm.2014.035

Wang, C., & Kurzer, M. S. (1998). Effects of phytoestrogens on DNA synthesis in MCF-7 cells in the presence of estradiol or growth factors. *Nutr Cancer*, *31*(2), 90-100. https://doi.org/10.1080/01635589809514686

Wang, Q., Jiang, J., Ying, G., Xie, X. Q., Zhang, X., Xu, W., Zhang, X., Song, E., Bu, H., Ping, Y. F., Yao, X. H., Wang, B., Xu, S., Yan, Z. X., Tai, Y., Hu, B., Qi, X., Wang, Y. X., He, Z. C., . . . Bian, X. W. (2018). Tamoxifen enhances stemness and promotes metastasis of ERα36(+) breast cancer by upregulating ALDH1A1 in cancer cells. *Cell Res*, *28*(3), 336-358. https://doi.org/10.1038/cr.2018.15

Wang, S., Ran, L., Zhang, W., Leng, X., Wang, K., Liu, G., Song, J., Wang, Y., Zhang, X., Wang, Y., Zhang, L., Ma, Y., Liu, K., Li, H., Zhang, W., Qin, G., & Song, F. (2019). FOXS1 is regulated by GLI1 and miR-125a-5p and

promotes cell proliferation and EMT in gastric cancer. *Sci Rep*, *9*(1), 5281. https://doi.org/10.1038/s41598-019-41717-w

Wang, W., Nag, S. A., & Zhang, R. (2015). Targeting the NFκB signaling pathways for breast cancer prevention and therapy. *Current medicinal chemistry*, *22*(2), 264-289. https://doi.org/10.2174/0929867321666141106124315

Wang, X., Reyes, M. E., Zhang, D., Funakoshi, Y., Trape, A. P., Gong, Y., Kogawa, T., Eckhardt, B. L., Masuda, H., Pirman, D. A., Jr., Yang, P., Reuben, J. M., Woodward, W. A., Bartholomeusz, C., Hortobagyi, G. N., Tripathy, D., & Ueno, N. T. (2017). EGFR signaling promotes inflammation and cancer stem-like activity in inflammatory breast cancer. *Oncotarget*, *8*(40), 67904-67917. https://doi.org/10.18632/oncotarget.18958

Wang, Z. Y., & Yin, L. (2015). Estrogen receptor alpha-36 (ER-α36): A new player in human breast cancer. *Mol Cell Endocrinol*, *418 Pt 3*, 193-206. https://doi.org/10.1016/j.mce.2015.04.017

Wei, L., Liu, T. T., Wang, H. H., Hong, H. M., Yu, A. L., Feng, H. P., & Chang, W. W. (2011). Hsp27 participates in the maintenance of breast cancer stem cells through regulation of epithelial-mesenchymal transition and nuclear factor-κB. *Breast Cancer Res*, *13*(5), R101. https://doi.org/10.1186/bcr3042

Wei, W., Chen, Z. J., Zhang, K. S., Yang, X. L., Wu, Y. M., Chen, X. H., Huang, H. B., Liu, H. L., Cai, S. H., Du, J., & Wang, H. S. (2014). The activation of G protein-coupled receptor 30 (GPR30) inhibits proliferation of estrogen receptor-negative breast cancer cells in vitro and in vivo. *Cell Death Dis*, *5*(10), e1428. https://doi.org/10.1038/cddis.2014.398

Wingo, P. A., Jamison, P. M., Young, J. L., & Gargiullo, P. (2004). Population-based statistics for women diagnosed with inflammatory breast cancer (United States). *Cancer Causes Control*, *15*(3), 321-328. https://doi.org/10.1023/b:Caco.0000024222.61114.18

Yamauchi, H., Woodward, W. A., Valero, V., Alvarez, R. H., Lucci, A., Buchholz, T. A., Iwamoto, T., Krishnamurthy, S., Yang, W., Reuben, J. M., Hortobágyi, G. N., & Ueno, N. T. (2012). Inflammatory breast cancer: what we know and what we need to learn. *Oncologist*, *17*(7), 891-899. https://doi.org/10.1634/theoncologist.2012-0039

Ye, Y., Tellez, J. D., Durazo, M., Belcher, M., Yearsley, K., & Barsky, S. H. (2010). E-cadherin accumulation within the lymphovascular embolus of inflammatory breast cancer is due to altered trafficking. *Anticancer Res*, *30*(10), 3903-3910.

Yersal, O., & Barutca, S. (2014). Biological subtypes of breast cancer: Prognostic and therapeutic implications. *World J Clin Oncol*, *5*(3), 412-424. https://doi.org/10.5306/wjco.v5.i3.412

Yu, T., Liu, M., Luo, H., Wu, C., Tang, X., Tang, S., Hu, P., Yan, Y., Wang, Z., & Tu, G. (2014). GPER mediates enhanced cell viability and motility via non-genomic signaling induced by 17β-estradiol in triple-negative breast cancer cells. *J Steroid Biochem Mol Biol*, *143*, 392-403. https://doi.org/10.1016/j.jsbmb.2014.05.003

Zafar, A., Singh, S., & Naseem, I. (2017). Cytotoxic activity of soy phytoestrogen coumestrol against human breast cancer MCF-7 cells: Insights into the

molecular mechanism. *Food Chem Toxicol*, *99*, 149-161. https://doi.org/10.1016/j.fct.2016.11.034

Zafar, A., Singh, S., Satija, Y. K., Saluja, D., & Naseem, I. (2018). Deciphering the molecular mechanism underlying anticancer activity of coumestrol in triple-negative breast cancer cells. *Toxicol In Vitro*, *46*, 19-28. https://doi.org/10.1016/j.tiv.2017.10.007

Zhang, H., Kong, Q., Wang, J., Jiang, Y., & Hua, H. (2020). Complex roles of cAMP-PKA-CREB signaling in cancer. *Exp Hematol Oncol*, *9*(1), 32. https://doi.org/10.1186/s40164-020-00191-1

Zhang, L., Cao, J., Dong, L., & Lin, H. (2020). TiPARP forms nuclear condensates to degrade HIF-1α and suppress tumorigenesis. *Proceedings of the National Academy of Sciences*, *117*(24), 13447-13456. https://doi.org/doi:10.1073/pnas.1921815117

Zhao, H., Martin, T. A., Davies, E. L., Ruge, F., Yu, H., Zhang, Y., Teng, X. U., & Jiang, W. G. (2016). The Clinical Implications of RSK1-3 in Human Breast Cancer. *Anticancer Res*, *36*(3), 1267-1274.

Zhou, X., Zhang, F.-y., Liu, Y., & Wei, D.-x. (2021). A Risk Prediction Model for Breast Cancer Based on Immune Genes Related to Early Growth Response Proteins Family [Original Research]. *Frontiers in Molecular Biosciences*, *7*. https://doi.org/10.3389/fmolb.2020.616547